# Pharmakologische Zielproteine von $\alpha_2$-Agonisten bei $\alpha_{2ABC}$-Rezeptor-defizienten Mäusen

Anne Elizabeth Knaus

Dissertation zur Erlangung des

Naturwissenschaftlichen Doktorgrades

Bayerische Julius-Maximilians-Universität

Fakultät für Chemie und Pharmazie

Würzburg

Mai, 2007

# Pharmakologische Zielproteine von $\alpha_2$-Agonisten bei $\alpha_{2ABC}$-Rezeptor-defizienten Mäusen

Anne Elizabeth Knaus

Dissertation zur Erlangung des

Naturwissenschaftlichen Doktorgrades

Bayerische Julius-Maximilians-Universität

Fakultät für Chemie und Pharmazie

Würzburg

Mai, 2007

Eingereicht am: ………………………………………………………………

1. Gutachter: Prof. Dr. Lutz Hein ……………………………………………….
2. Gutachter: Prof. Dr. Tanja Schirmeister ……………………………………….

1. Prüfer: Prof. Dr. Lutz Hein …………………………………………………
2. Prüfer: Prof. Dr. Tanja Schirmeister …………………………………………
3. Prüfer: Prof. Dr. Martin J. Lohse ……………………………………………….

Tag des öffentlichen Promotionskolloquiums: ……………………………………….
Doktorurkunde ausgehändigt am: ……………………………………………………

**Erklärung**

Hiermit erkläre ich an Eides statt, dass ich die Dissertation "Pharmacological targets of $\alpha_2$-agonists in $\alpha_{2ABC}$-receptor deficient mice" selbständig angefertigt und keine anderen als die von mir angegebenen Quellen und Hilfsmittel benutzt habe.

Ich erkläre außerdem, dass diese Dissertation weder in gleicher oder anderer Form bereits in einem anderen Prüfungsverfahren vorgelegen hat.

Ich habe früher außer den mit dem Zulassungsgesuch urkundlich vorgelegten Graden keine weiteren akademischen Grade erworben oder zu erwerben versucht.

Würzburg, den …………………………………………………...

# I.  Summary / Zusammenfassung

# II.  Introduction

## 1.  Autonomic nervous system

## 2.  Adrenergic system

## 3.  $\alpha_2$-adrenergic receptors

## 4.    Project goals

# III.   Methods

## 1.    Generation of $\alpha_2$-deficient mice

## 2.    Basal characterization of $\alpha_{2ABC}$-deficient mice

## 3.    Radioligand binding

# IV.      Materials

# V.  Results

# VI. Discussion

# VII. References

# VIII. Attachments

# I.  Summary / Zusammenfassung

Clonidine is an agonist at $\alpha_2$-adrenergic receptors that mediate a wide variety of the physiological responses to epinephrine and norepinephrine, such as inhibition of neurotransmitter release as well as sedation and analgesia.  As with other therapeutically used $\alpha_2$-agonists such as moxonidine and rilmenidine, clonidine possesses an imidazoline structure and is believed to lower blood pressure not only via central and peripheral $\alpha_2$-receptors, but perhaps even more so by acting on central "imidazoline $I_1$ receptors" in the brain stem.  The molecular structure of these hypothetical "imidazoline $I_1$ receptors" has not yet been identified.  In order to test whether ligands with an imidazoline structure elicit pharmacological effects via $\alpha_2$-adrenergic receptors or via "imidazoline receptors", mice were generated with a targeted deletion of all three $\alpha_2$-adrenergic receptor subtypes ($\alpha_{2ABC}$-KO).  These $\alpha_{2ABC}$-KO mice were an ideal model in which to examine the pharmacological effects of the centrally acting antihypertensives clonidine, moxonidine and rilmenidine in the absence of $\alpha_2$-adrenergic receptors.  As expected, sedative and analgesic actions of clonidine were completely absent in $\alpha_{2ABC}$-KO mice, confirming the sole role of $\alpha_2$-receptors in these properties of clonidine.  Clonidine significantly lowered heart rate in anesthetized $\alpha_{2ABC}$-KO and wild-type mice by up to 150 beats/min.  A similar bradycardic effect of clonidine was observed in isolated spontaneously beating right atria from $\alpha_{2ABC}$-KO mice.  After treatment with the specific $I_f$ inhibitor ZD 7288, clonidine was no longer able to lower spontaneous beating frequency, suggesting a common site of action. Furthermore, in HEK293 cells stably transfected with HCN2 and HCN4, it could be shown that clonidine inhibits the $I_f$ current via blockade of pacemaker channels with similar affinity as in isolated $\alpha_{2ABC}$-KO and wild-type atria.  This inhibition was demonstrated again in isolated sinoatrial node (SAN) cells from $\alpha_{2ABC}$-KO mice and was identical in potency and efficacy to clonidine inhibition observed in isolated wild-type SAN cells, confirming that inhibition of atrial HCN channels constitutes the $\alpha_2$-independent bradycardic action of clonidine. Direct inhibition of cardiac HCN pacemaker channels contributes to the bradycardic effects of clonidine in gene-targeted mice.  Thus clonidine-like drugs represent novel structures for future HCN channel inhibitors.

$\alpha_2$-adrenerge Rezeptoren vermitteln die vielfältigen Wirkungen der endogenen Catecholamine Noradrenalin und Adrenalin, darunter auch eine Hemmung der Noradrenalin-Freisetzung sowie Sedierung und Analgesie. Clonidin und die ebenfalls therapeutisch eingesetzten $\alpha_2$-Agonisten Moxonidin und Rilmenidin besitzen eine Imidazolin-Teilstrukur. Es wird zur Zeit diskutiert, ob die hypotensive Wirkung dieser Arzneimittel nicht nur auf zentrale und periphere $\alpha_2$-Rezeptoren zurückzuführen ist, sondern auch auf sogenannte "$I_1$ Imidazolin-Rezeptoren" in der ventrolateralen Medulla. Bis heute ist die molekulare Struktur dieser hypothetischen Rezeptoren nicht bekannt. Um diese Imidazolin-Hypothese zu überprüfen wurden Mäuse mit einer gezielten Deletion in allen drei $\alpha_2$-Rezeptor Genen generiert ($\alpha_{2ABC}$-KO). Dieses Mausmodell eignete sich hervorragend, um die pharmakologische Wirkung von den zentral-wirksamen Antihypertensiva Clonidin, Moxonidin und Rilmenidin in der völligen Abwesenheit von $\alpha_2$-Rezeptoren zu untersuchen. Wie erwartet fehlten die sedativen und analgetischen Wirkungen des Clonidins bei $\alpha_{2ABC}$-KO Mäusen, wodurch die alleinige Beteiligung von $\alpha_2$-Rezeptoren an diesen Eigenschaften des Clonidins bestätigt wurde. Bei anästhesierten $\alpha_{2ABC}$-KO und Wildtyp-Mäusen zeigte Clonidin eine signifikante Senkung der basalen Herzfrequenz in beiden Genotypen von bis zu 150 Schlägen/min. In ähnlicher Weise setzte Clonidin in isolierten, spontan schlagenden rechten Vorhöfen von $\alpha_{2ABC}$-KO die Schlagfrequenz herab. Nach Vorbehandlung der Vorhöfe mit dem spezifischen $I_f$ Inhibitor ZD 7288 fand keine weitere Senkung der Schlagfrequenz durch Clonidin mehr statt, was auf einen gemeinsamen Wirkort der beiden Substanzen hindeutete. In stabil transfizierten HEK293 Zellen zeigte Clonidin eine Inhibition des $I_f$ Stromes durch Blockade von HCN2- und HCN4-Kanälen mit ähnlicher Potenz wie in den isolierten Vorhöfen. Ebenfalls in isolierten Sinusknoten (SAN) Zellen von $\alpha_{2ABC}$-KO und Wildtyp-Mäusen inhibierte Clonidin den $I_f$ Strom mit gleicher Potenz. Diese Befunde bestätigen, dass die Blockade von atrialen HCN-Kanälen den Mechanismus der $\alpha_2$-unabhängigen, Clonidin-induzierten Bradykardie darstellt. Die direkte Hemmung von kardialen HCN-Schrittmacher-Kanälen trägt wesentlich zur bradykarden Wirkung von Clonidin bei transgenen Mäusen bei. Clonidin-Derivate bilden somit die Basis für die Entwicklung neuer HCN-Kanal-Inhibitoren.

# II. Introduction

## 1. Autonomic nervous system

Although this project examined the effects of $\alpha_2$-adrenergic agonists, their pharmacological targets are by no means exclusively $\alpha_2$-receptors. While $\alpha_2$-mediated effects predominate, it was possible – with the aid of mice deficient in all three $\alpha_2$-receptor subtypes – to identify an additional target of one $\alpha_2$-agonist, clonidine. Therefore, it is appropriate to begin with a broad overview of the nervous system, and then narrow the focus to the level of $\alpha_2$-adrenergic receptors in order to better understand the context in which they function.

### 1.1. Nervous system classification

The nervous system of vertebrate animals can be classified either according to its localization or to its function in the body (figure 1). Anatomically, the nervous system can be divided into a central and a peripheral component. The central nervous system (CNS) contains the brain and spinal cord; the peripheral nervous system (PNS) encompasses the afferent (sensory) and efferent (motor) neurons, transmitting information received from sensory receptors to the central nervous system, as well as coordinating impulses received from the central nervous system and relaying them to effector organs in the periphery.

On a functional level, the peripheral nervous system can be divided into a voluntary, or sensory-somatic, nervous system, as well as an involuntary, or autonomic, nervous system. Both somatic and autonomic nervous systems communicate with the central nervous system via sensory and motor neurons. However, the somatic nervous system is responsible for conveying information received from the external environment to the CNS and responding to the external stimulus, while the autonomic nervous system serves as a regulator of the body's internal environment and is crucial for maintaining life-sustaining bodily functions as well as for adaptation to changing external influences. The autonomic nervous system can be further subdivided into a parasympathetic (1.1.1.) and a sympathetic (1.1.2.) nervous system.
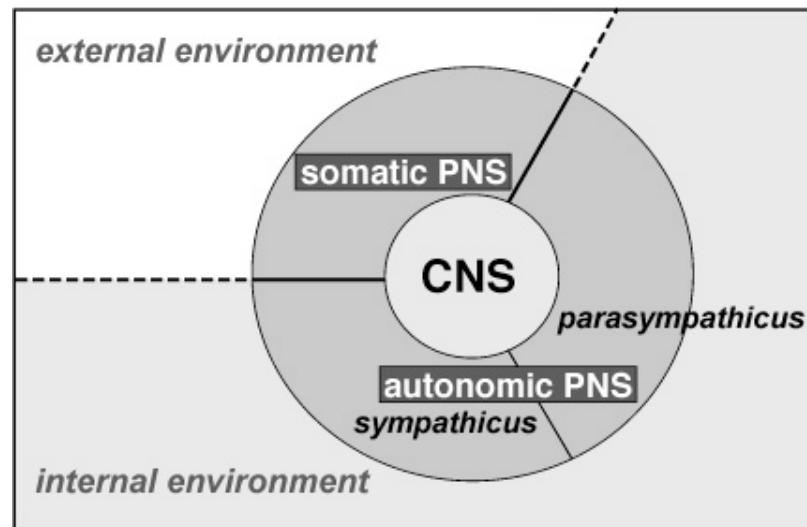
**Fig. 1:** *Scheme depicting the vertebrate nervous system. The interrelation of somatic and autonomic nervous systems, as well as the complex interplay of the sympathicus and parasympathicus within the autonomic nervous system, facilitates the tremendous capabilities of the organism to perceive and respond to an ever-changing external and internal milieu.*

1.1.1. Parasympathetic nervous system

The parasympathetic nervous system is responsible for maintaining the organism in the resting state and, upon stimulation, promotes digestion, lowers heart rate and blood pressure, and upholds the tonus of sphincter muscles of the bladder and bowel. In contrast to the somatic nervous system which only requires one neuron as a link between central and peripheral nervous systems, the parasympathetic nervous system employs a preganglionic neuron originating from either one of the cranial nerves III, VII, IX or X or from the sacral region of the spinal cord in the central nervous system (Hoffman and Taylor, 2001). This neuron synapses with a postganglionic neuron at a ganglion near or in the target organ in the peripheral nervous system. Acetylcholine serves as the neurotransmitter at all preganglionic as well as postganglionic neurons and modulates the parasympathetic nervous system via interactions with muscarinic receptors ($M_1$-$M_5$) at parasympathetic synapses and with nicotinic receptors in the ganglia and at neuromuscular junctions (Dale, 1914; Bonner, 1989).

## 1.1.2. Sympathetic nervous system

The sympathetic nervous system plays an opposing role to that of the parasympathetic nervous system (1.1.1.). Sympathetic stimulation prepares the body for "fight or flight" by redirecting the blood flow away from the gastrointestinal tract and instead to the skeletal muscles, brain and heart. In addition, heart rate and blood pressure increase, and the trachea and bronchi dilate, further allowing the body to better cope with the stressful situation. Like the parasympathetic nervous system, the sympathetic nervous system utilizes a preganglionic as well as a postganglionic neuron to relay information from the central nervous system to the periphery. While acetylcholine is the neurotransmitter at the sympathetic as well as parasympathetic ganglia, norepinephrine (noradrenaline) is unique to the sympathetic nervous system, where it serves as the postganglionic neurotransmitter at the effector organ. In addition, sympathetic stimulation results in a much more generalized signal than parasympathetic stimulation because one preganglionic neuron (located in the T1 to L2 region of the spinal cord) is able to synapse with any number of postganglionic neurons located along the sympathetic chain (paravertebral ganglia) or with a postganglionic neuron located in an effector organ or in the adrenal medulla (Hoffman and Taylor, 2001). Stimulation of adrenal chromaffin cells releases epinephrine (adrenaline) into the blood stream, further activating adrenergic receptors throughout the body. Adrenergic receptors are discussed in detail in chapter 2.

## 1.2. Regulation of blood pressure and heart rate

Although adrenergic regulation of the cardiovascular system is discussed later in the Introduction (2.3.1.), the regulation of blood pressure and heart rate is far more complex and requires both parasympathetic and sympathetic input. The heart rate is influenced by the nervous system; however, the frequency of the beating heart is generated within the heart itself, allowing the heart to beat autonomously. Cardiac pacemaker (HCN) channels are crucial to the spontaneous generation of the beating impulse and will be discussed in depth here (1.2.2.). During this project, the HCN channel was identified as a pharmacological target of the $\alpha_2$-agonist clonidine.

1.2.1. Blood pressure

Cardiovascular tone is regulated on both a short-term and on a long-term basis through a number of reflex pathways. Afferent pathways relay information from pressor receptors (baroreceptors) in both arterial walls and the heart. The body is able to quickly respond to deviations in blood pressure from a given norm ("set point") by means of arterial baroreceptors located on the aortic arch and the carotid sinus that register stretch (changes in vessel diameter). Action potentials are generated according to the degree of stretch, and these impulses are relayed from the arterial baroreceptors to the central nervous system where they terminate in the nucleus of the tractus solitarius (NTS). Stimulation of this region in the brain stem elicits a bradycardic vagal response in no more than 0.5 s (Levick, 1998). Baroreceptor activation not only exerts a parasympathomimetic effect; the activated NTS also represses sympathetic tone, with both effects leading to a rapid decrease in heart rate, contractility and therefore cardiac output. As a result, blood pressure decreases. In contrast, an increase in blood pressure occurs indirectly and somewhat more slowly (after circa 1.5 s), as the unstimulated baroreceptor and consequent decrease in vagal activity no longer inhibit sympathetic tone (Levick, 1998).

1.2.2. Heart rate

Although the frequency of the beating heart is modified by both sympathetic and parasympathetic nervous systems in response to external and internal stimuli, the heart beats autonomously. The electrical impulses leading to depolarization of the working myocardium originate within the heart itself, following a hierarchical arrangement of pacemaker regions, each characterized by its own rate of spontaneous depolarization. Under physiological conditions, the sinus node, a small bundle of cells located near the superior vena cava in the back of the right atrium, determines the frequency of the beating heart. The sinus node, also known as the cardiac pacemaker, possesses an unstable resting potential and depolarizes spontaneously approximately once every second in the human heart (Levick, 1998). The depolarization wave passes through the atrium to the ventricle via the atrioventricular node (AV-node), where its velocity is greatly reduced, allowing the atria adequate time to contract before the ventricles are stimulated. Immediately following the AV-node, the electrical impulse enters the ventricle via the His bundle. The long strands of the His bundle are

composed of electrically connected myocytes (also known as Purkinje fibers); these conduct the electrical impulse rapidly along the septum wall and distribute it to the entire ventricle wall, allowing a nearly simultaneous contraction of each ventricle (Levick, 1998). When one of the pacemaker centers is impaired, the next lower center can take over and maintain the beating of the heart, albeit at a lower heart rate. Patients suffering from AV-block generally require a cardiac pacemaker, as the heart rate originating from the His-bundle (approximately 40 beats per minute) in this condition is too low for most activities (Levick, 1998).

Within the sinus node, several different ion currents contribute to the maintenance of pacemaker activity. At the beginning of each new impulse, the membrane potential of the sinus node cell slowly decreases (in humans) from -60 mV to -40 mV (Levick, 1998). This slow decrease, also known as the pacemaker potential, is due in large part to activation of the "pacemaker" or $I_f$ current, characterized by an increased membrane permeability for (mostly) $Na^+$ ions, thereby making the intracellular membrane potential more positive (Baruscotti and DiFrancesco, 2004). Hyperpolarization activated, cyclic nucleotide-gated cation (HCN) channels provide the basis for this current. To date, four isoforms (HCN1, HCN2, HCN3 and HCN4) have been cloned (Stieber et al., 2004), although HCN4 appears to dominate in the sinoatrial node cells of all mammals studied (Ishii et al., 1999). While the membrane potential becomes less negative, the membrane permeability for $K^+$ ions decreases as well, prohibiting a repolarization of the cell. As the membrane potential approaches -40mV, voltage-gated L-type $Ca^{2+}$ channels are activated; the inward flow of $Ca^{2+}$ contributes to the last third of the pacemaker potential and "pushes" it over the threshold potential of -40 mV, thereby inducing the next action potential. $Ca^{2+}$ influx prolongs the duration of the action potential. Unlike the action potential of the working myocytes (characterized by a stable membrane potential) and of nerve cells, both sinus node and AV-node cells lack a fast $Na^+$ current, which is evident by the missing spike at the beginning of the action potential. During the action potential, delayed rectifier $K^+$ channels activate to slowly induce repolarization. Other ion channels, particularly $K^+$ channel subtypes, play a lesser contribution to the maintenance of pacemaker activity (for a comprehensive review see Satoh, 2003).

## 2. Adrenergic system

### 2.1. Historical aspects of adrenergic receptors

The concept of a "receptor" as the site of drug action emerged slowly during the late nineteenth and early twentieth centuries. The delineation of the paralyzing action of curare by Claude Bernard (1844) aroused the idea of a specific interaction between drug and physiological target (Bennett, 2000). Bernard demonstrated in a curarized frog that, while direct electrical stimulation of a motor neuron failed to elicit a response, stimulation of the muscle nevertheless lead to a contraction. These results were later interpreted by E. Vulpian, suggesting that curare acts on some intermediate zone between nerve and muscle (Vulpian, 1866). However, it was first John Langley whose experiments with agonists and antagonists of the autonomic nervous system and later the neuromuscular junction lead him to correctly deduce the presence of a "receptive substance" (Langley, 1905). Around this time, Paul Ehrlich had envisioned his own "receptor" independent of Langley. In 1885, Ehrlich first described his "side chain theory" of cellular action in his thesis to the University of Leipzig. Ehrlich proposed that a particular toxin could bind specifically to a certain side chain and become neutralized. While this did provide an insightful view of the immune system, it wasn't until several years later that Ehrlich expanded his theory to include pharmacological substances (Ehrlich, 1900). Ehrlich later went on to introduce the concept of a "chemoreceptor" (Ehrlich, 1914).

Around this time, many researchers became interested in acetylcholine and its nearly identical effects in vivo as those following parasympathetic stimulation (Hunt and Taveau, 1906; Dixon, 1906). However, it wasn't until 1926 that Loewi and Navratil unequivocally demonstrated that acetylcholine was indeed the neurotransmitter at the autonomic neuromuscular junction (Hoffman and Taylor, 2001). Despite the early report from Cannon and Uridil (1921) that a stimulatory counterpart to acetylcholine was released in postganglionic synapses after sympathetic stimulation of the effector organ, it took another two decades for Ulf von Euler to identify this adrenaline-like neurotransmitter as noradrenaline (Hoffman and Taylor, 2001). Following this discovery, understanding of the adrenergic receptors grew rapidly. In 1948, R. Ahlquist proposed that two subtypes of adrenergic receptors, $\alpha$ und $\beta$, mediate the physiological responses of the body to epinephrine and norepinephrine (Black, 1976). This, together with the growing knowledge of the detrimental effects of

17

epinephrine, led Sir James Black to develop a new class of drugs, the β-blockers, during the early 1960s (Black and Stephenson, 1962). Finally, beginning with the first cloning of an adrenergic receptor (Kobilka et al., 1987), it became gradually clear that all adrenergic receptors represent G protein coupled receptors (chapter 2.4.). Soon thereafter, the human $\alpha_2$-subtypes $\alpha_{2A}$, $\alpha_{2B}$ and $\alpha_{2C}$ were identified and characterized (Kobilka et al., 1987; Weinshank et al., 1990; Regan et al., 1988).

2.2.    Receptor subtypes of the adrenergic system

## adrenergic receptors
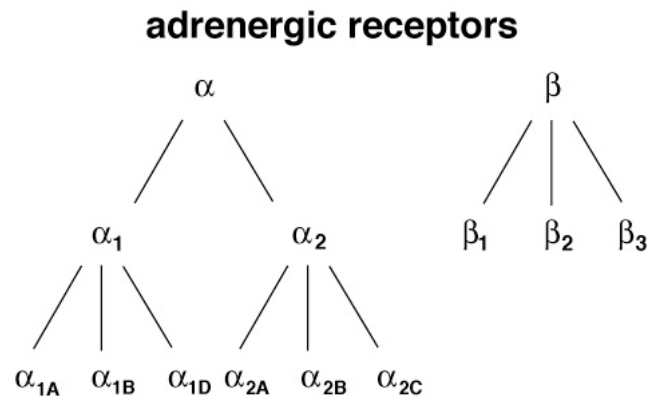


**Fig. 2:  *Adrenergic receptor families.*** *$\alpha$- and $\beta$-adrenergic receptors are categorized into three families $\alpha_1$, $\alpha_2$ and $\beta$, which can themselves be divided into three subtypes each.*

The sympathetic nervous system imparts its effects on the body via the sympathetic postganglionic neurotransmitter, norepinephrine, and via the endogenous hormone epinephrine, produced by and released from the adrenal glands. While epinephrine conveys a global signal by traveling throughout the body, norepinephrine evokes a much more local signal confined to the area near the presynaptic vesicles from which it was released. The adrenergic system consists of three receptor groups – $\alpha_1$-, $\alpha_2$- and $\beta$-adrenergic receptors (figure 2). Each of these three families can be divided into three receptor subtypes: $\alpha_{1A}$, $\alpha_{1B}$, $\alpha_{1D}$; $\alpha_{2A}$, $\alpha_{2B}$, $\alpha_{2C}$ and $\beta_1$, $\beta_2$ and $\beta_3$ (Bylund et al., 1994) Although the subtypes of a given family show many similarities, they tend to display characteristic distribution throughout different organs and different tissues. They may also differ in part in their intracellular localization, as in the case of $\alpha_2$-adrenergic receptors (chapter 3.2.). Another distinctive feature of the adrenergic receptor subtypes lies in their interactions

18

with norepinephrine and epinephrine. The two endogenous ligands act on the adrenergic receptor subtypes with different affinities (Hoffman, 2001).

### 2.3. Role of adrenergic receptors in the sympathetic nervous system

Adrenergic receptors mediate the wide range of physiological responses to norepinephrine and epinephrine in vivo. The three families of adrenergic receptors each contain three receptor subtypes with varying affinities for norepinephrine and epinephrine. This, together with their heterogeneous distribution at both organ as well as cellular levels, facilitates their great pharmacological diversity. Only the adrenergic moderation of the cardiovascular system and metabolism will be discussed here, as these were covered in the scope of this project.

### 2.3.1. Cardiovascular system

The sympathetic nervous system is best characterized for its role in the modulation of heart rate and blood pressure. Indeed, all three families of adrenergic receptors, $\alpha_1$, $\alpha_2$ and $\beta$, represent popular pharmacological targets for antihypertensive drugs. Activation of $\alpha_1$-receptors normally elicits a vasoconstrictor response in vascular smooth muscle cells. Although all three $\alpha_1$-subtypes have been shown to be present in the endothelium (Miller et al., 1996), $\alpha_{1A}$ and $\alpha_{1D}$ appear to mediate smooth muscle contraction in most arteries in response to $\alpha_1$-adrenergic agonists (Guimaraes and Moura, 2001).

Presynaptic $\alpha_2$-receptors are located both centrally – $\alpha_{2A}$- and $\alpha_{2C}$- subtypes – and peripherally – $\alpha_{2A}$, $\alpha_{2B}$ and $\alpha_{2C}$ – (Hein et al., 1999; Trendelenburg et al., 2003); as regulators of sympathetic activity, $\alpha_2$-autoreceptors indirectly influence blood pressure and heart rate. $\alpha_2$-agonists such as clonidine are therefore well-established antihypertensives, although some of these agonists find other uses as well. Endothelial $\alpha_2$-receptors promote the release of endothelium-derived relaxing factor (NO) in some blood vessels (Vanhoutte, 2001). Interestingly, the $\alpha_{2B}$-subtype exhibits a vasoconstriction in the smooth muscle cells of veins and arteries similar to that of the $\alpha_1$-subtypes (Link et al., 1996). This effect is clearly demonstrated after iv bolus injection of an $\alpha_2$-agonist by an initial increase in blood pressure, which gradually decreases to below baseline level several minutes later. However, this brief hypertension after $\alpha_2$-agonist administration is not observed when the drug is taken perorally. $\alpha_2$-receptors in the kidney also regulate blood pressure by

influencing the reuptake of salt and water at various locations in the tubule and collecting duct (Wallace et al., 2004).

The family of $\beta$-receptors contains three subtypes $\beta_1$, $\beta_2$ and $\beta_3$, and both $\beta_1$- and $\beta_2$-subtypes play key roles in sympathetic regulation of the cardiovascular system. Stimulation of $\beta_2$-receptors promotes vasodilation, not only via relaxation of vascular smooth muscle cells, but also indirectly by increasing the activity of endothelial-type nitric oxide synthase (Ferro et al., 2004). Sympathetic activation of $\beta_1$-receptors in the heart elicits positive inotropic and positive chronotropic effects, allowing a greater volume of blood to flow through the body per unit of time, providing more oxygen and a more rapid removal of metabolic wastes. At the same time, $\beta_1$-receptors in the vasculature also contribute to the dilative effect of mixed $\beta_1$- / $\beta_2$-agonists, albeit to a much lesser extent than $\beta_2$-receptors (Chruscinski et al., 1999).

## 2.3.2. Metabolism

In the resting state, there is little sympathetic intervention into metabolic processes; this is the role of the parasympathetic nervous system. In contrast, activation of the sympathetic nervous system has a tremendous effect on metabolic processes. Glucose is needed to prepare the organism for "fight or flight", and this sudden increase of available glucose in the bloodstream comes from glycogenolysis of glucose stores largely in the liver and skeletal muscle, followed by glycolysis. Overall energy requirements are elevated, and lipolysis also increases to meet these demands. $\alpha_1$-receptor stimulation raises blood glucose levels by promoting glycogenolysis as well as gluconeogenesis. Activation of $\alpha_2$-receptors in the $\beta$-cells of the pancreas inhibits the $Ca^{2+}$-induced exocytotic release of insulin via $G_o$-mediated inhibition of voltage activated $Ca^{2+}$ channels (Wozniak et al., 1995). This acute hyperglycemic response should not be confused with the long-term beneficial effect on blood glucose levels observed with $\alpha_2$-agonists such as moxonidine (Jacob et al., 2004). Both $\beta_2$- and $\beta_3$-receptor subtypes stimulate insulin release, while the $\beta_2$-subtype additionally promotes glucose synthesis.

## 2.4. G protein coupled receptors

The adrenergic receptors belong to the superfamily of G protein coupled receptors (GPCRs). GPCRs, which comprise the majority of all receptors, represent seven-transmembrane proteins with an extracellular N-terminus and

an intracellular C-terminus. Ligand binding occurs typically inside the transmembrane region; only for large ligands such as peptides do extracellular domains play a role in receptor specificity (Krauss, 1997). GPCR ligands include hydrophilic hormones such as gonadotropin, glucagon and parathyroid hormone, as well as most neurotransmitters, including norepinephrine (Dohlman et al., 1991). It is therefore not surprising that a great number of pharmaceuticals target GPCRs, either as agonists or antagonists. The great prevalence of GPCRs in mammals is very likely due to the almost innumerable signaling possibilities after receptor activation; this, in turn, is accomplished by the many possible combinations of different subunit isoforms in heterotrimeric G proteins, as well as by the specificity of the receptor / G protein interaction (Neer, 1995).

Upon ligand binding, the activated receptor undergoes a conformational change (Fig. 3, $1^{st}$ step). A nearby G protein, consisting of an $\alpha$ subunit bound in its inactive state to guanosine diphosphate (GDP) and associated $\beta$ and $\gamma$ subunits, binds to the activated receptor, thereby undergoing a conformational change itself. The $\alpha$ subunit, having lost its high affinity to GDP, releases this and quickly binds a molecule of guanosine triphosphate (GTP). GTP binding allows a dissociation of the now active $\alpha$ subunit from the $\beta\gamma$ complex (Fig. 3, $2^{nd}$ step). At the same time, the active $\alpha$ subunit is released from the receptor complex, leaving the receptor to either react with further G proteins or to become inactive via phosphorylation or by binding of arrestins (Krauss, 1997). Now both $\alpha$ and $\beta\gamma$ subunits are free to interact with effector proteins, leading to different signaling cascades in the cell (Fig. 3, $3^{rd}$ step).

Effectors are, depending on the G protein subtype, either stimulated or inhibited by the $\alpha$ and $\beta\gamma$ subunits. In the case of $G_s$ proteins which are activated by the family of $\beta$-adrenergic receptors, the effector adenylyl cyclase (AC) is stimulated by $G_{\alpha s}$, resulting in an increased production of the second messenger cyclic adenosine monophosphate (cAMP). This in turn leads to activation of different signaling pathways in the cell (Ross and Gilman, 1977; Gilman, 1987). On the other hand, $G_{\alpha i}$, the $\alpha$ subunit of the inhibitory $G_{i/o}$ protein subfamily stimulated by $\alpha_2$-adrenergic receptors, represses the activity of the AC, resulting in a decrease of second messenger cAMP. The $G_{i/o}$ protein $\beta\gamma$ subunits facilitate opening of G protein-activated inwardly rectifying $K^+$ (GIRK) channels and inhibit N-type $Ca^{2+}$ channels (Bünemann et al., 2001; Starke, 2001). Another G protein subfamily, $G_q$, activates phospholipase C$\beta$, which in turn liberates the second messengers diacylglycerol and inositol-1,4,5

triphosphate; this subfamily binds to $\alpha_1$-adrenergic receptors upon activation. Thromboxane receptors may activate the fourth G protein subfamily $G_{12}$.
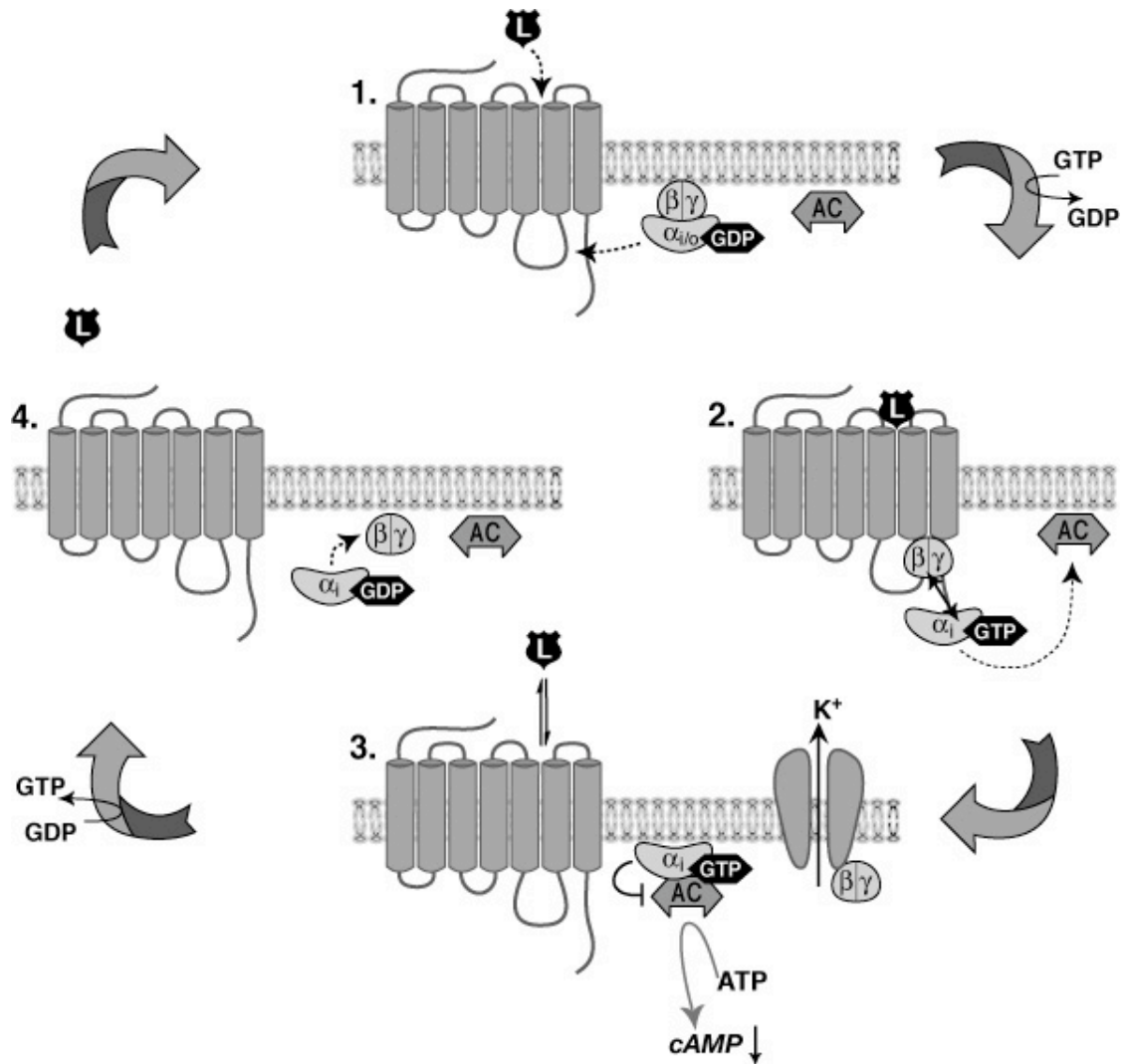


**Fig. 3:** *G protein activation cycle as exemplified by the $\alpha_2$-adrenergic receptor.* *Ligand (L) binding to the $G_i$-coupled receptor induces a conformational change that facilitates binding of a nearby G protein. The G protein similarly undergoes a change in conformation, prompting an exchange of GDP for GTP in the G$\alpha$ subunit (1.). The active G$\alpha$ subunit dissociates from the $\beta\gamma$ complex, allowing each to interact with nearby effector molecules (2.). The $\alpha_2$-receptor recruits an inhibitory $G_i$ protein whose $G\alpha_i$ subunit inhibits adenylyl cyclase (AC). The inhibitory $\beta\gamma$ complex interacts with several partners including GIRK ($K^+$) channels (3.). The intrinsic GTPase capacity of*

*the Gα subunit prompts hydrolysis of GTP to GDP, permitting reassociation of Gα and Gβγ subunits, thereby terminating G protein signaling (4.).*

The active Gα-GTP subunit is endowed with an intrinsic GTPase activity, ensuring a limited signaling capacity of the G protein. Through hydrolysis of GTP to GDP, the αsubunit reacquires its inactive conformation and reassociates with the βγ subunit, thus terminating the further interaction with effector proteins (Fig. 3, 4th step). The length of activation time is dependent on the G protein as well as on other regulatory proteins (e.g. RGS proteins). In addition, proteins may either shorten (GTPase activating proteins, GAP) or lengthen (guanine nucleotide exchange factor, GEF) the duration of the G protein signal. Through such modulation, as well as through various combinations of the 20 α, 5 βand 12 γ subunits, a fine-tuned, individual regulation of numerous physiological processes is achieved.

## 3.    $\alpha_2$-adrenergic receptors

Negative feedback regulation of sympathetic activity by autoinhibitory $\alpha_2$-receptors is crucial in regulating norepinephrine release and maintaining normal levels of plasma catecholamines. Postsynaptic $\alpha_2$-receptors are found throughout the body, where they play highly diversified roles (3.4.2.). Often, however, it is difficult to associate a specific physiological process with a certain $\alpha_2$-receptor subtype due to high similarities in signaling, (sub)cellular localization and tissue distribution.

### 3.1.    Signal transduction of $\alpha_2$-adrenergic receptors

### 3.1.1. Interaction with inhibitory $G_{i/o}$ proteins

All three $\alpha_2$-receptor subtypes belong to the large family of transmembrane G protein coupled receptors and couple mainly to inhibitory $G_{i/o}$ proteins. As previously described in chapter 2.4., dissociation of the heterotrimeric G protein following $\alpha_2$-receptor activation and G protein binding allows the free α and βγ subunits to interact with a number of downstream partners (Neer, 1995). Although a number of α, β and γ subunit isoforms have been cloned, it has been recently demonstrated, using fluorescence resonance energy transfer (FRET)-labeled $G_i\alpha$ and Gβγ subunit isoforms activated by $\alpha_2$-receptors in HeLa cells, that not the individual α and β isoforms but rather the combination of Gα and Gβγ isoforms determines the degree of G protein

23

activation (Gibson and Gilman, 2006). The $G\alpha_i$ subunit, and perhaps the $G\alpha_o$ subunit as well, inhibits the activity of adenylyl cyclase (AC), thus decreasing the amount of intracellular cyclic AMP (cAMP) and inhibiting cAMP-mediated downstream signaling (Duman and Nestler, 1995). The inhibitory $G\beta\gamma$ subunit both stimulates inward-rectifier $K^+$ (GIRK) channels as well as inhibits voltage-gated $Ca^{2+}$ channels, resulting in a hyperpolarization of the cell membrane. This dual role is played by $\beta\gamma$ dimers from both $G_i$ and $G_o$ proteins, although each G protein subtype may uniquely contribute to these effects (Duman and Nestler, 1995). In rat sympathetic neurons, $G\alpha_o$-associated $\beta\gamma$ subunits effected voltage-dependently the norepinephrine-mediated inhibition of N-type $Ca^{2+}$ channels, while the inhibition resulting from $\beta\gamma$ subunits associated with $G\alpha_i$ was voltage-independent (Delmas et al., 1999). This $G\alpha_{i/o}\beta\gamma$-mediated inhibition of $Ca^{2+}$ channels appears fundamental in the autoinhibition of presynaptic $\alpha_2$-receptors (Stephens and Mochida, 2005). It has even been demonstrated that free $G\beta\gamma$ subunits inhibit some forms of AC (types I, III and VIII), while contrarily they stimulate other AC forms (II and IV) in vitro (Duman and Nestler, 1995).
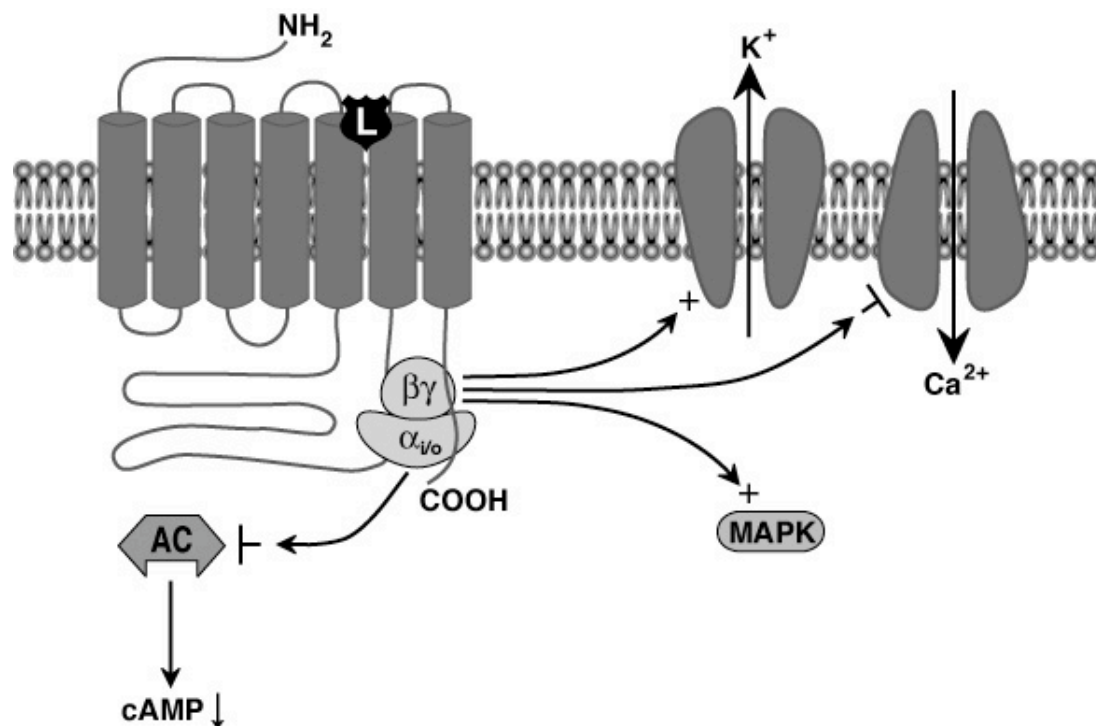


**Fig. 4:** ***$G_{i/o}$ protein mediated signal transduction of $\alpha_2$-adrenergic receptors.*** *The ligand (**L**)-bound receptor assumes a new conformation preferable to $G_{i/o}$ protein binding, triggering a cascade of events resulting in*

*either the activation or inhibition of effector proteins (here adenylyl cyclase, GIRK and N-type $Ca^{2+}$ channels) by the liberated $G\alpha_{i/o}$ and $G\beta\gamma$ subunits.*

### 3.1.2. Activation of mitogen-activated protein kinase (MAPK) cascade

Aside from the direct downstream signaling pathway of $G_{i/o}$ proteins (inhibition of AC, GIRK channel stimulation, $Ca^{2+}$ channel blockade), G protein stimulation elicits additional downstream effects as well. The ability of free $G\alpha_{i/o}$ and $G\beta\gamma$ subunits following $\alpha_2$-adrenergic activation to interact with downstream effectors of various growth hormone receptors (tyrosine kinase receptors) is well documented and illustrates again the wide diversity of $\alpha_2$-receptors in a multitude of physiological processes including indirect mediation of cell growth and proliferation (Duman and Nestler, 1995). Many circulating hormones such as insulin and other growth factors mediate their physiological effects via activation of complementary growth factor receptors. Hormone binding precipitates dimerization of two adjacent transmembrane receptors, triggering a cascade of phosphorylation of both receptor (autophosphorylation) and of downstream target proteins (Duman and Nestler, 1995). These events lead to the activation of a family of serine / threonine kinases, or MAP-kinases (mitogen-activated protein kinases), which translate the extracellular stimulus into a resulting change in transcription of the target gene(s) and ultimately into changes in cell growth and differentiation (Cano and Mahadevan, 1995). MAP-kinases can be divided into the subfamilies of extracellular signal regulated kinases (ERK1/2 and ERK5), stress-activated protein kinases (SAPK, synonymous with c-jun N-terminus kinases or JNK) and p38 kinase (Lopez-Ilasaca, 1998). Each subfamily displays a unique signal transduction pathway, as depicted in figure 5.

25
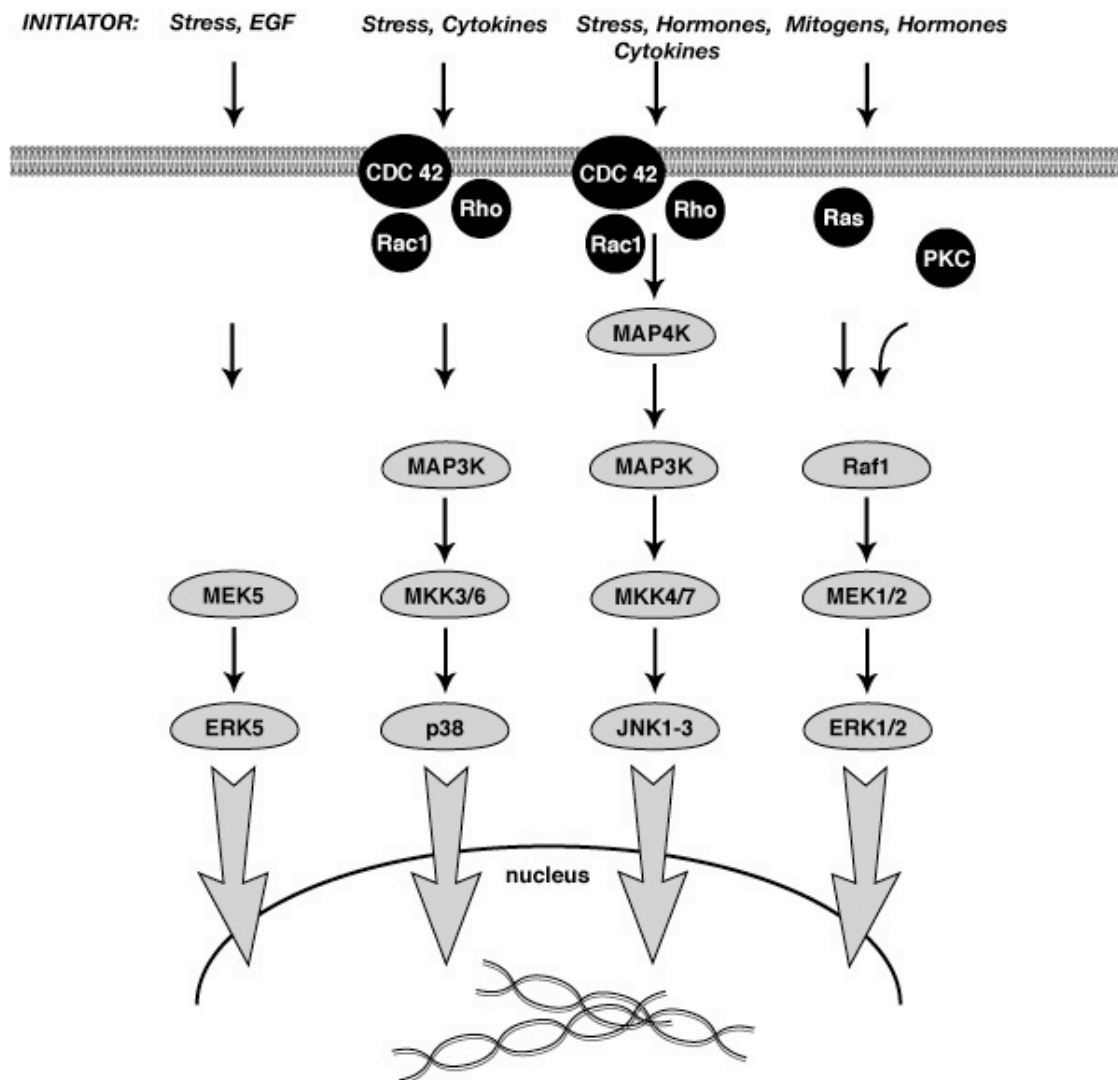
**Fig. 5:** *The four subfamilies of MAP-kinases: ERK5, p38, JNK1-3 and ERK1/2.* *The MAPK cascades can be further grouped into the stress-activated (ERK5, p38 and JNK1-3) or growth hormone-activated (ERK1/2) pathways. Each pathway, though comprised of different members, shares a similar stimulus which is transmitted via successive phosphorylation (and activation) of cascade members down the four-tiered signaling pathway. The original stimulus is then converted into a nuclear signal, prompting the transcription of genes regulating cell growth and differentiation (modified after Seger et al., 2000).*

26

These complex signaling cascades offer many potential partners with which free $G\alpha_{i/o}$ and $G\beta\gamma$ subunits can interact. Indeed, though the exact mechanisms are long from being clearly established, there has been much experimental evidence generated for the $\alpha_2$-adrenergic-stimulated, $G\beta\gamma$-mediated activation of Rho (Roberts, 2004), epidermal growth factor (EGF) receptor (Pierce et al., 2001; Cussac et al., 2002), Pyk2 (Della Rocca et al., 1997), Src (Pierce et al, 2000), Shc (Cussac et al., 2002), PLC with subsequent activation of Ras-dependent ERK1/2 (Della Rocca et al, 1997), and MEK (Kribben et al., 1997; Taraviras et al., 2002), to name but a few examples. Another proposed pathway of ERK1/2 activation, documented for both $\alpha_{2A}$- and $\alpha_{2B}$-subtypes in certain cell types, is the $\alpha_2$-agonist-mediated transactivation of EGF-receptors as shown in figure 6 (Cussac et al., 2002; Daub et al., 1996; Prenzel et al., 1999). This transactivation process was similarly demonstrated in the mouse placenta, and is believed to provide a mechanism for the involvement of the $\alpha_{2B}$-subtype in vascularization of the placenta during early embryonic development (Philipp et al., 2002c).
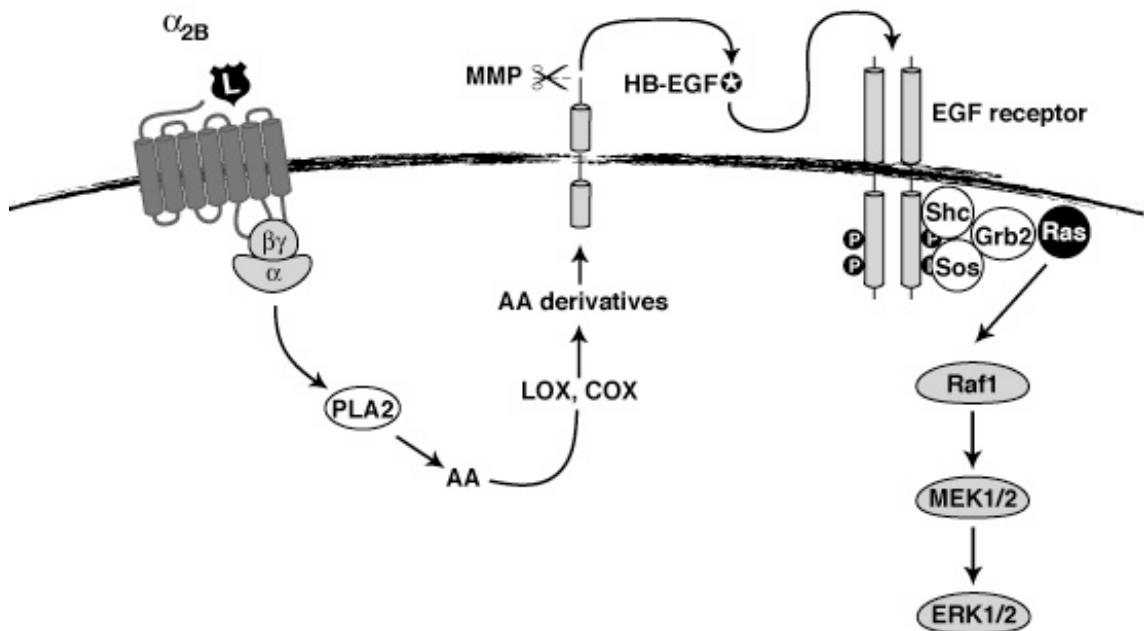


**Fig. 6: $\alpha_2$-adrenoceptor-mediated activation of MAPK cascade.** *A proposed mechanism of ERK1/2 activation by the $\alpha_{2B}$-adrenergic receptor via transactivation (modified after Cussac et al., 2002) is depicted above. Following $\alpha_2$-agonist binding and subsequent $G_i$ protein activation, $G_i\beta\gamma$ subunits appear to increase production of arachidonic acid (AA) via stimulation*

*of phospholipase $A_2$ (PLA2). Cytoplasmic lipoxygenase (LOX) and cyclooxygenase (COX) convert AA into metabolites which stimulate matrix metalloproteinases (MMP) to cleave heparin-binding EGF-like growth factor (HB-EGF) from its transmembrane receptor. HB-EGF binds to the EGF receptor, inducing autophosphorylation of the tyrosine kinase receptor and recruiting the adaptor protein Shc, which then interacts with the Grb2-Sos complex. Sos, a guanine nucleotide exchange factor for Ras, activates this, thereby initiating the ERK1/2 MAPK-signaling cascade (Lotti et al., 1996).*

## 3.2.    Subtype-specific cellular localization

Despite the high degree of amino acid homology within the transmembrane regions of the three $\alpha_2$-adrenergic receptor subtypes, each subtype exhibits a unique pattern of cellular distribution. Characteristic of transmembrane G protein coupled receptors, both $\alpha_{2A}$- and $\alpha_{2B}$-subtypes are located primarily at the cell membrane under basal conditions (figure 7). In contrast, the $\alpha_{2C}$-subtype is found to a large extent in intracellular compartments (endoplasmic reticulum and cis / medial Golgi compartments) in many cell types (Daunt et al., 1997; Saunders and Limbird, 1999). Neither the molecular basis for nor the (possible) significance of this deviant location of the $\alpha_{2C}$-subtype is known at present, although the growing concept of "microdomains", in which reaction partners of a signaling cascade may preferentially interact, may offer an attractive explanation (Neer and Clapham, 1988). Indeed, $\alpha_{2C}$-receptors in PC-12 cells, a neuroendocrine-derived cell line, were observed to be concentrated in the cell membrane of neurite outgrowths, suggesting a cell-type specific targeting of the $\alpha_{2C}$-subtype in this cell line (Hurt et al., 2000).

Furthermore, all $\alpha_2$-subtypes differ in the extent of desensitization and internalization following receptor activation. In transfected CHO cells, $\alpha_{2A}$- and $\alpha_{2B}$-receptor subtypes underwent desensitization following 30 minutes exposure to epinephrine, while the $\alpha_{2C}$-subtype did not (Eason and Liggett, 1992). Differences in the amino acid sequences of the third intracellular loop, a highly heterogeneous region between the subtypes, appeared to dictate the degree of phosphorylation by $\beta$-adrenergic receptor kinase ($\beta$ARK) and therefore receptor desensitization (Jewell-Motz and Liggett, 1996). Following agonist exposure in transfected HEK293 cells, the $\alpha_{2B}$- but not $\alpha_{2A}$-subtype internalized and appeared to be sequestered in the same endosomes as the $\beta_2$-adrenergic receptor, suggesting a common mechanism (Daunt et al., 1997). The authors found evidence of agonist-induced internalization of the $\alpha_{2C}$-

subtype as well, although internalization of the small percentage of surface $\alpha_{2C}$-receptors was initially obscured by the high background of intracellular $\alpha_{2C}$-receptors (Daunt et al., 1997).
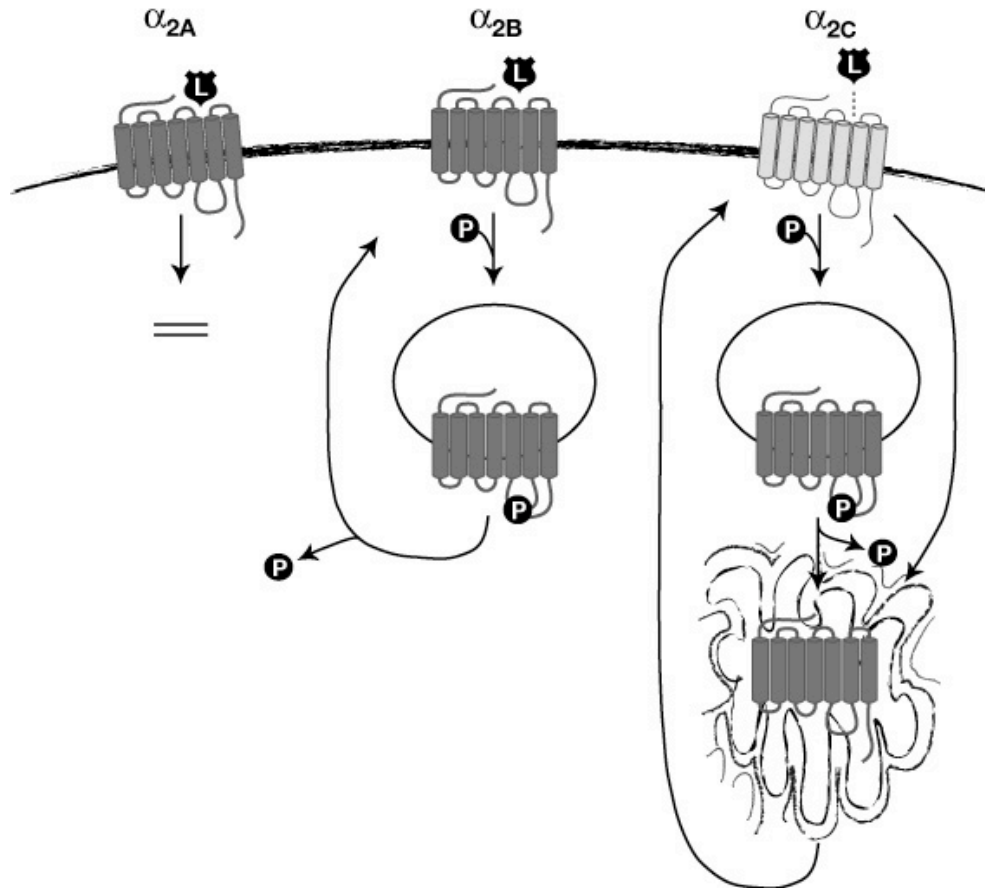


**Fig. 7:** *Differences in $\alpha_2$-receptor subtype subcellular localization and trafficking.* *As G protein coupled receptors, all three $\alpha_2$-subtypes are located at the cell membrane; however, the $\alpha_{2C}$-subtype has also been found in intracellular compartments in many cell types. Following receptor activation, the $\alpha_{2B}$- and to a lesser degree the $\alpha_{2C}$-subtypes, but not $\alpha_{2A}$, internalize and are recycled to the plasma membrane.*

In polarized cultured Madin-Darby canine kidney II (MDCKII) cells, a similar pattern of $\alpha_2$-receptor subtype subcellular localization was observed as described above (Saunders and Limbird, 1999). While all three subtypes were detected nearly exclusively at the basolateral membrane (excluding the intracellular pool of $\alpha_{2C}$-receptors), the authors observed that only the $\alpha_{2A}$- and $\alpha_{2C}$-receptor subtypes were directly delivered to this membrane. In contrast,

29

the $\alpha_{2B}$-subtype was randomly delivered to either the basolateral or the apical membrane; merely the short duration of the $\alpha_{2B}$-receptor on the apical membrane (half-life 0.25-0.5 h) compared to the long half-life (12 h) at the basolateral membrane surface gave the appearance of a true targeting, as was the case with the $\alpha_{2A}$- and $\alpha_{2C}$-receptor subtypes. Post-translational receptor modifications, e.g. palmitoylation and glycosylation, have not been found to influence either receptor trafficking or subcellular localization of the $\alpha_{2A}$-subtype (Saunders and Limbird, 1999), and deletion of the third intracellular loop was likewise without effect on trafficking of the $\alpha_{2A}$-subtype to the MDCK cell membrane (Keefer et al., 1994).

## 3.3. Tissue distribution of $\alpha_2$-receptor subtypes

As implied by the vast array of physiological processes mediated exclusively or partially by catecholamines, $\alpha_2$-adrenergic receptors are widely distributed throughout the entire organism. The role of central presynaptic regulator of norepinephrine release suggests a high density of $\alpha_2$-receptors in the brain (figure 8). This is indeed the case; mRNA for $\alpha_{2A}$-receptors, the predominant presynaptic inhibitor both centrally as well as in the periphery, was located abundantly in the locus ceruleus, but also found in the cerebral cortex, septum, hypothalamus, hippocampus, amygdala and the nucleus tractus solitarius (NTS) and rostral ventrolateral medulla (RVLM) regions of the brain stem in rat brain (Nicholas et al., 1993; Scheinin et al., 1994). The $\alpha_{2C}$-subtype, playing a subordinate role in presynaptic inhibition, displayed a unique pattern of mRNA expression primarily in cerebral cortex, hippocampus, olfactory bulb and basal ganglia in rat brain (Scheinin et al., 1994). Immunohistochemical studies affirmed the location of the corresponding $\alpha_{2A}$- and $\alpha_{2C}$-receptor proteins (Talley et al., 1996; Rosin et al., 1996). In contrast, mRNA for the $\alpha_{2B}$-subtype in rat brain was found in modest amounts exclusively in the thalamus (Nicholas et al., 1993; Scheinin et al., 1994).

In peripheral tissues, pharmacological and radioligand binding studies have shown a heterogeneous distribution of $\alpha_2$-receptor subtypes as well. In contrast to central regulation of norepinephrine release, all three $\alpha_2$-receptor subtypes contribute to presynaptic autoinhibition in the periphery, as demonstrated in the atria and vas deferens of $\alpha_{2AC}$-KO mice (Trendelenburg et al., 2003). The $\alpha_{2B}$-subtype appears to mediate contraction of vascular smooth muscle cells, as this response to $\alpha_2$-agonist stimulation was absent in mice lacking the $\alpha_{2B}$-subtype (Link et al., 1996). However, there is evidence

that the $\alpha_{2A}$-subtype may contribute to this effect as well (Philipp et al., 2002a). Platelets contain the $\alpha_{2A}$-subtype, which was originally cloned from this source (Kobilka et al., 1987). The kidney is also rich in $\alpha_2$-receptors. mRNA of the $\alpha_{2B}$-subtype was concentrated in the kidney (Nicholas et al., 1993), and immunoblotting identified both $\alpha_{2A}$- and $\alpha_{2B}$-subtypes in human medullary collecting duct cells (Wallace et al., 2004). While mRNA of all three $\alpha_2$-subtypes was detected in the adrenal medulla (Takeda et al., 2001), it has been clearly demonstrated that the $\alpha_{2C}$-subtype is the sole regulator of epinephrine release from chromaffin cells (Brede et al., 2003). Both $\alpha_{2A}$- and $\alpha_{2C}$-subtypes are located in the $\beta$-cells of the pancreas and appear to independently support the acute hyperglycemic response to sympathetic activation (Peterhoff et al., 2003). $\alpha_2$-receptors have also been found in lung, submandibular and salivary glands (Bylund and Martinez, 1981 and 1980), liver (Lomasney et al., 1990), ileum (Chang et al., 1982), spleen and stomach (Saunders and Limbird, 1999).
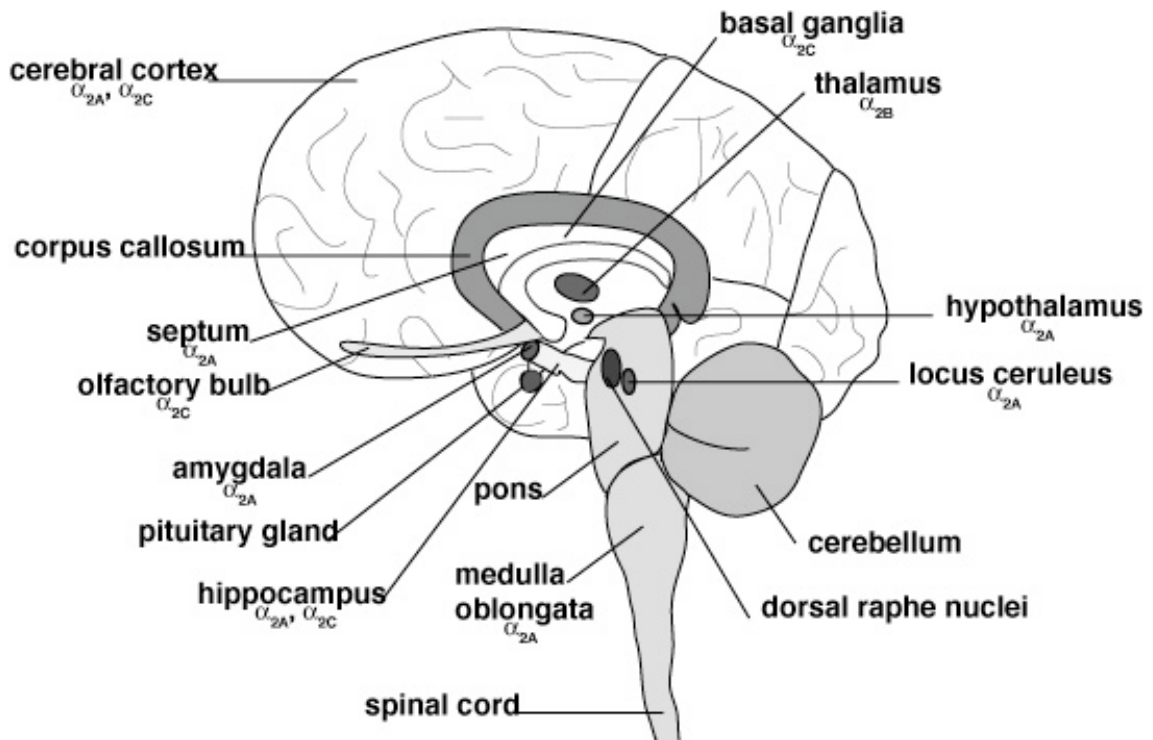


**Fig. 8: *Sagittal view of the human brain.*** $\alpha_2$-receptors are widely distributed throughout the brain, with $\alpha_2$-subtypes often occupying distinct areas. The predominant central autoreceptor, $\alpha_{2A}$, is found abundantly within the locus ceruleus. Other areas with considerable $\alpha_{2A}$ density include the medulla oblongata, hippocampus, amygdala, hypothalamus, septum and cortex. The

*other central autoreceptor, $\alpha_{2C}$, is located mainly in the cortex, hippocampus, olfactory bulb and basal ganglia, while the $\alpha_{2B}$-subtype is found only in significant amounts in the thalamus (for references, see text).*

## 3.4. Physiological importance of $\alpha_2$-receptors

Presynaptic $\alpha_2$-receptors play an essential role in the regulation of sympathetic outflow from adrenergic neurons in both central and peripheral sympathetic nervous systems. Norepinephrine released from neurons activates $\alpha_2$-receptors, which in turn via coupling to $G_i/G_o$ proteins leads to a decrease both in further norepinephrine release as well as in the firing frequency of adrenergic neurons (Foote and Aston-Jones, 1995; Starke, 2001).

### 3.4.1. Presynaptic $\alpha_2$-receptors

Presynaptic $\alpha_2$-receptors are located throughout the entire central and sympathetic nervous systems on adrenergic neurons. Because they regulate sympathetic activity, $\alpha_2$-autoreceptors influence blood pressure and heart rate. $\alpha_2$-receptors on presynaptic termini of the ventrolateral medulla, a region in the brainstem encompassing the nucleus reticularis lateralis (NRL), elicit a decrease in sympathetic outflow and consequently hypotension and bradycardia. In its role as the final relay station in the baroceptor reflex pathway, the NRL is considered to be the major site of action for clonidine and clonidine-like drugs (Szabo, 2002). Likewise, the nucleus tractus solitarius (NTS), the medullar region where afferent baroreceptors terminate, also possesses a high density of $\alpha_2$-receptors which elicit the same response as in the NRL. However, the hypotensive effect of presynaptic $\alpha_2$-receptors is not limited solely to sympathetic inhibition. In the dorsal vagal nucleus, the origin of parasympathetic fibers of the vagus nerve, $\alpha_2$-receptors stimulate parasympathetic outflow and similarly evoke cardiac negative inotropic and bradycardic responses (Wozniak et al., 1995). With the many sites of blockade of central cardiac stimulation, the use and success of clonidine-like drugs as antihypertensive agents is easily understandable. In release experiments with tissue from mice lacking one or two of the three $\alpha_2$-receptor subtypes, it could be shown that the $\alpha_{2A}$-subtype was responsible for approximately 70% of the centrally mediated presynaptic inhibition of norepinephrine release following electrical stimulation of hippocampus sections; the $\alpha_{2C}$-subtype accounted for the remaining 30% of adrenergic inhibition, while the $\alpha_{2B}$-subtype appeared to play little or no role either in the

hippocampus or in the periphery (Hein et al., 1999). Several years later, these experiments were repeated with the previously used agonist, UK 14304 (brimonidine), as well as with medetomidine, a full agonist at all three $\alpha_2$-receptor subtypes. Medetomidine unveiled the contribution of the $\alpha_{2B}$-subtype to presynaptic inhibition in peripheral tissues, very similar to that of the $\alpha_{2C}$-subtype (Trendelenburg et al., 2003). In hippocampus slices, no difference in the inhibition curves obtained with UK 14304 and medetomidine was observed, confirming that the $\alpha_{2B}$-subtype does not contribute to central inhibition (Trendelenburg et al., 2003).

Catecholamines influence not only physical processes but also behavioral aspects and emotional states as well. The locus ceruleus, an area in the brain stem strongly associated with clinical depression, panic disorder and anxiety, is rich in noradrenergic neurons projecting to the hippocampus, thalamus and cortex (Valentino and Aston-Jones, 1995). Presynaptic $\alpha_2$-receptors in the hippocampus suppress norepinephrine release from these neurons, and autoinhibitory overstimulation may contribute to the development of depression, which is according to the widely accepted monoamine theory of depression believed to be linked in part to a norepinephrine depletion in the hippocampus (Delgado and Moreno, 2000). Antidepressants with $\alpha_2$-antagonistic action such as mianserin (Dam et al., 1998) and mirtazepine (Guelfi et al., 2001, Leinonen et al., 1999) have been clinically shown to successfully alleviate depressive symptoms, suggesting that $\alpha_2$-receptors may indeed be involved in the emergence of the illness.

### 3.4.2. Postsynaptic $\alpha_2$-receptors

In contrast to the antihypertensive use of clonidine, the growing use of clonidine as a pre-, peri-, and/or post-operative adjunct to general anesthetics and analgesics exploits the sedative as well as analgesic properties of the drug. Clonidine given prior to and / or during surgery has generally been found to decrease the amount of anesthetic used perioperatively (Watanabe et al., 2006) and even the amount of analgesic used postoperatively in some cases (Segal et al., 1991; Tripi et al., 2005), though the route of clonidine administration may play a role in its post-operative analgesic efficacy (Mannion et al., 2005). Clonidine is also used to maintain blood pressure stability during endotracheal intubation (Zalunardo et al., 1997). The strong analgesic efficacy of clonidine complements that of opioid analgesics. However, these mechanisms appear to be independent of each other, as mice

lacking the $\alpha_{2A}$-subtype displayed the expected lack of analgesic response to clonidine yet were not impaired in their reaction to morphine (Özdogan et al., 2004). With the aid of $\alpha_{2A}$- and $\alpha_{2C}$-deficient mice crossed with Flag-tagged $\alpha_{2A}$-transgenic mice under the control of the dopamine $\beta$-hydroxylase promoter, it could be unequivocally demonstrated that an analgesic response to the $\alpha_2$-agonist medetomidine failed to return with the reintroduction of $\alpha_{2A}$-receptors. Dopamine $\beta$-hydroxylase, a hallmark of noradrenergic neurons, is restricted to adrenergic neurons. In contrast, the sedative effects of $\alpha_2$-agonists returned to $\alpha_{2A}$- and $\alpha_{2C}$-deficient mice after crossing them with Flag-tagged $\alpha_{2A}$-transgenic mice, indicating that presynaptic $\alpha_2$-receptors mediate sedation (Röser, 2005). Postsynaptic $\alpha_2$-receptors contributing to analgesia occur at both spinal as well as supraspinal loci (Guo et al., 1996; Pertovaara et al., 1991).

Postsynaptic $\alpha_2$-receptors modulate hemodynamic responsiveness to adrenergic stimulation. Most notably the $\alpha_{2B}$-subtype mediates vasoconstriction such as that exhibited by clonidine in arterial vessels (Kiowski et al., 1983, Link et al., 1996). However, depending on the vascular bed, either the $\alpha_{2A}$- or the $\alpha_{2C}$-subtype may be involved as well (MacMillan et al., 1996; Philipp et al., 2002a). Uniquely, certain "silent" $\alpha_{2C}$-receptors seem to be activated upon cooling below 37 C and in HEK293 cells have been found to relocate from an intracellular pool to the cell membrane, where they induce vasoconstriction (Chotani et al., 2000; Jeyaraj et al., 2001). It is interesting that both $\alpha_2$-antagonists (phenoxybenzamine) as well as agonists (guanethidine) are therapeutically used to treat the symptoms of Raynaud's disease, which is characterized by paroxysmal vasospasms of the fingers, and sometimes nose and tongue, often triggered by exposure to cold. $\alpha_2$-receptors contribute to the maintenance of blood hemostasis as well. Platelets are endowed with $\alpha_2$-receptors which, upon stimulation with endogenous epinephrine and consequent coupling to $G_i$ proteins, inhibit adenylyl cyclase, leading to a decrease in antiaggregatory cAMP and to an increase in the potent platelet activator ADP (adenosine diphosphate), thereby promoting platelet aggregation (Siess, 1989).

Blood glucose homeostasis is maintained in part by postsynaptic $\alpha_2$-adrenergic receptors (Nakaki et al., 1981). Sympathetic activation of $\alpha_2$-receptors on the $\beta$-cells of the pancreas decreases intracellular $Ca^{2+}$ via coupling to inhibitory G proteins (2.4.). $Ca^{2+}$, however, is necessary for the exocytotic release of insulin from vesicles of the Golgi apparatus. In general

there are two mechanisms of glucose-mediated insulin release. A rise in blood glucose triggers insulin release directly via closure of ATP-sensitive $K^+$ ($K^+_{ATP}$) channels by ATP generated from the oxidative metabolism of glucose. ATP is an endogenous regulator of insulin release; closure of $K^+_{ATP}$ channels and subsequent depolarization of the β-cell membrane leads to an increase of intracellular $Ca^{2+}$ which liberates insulin in the aforementioned manner (Mutschler, 1997). In addition, glucose has been found to enhance insulin release independent of $K^+_{ATP}$ channels (Gembal et al., 1992), although the exact mechanism remains unclear. Studies with mice deficient in one or more $α_2$-subtypes have revealed that the $α_{2A}$-subtype is the main regulator of the epinephrine-induced suppression of insulin release via activation of $α_2$-receptors; however, the role of the $α_{2C}$-subtype is not negligible and appears to act independently of cAMP in contrast to the $α_{2A}$-subtype (Peterhoff et al., 2003). Yet another mechanism of $α_2$-mediated hyperglycemia may be the stimulation of glucagon secretion, which was first observed in sheep (Oda et al., 1990).

The involvement of postsynaptic $α_2$-receptors in a variety of behaviors, affect disorders and cognitive skills has been proposed. $α_2$-receptors have been associated with a number of psychological disorders including post-traumatic stress syndrome, attention deficit hyperactivity disorder (ADHD) and schizophrenia (Perry et al., 1987; Morris et al., 2004; Arnsten et al., 1996; Hornykiewicz, 1982; Lindström, 2000). Several studies using $α_{2C}$-deficient mice have suggested a contribution of this receptor subtype to startle response and the execution of complex navigation patterns (Sallinen et al., 1998; Bjorklund et al., 1999). Particularly the role of the $α_{2C}$-subtype in aggressive behavior has been observed. $α_{2C}$-deficient mice have shown a decrease in attack latency in the isolation-aggression test, whereas mice with a tissue-specific overexpression of the $α_{2C}$-subtype displayed the opposite behavior (Sallinen et al., 1998). More recently, however, attention has been focused on the $α_{2A}$-subtype, which was shown in experiments with $α_{2A}$-deficient mice to stimulate functions in the prefrontal cortex involved in memory and attention (Franowicz et al., 2002). These authors similarly identified the $α_{2A}$-subtype as the molecular target of guanfacine, an $α_2$-agonist used, like clonidine, as a non-stimulant drug in the treatment of ADHD in patients not responding to or not tolerating standard psychostimulant treatment, as well as in patients exhibiting tics either comorbidly with ADHD or alone, as in Tourette's syndrome (Chappell et al., 1995; Hunt et al., 1995; Jimenez-Jimenez and Garcia-Ruiz, 2001; Pliszka, 2003). Finally, there is

much evidence to justify the use of $\alpha_2$-agonists, notably clonidine, for the treatment of symptoms resulting from opiate and alcohol withdrawal (Gold et al., 1978). A recent study identified the $\alpha_{2A}$-subtype as the main pharmacological target of clonidine in the alleviation of opiate withdrawal, as $\alpha_{2A}$-deficient mice showed 70% fewer naloxone-precipitated jumps than wild-type mice (Özdogan et al., 2004). Despite the general consensus that the clonidine-mediated attenuation of withdrawal symptoms is dependent on inhibition of the overstimulation of both central and peripheral noradrenergic pathways (Devoto et al., 2002; Delfs et al., 2000; Milanés et al., 2001), the precise involvement of certain $\alpha_2$-subtypes and the relative contribution of pre- and / or postsynaptic $\alpha_2$-receptors is still not known.

## 3.5. $\alpha_2$-receptor ligands

The catecholamines norepinephrine and epinephrine are the endogenous ligands of $\alpha_2$-adrenergic receptors. It is therefore reasonable that other small molecules with a 2-phenylethylamine structure could be potential $\alpha_2$-agonists or antagonists. However, the $\alpha_2$-agonists commonly used as centrally acting antihypertensives or sedatives do not resemble catecholamines at a first glance. This second class of $\alpha_2$-ligand, which finds much wider use than the endogenous catecholamines, represents 2-amino imidazolines. A closer look at the prototypical $\alpha_2$ / imidazoline agonist clonidine reveals a preferred conformation spatially similar to that of norepinephrine, indicating that the 2-amino imidazoline structure is a potentially potent agonist or also antagonist at the three $\alpha_2$-receptor subtypes (Roth and Fenner, 2000).

### 3.5.1. Catecholamine ligands of $\alpha_2$-receptors

Despite the highly diverse physiological roles both between as well as within the $\alpha_1$-, $\alpha_2$- and $\beta$-adrenergic receptor families, the catecholamines norepinephrine and epinephrine serve as the endogenous ligands of all these adrenergic receptors. The 2-phenylethylamine moiety of the model substance norepinephrine permits little variability, and each receptor family displays its own 'preferences' as to which manipulations of the leading structure are tolerated before receptor affinity is lost. The stepwise modification of many residues of the norepinephrine structure has been documented along with the resulting changes in the affinity and activity of the new molecule at the $\beta$-receptor (Roth and Fenner, 2000). In contrast, the $\alpha_2$-receptor has a more stringent structure-activity relationship; only a substitution of the residues on

the amino group is practicable, and increasing the size of the amino substituent tends to diminish the $\alpha$-activity while increasing the affinity of the drug to the $\beta$-receptor (Hoffman, 2001). The deletion of one of the two aromatic hydroxyl groups of the catecholamine allows the drug to be given perorally without inactivation via 3-O-methylation by catechol-O-methyltransferase (COMT). Together with monoamine oxidase (MAO), COMT is a key enzyme in the metabolism of endogenous catecholamines. Loss of the aromatic hydroxyl group(s) renders the molecule devoid of activity at the $\alpha_2$-receptor; however, drugs such as amphetamine and ephedrine act as indirect agonists and derive their pharmacological activity by competing with norepinephrine for uptake into storage vesicles (Roth and Fenner, 2000).
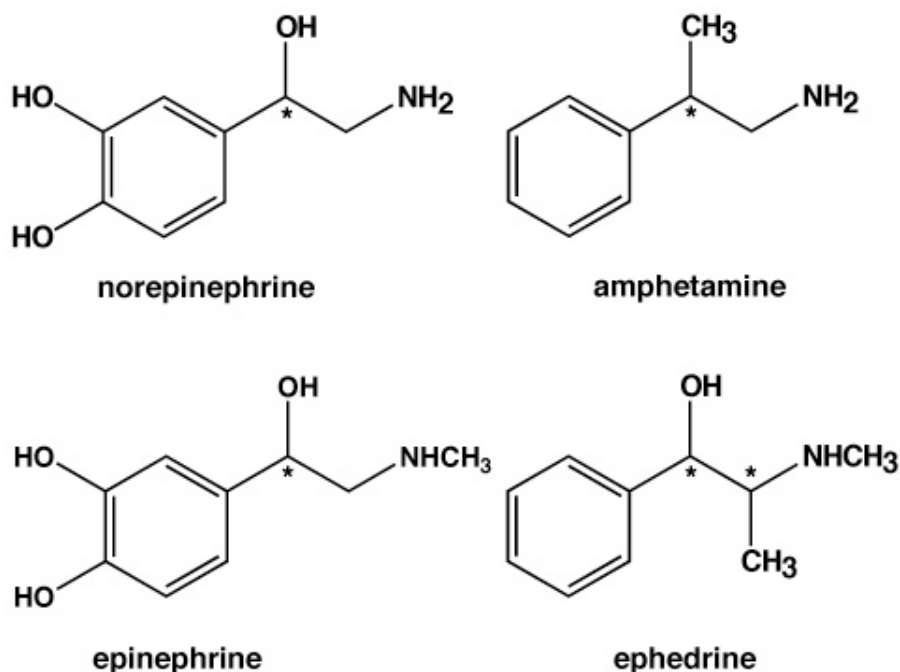


**Fig. 9:** *Structures of norepinephrine and epinephrine as well as of the indirect sympathomimetic drugs amphetamine and ephedrine.* *The latter two substances do not bind to adrenergic receptors. Instead, they compete with the endogenous neurotransmitter norepinephrine for uptake into storage vesicles, thereby increasing the concentration of norepinephrine at the synapse. The asterisk denotes a stereogenic center.*

The $\alpha_2$-receptor distinguishes itself from the $\alpha_1$-adrenergic receptor in its ability to recognize the stereo conformation of the $\alpha$-methyl residue; Ruffolo and Waddell observed the highly preferential interaction of the $\alpha_2$-receptor with

2S(+)-$\alpha$-methyldopamine, whereas the $\alpha_1$-receptor did not prefer either stereoisomer (Ruffolo and Waddell, 1982). Differences in receptor affinity of norepinephrine and epinephrine exist within the $\alpha_2$-family as well; these may, at least partially, account for the unequal contribution of the three $\alpha_2$-subtypes to presynaptic inhibition (Bünemann et al., 2001).

### 3.5.2. Imidazoline and imidazoline-like ligands of $\alpha_2$-receptors

The chemical and metabolic instability of the catecholamine derivatives was surely impetus for the development of $\alpha$-agonists lacking phenolic and catechol structures. Tolazoline was the first fruit of the combination of the catechol phenylethylamine moiety with the imidazole structure of histamine, successfully undertaken by scientists at Ciba in Switzerland in 1939 (Szabo, 2002). Clonidine was first synthesized in 1962 by H. Stähle, a chemist at Boehringer Ingelheim. The compound known as St155 was originally conceived as an improvement on the imidazoline-derived nasal decongestants of the time, such as naphazoline and xylometazoline (Scholz, 2002). Despite the structural relation to these previous $\alpha$-adrenergic agonists, clonidine distances itself from its 2-arylmethyl imidazoline cousins due to a 2-amino imidazoline structure. Clonidine therefore exists predominantly in the more favorable 2-imino imidazolidine form (figure 10), which allows the protonated base to distribute its positive charge throughout the guanidine moiety (Remko et al., 2006). Another unique feature of clonidine compared to the naphazoline-type nasal decongestants is the sterical hindrance of the ortho-chloro substituents, which likely restrain the clonidine molecule in a perpendicular conformation in which the guanidine moiety lies at a 90 angle to the phenyl ring, perhaps "fixed" by the exocyclic C=N double bond (Avbelj and Hadzi, 1985; Roth and Fenner, 2000). The ability of clonidine to adopt this perpendicular conformation appears to permit a nearly identical sterical conformation as the catecholamine neurotransmitter norepinephrine. Using docking simulations, Salminen and colleagues suggested that both clonidine and norepinephrine were able to form two hydrogen bonds with Asp113 in the binding pocket of $\alpha_{2A}$ (Salminen et al., 1999). In contrast, the naphazoline-type $\alpha$-sympathomimetics are not constrained by similar substituents and are likely free to rotate and assume a coplanar form. A general prerequisite for the strong antihypertensive effect of clonidine and related drugs has been found to be an impediment of free rotation of the phenyl ring around the C-N single bond (Roth and Fenner, 2000). Given the stereo selective nature of the $\alpha_2$-receptor (2.5.1.), this "fixed" conformation of clonidine, compared to

naphazoline, may well determine the selectivity for $\alpha_2$- and $\alpha_1$-receptors, respectively.
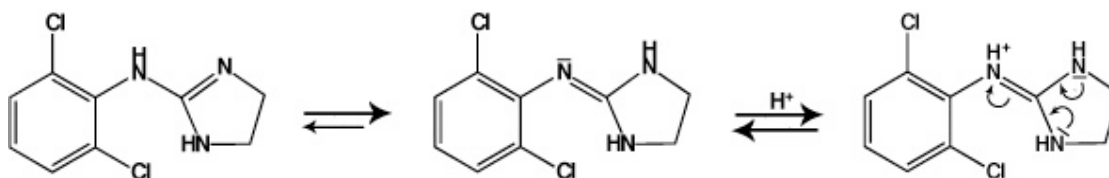


**Fig. 10:** *Tautomeric isomers of clonidine.* The 2-amino imidazoline structure of clonidine facilitates a shift of the imidazoline C=N double bond to the bridging amino nitrogen. Upon protonation of the molecule, the positive charge is more evenly distributed over the molecule (+M effect of the ortho-chlorophenyl substituent and the free electron pairs of the two imidazolidine nitrogen atoms). Consequently, clonidine may be more correctly described as a guanidine derivative than a 2-imidazoline compound.

While effective as a topical vasoconstricting agent, clonidine proved to possess other pharmacological effects that made it undesirable in the treatment of nasal decongestion. Sedation was a known side effect of imidazoline derivates; however, the bradycardic and hypotensive properties exhibited by clonidine were unexpected, as described by Hoefke and Kobinger in 1966. These unique qualities led to the realization of a new class of centrally acting antihypertensive drug. While clonidine (Catapresan®) remains the classic $\alpha_2$-imidazoline agonist, it has gradually lost its therapeutic importance as an antihypertensive with the emergence of the newer $\alpha_2$-imidazoline compounds rilmenidine (Laubie et al., 1985) and moxonidine (Armah, 1988). These "second generation" central antihypertensives are comparable to clonidine in their ability to lower blood pressure, yet are recognized as eliciting fewer side effects than their predecessor such as sedation and xerostomia.

There is much controversy surrounding the mechanism of action of these centrally acting $\alpha_2$-agonists with imidazoline structure depicted in figure 11 (see Szabo, 2002 for a thorough review of both sides). Two general hypotheses can be distinguished to explain the pharmacological target(s) of the antihypertensive effect of these drugs. Prior to the discovery of imidazoline binding sites, the mode of action of clonidine was attributed solely to the activation of $\alpha$-adrenergic receptors, primarily sympathoinhibitory $\alpha_2$-receptors in the medulla oblongata, with a lesser contribution of peripheral $\alpha_2$-

autoreceptors (van Zwieten et al., 1984). This $\alpha_2$-hypothesis still receives much support (see Guyenet, 1997 for a critical review).

In 1984, however, the imidazoline hypothesis was introduced by Bousquet and colleagues who observed that clonidine, but not $\alpha$-methylnorepinephrine, lowered blood pressure when injected directly into the rostral ventrolateral medulla (RVLM). Moreover, the authors observed a similar hypotensive effect with two selective $\alpha_1$-agonists with imidazoline structure, cirazoline and ST 587, as with clonidine, leading them to speculate that not $\alpha_2$-receptors but rather certain "imidazoline-preferring" binding sites mediate the hypotensive effect of centrally acting $\alpha_2$-imidazoline agonists (see Bousquet and Feldman [1999] and Ernsberger and Haxhiu [1997] providing evidence in favor of the imidazoline hypothesis). Numerous radioligand binding studies with [$^3$H]clonidine or clonidine-related radioligands such as [$^{125}$I]p-iodoclonidine in various tissues, classically in bovine brain stem, have identified imidazoline binding sites, although the relative selectivity of $\alpha_2$-imidazoline ligands to either binding site may vary greatly depending on the tissue and the donating species (see Szabo, 2002 for a comprehensive summary). Therefore, the imidazoline-preferring binding site has remained difficult to define absolutely. Due to the varying affinity of clonidine to these binding sites, three classes of imidazoline binding sites can now be differentiated. $I_1$ imidazoline binding sites are located in the RVLM and are therefore believed to participate in blood pressure regulation; $I_1$ binding sites have been found on platelets and in PC-12 cells as well (Piletz et al., 1991; Lanier et al., 1993). The molecular identity of the $I_1$ site is still unknown. Piletz and colleagues succeeded in isolating the full-length cDNA clone of a protein recognized by an antibody raised against an affinity-purified imidazoline binding protein (Piletz et al., 2000). It is not yet clear, however, if this isolated protein termed "IRAS-1" represents a functional receptor. $I_2$ binding sites are better characterized and appear to be allosteric binding sites on monoamine oxidase (Tesson et al., 1995). $I_3$ binding sites may or may not represent a unique class; however, they appear to facilitate insulin release (Morgan and Chan, 2001).
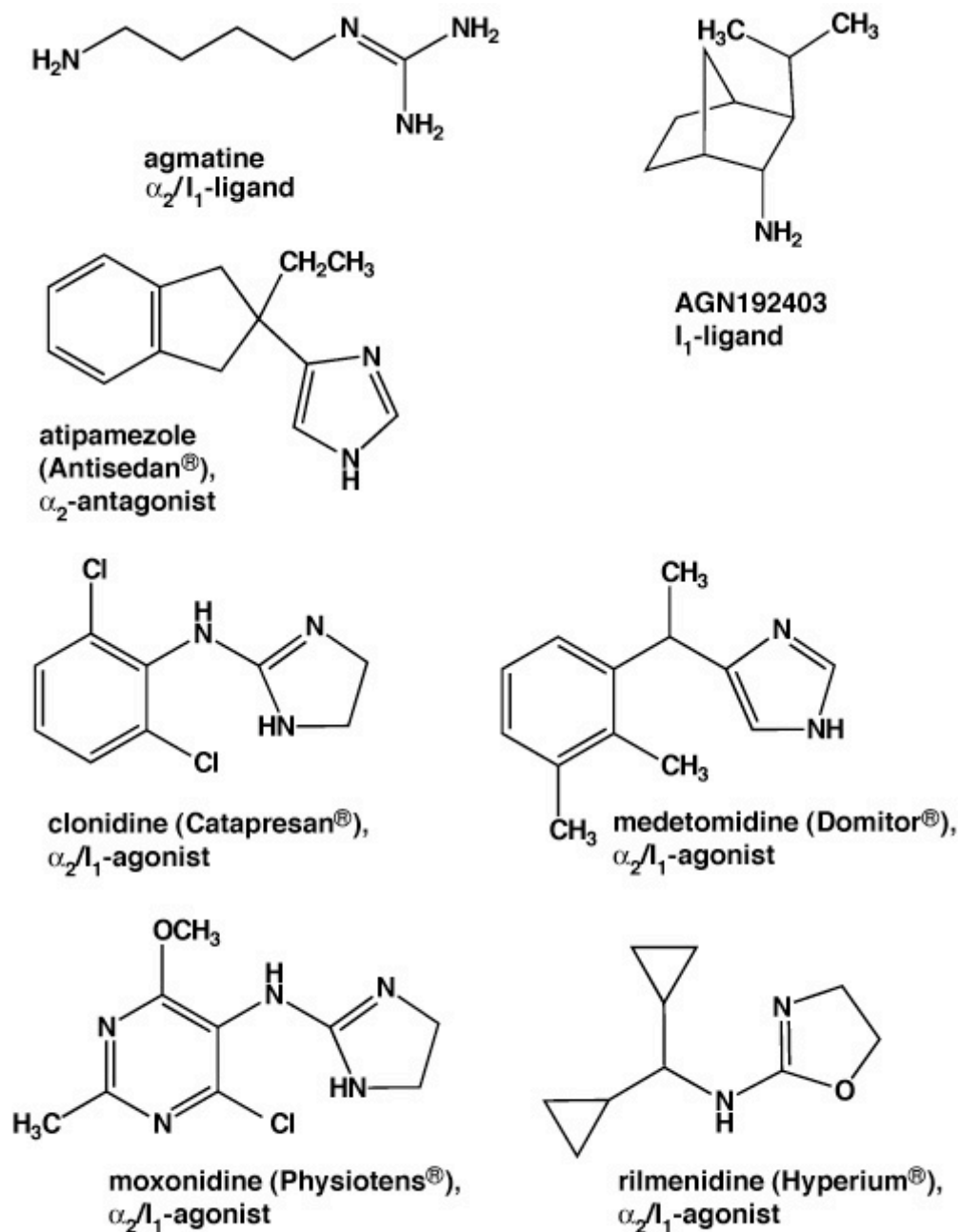
**Fig. 11:** *Structures of $\alpha_2$-imidazoline agonists with varying affinities at $\alpha_2$-receptors and $I_1$ binding sites.*

3.6.    Mice carrying targeted deletions for one or more $\alpha_2$-receptor subtypes

### 3.6.1. Introduction to gene targeting

Genetic manipulation of mouse DNA has become a common technique to elucidate the function and biochemical pathways of proteins. Although the genetic code of many standard laboratory animals is well established, the species Mus musculus (the house mouse) has been used nearly exclusively for (mammalian) genetic studies due to its short reproductive cycle and established techniques of introduction of foreign genetic material into germ cells. Two widespread methods of genetic manipulation, transgenesis and mutagenesis (gene targeting), can be distinguished (Silver, 1995).

Unlike transgenesis, gene targeting modifies the endogenous genetic locus of a specific gene. After subcloning the genetic region of interest into a suitable vector, the targeted gene is modified via site-directed mutagenesis to create either a deletion, insertion or a substitution. The genetic construct is then introduced into embryonic stem (ES) cells via homologous recombination (Stryer, 1995). Properly targeted cells are then injected into blastocysts and implanted into the ovary ducts of pseudopregnant foster mice. The mice born are chimera, carrying both wild-type and mutant cells. In case of germline transmission of targeted cells, these chimera become founders of the mutant line (Silver, 1995).

### 3.6.2. Generation of $\alpha_2$-"knockout" mice

Genetic manipulation of the $\alpha_2$-receptor has tremendously increased understanding of the individual receptor subtypes. Because of the high homology between the three subtypes and the related lack of subtype-specific ligands, deletion of each subtype has proven a powerful tool in the elucidation of their physiological roles. The first published targeted deletion of an $\alpha_2$-receptor subtype was the $\alpha_{2C}$-"knockout" mouse by Link and colleagues (1995). These mice showed no obvious abnormalities, and no up-regulation in the mRNA levels of the remaining two $\alpha_2$-subtypes, suggesting that the $\alpha_{2C}$-subtype was more or less dispensable (Link et al., 1995). One year later, the same group succeeded in deleting the $\alpha_{2B}$-subtype (Link et al., 1996). The targeted deletion of the $\alpha_{2A}$-subtype was not described until three years later (Altman et al., 1999). Loss of the $\alpha_{2A}$-subtype divulged resting tachycardia in these mice (Altman et al., 1999), which was not evident in mice expressing 80% less of the $\alpha_{2A}$-subtype due to a mutation of a single amino acid ($\alpha_{2A}$D79N-mutant, MacMillan et al., 1996).

## 4.    Project goals

Autoinhibitory $\alpha_2$-receptors play a key role in the regulation of sympathetic activity.  Functionally and molecularly the $\alpha_2$-receptor subtypes are very similar.  Because no $\alpha_2$-ligands with sufficient subtype selectivity are available, mice deficient in two or all three $\alpha_2$-receptor subtypes were generated by crossing existing $\alpha_2$-KO lines.  The first goal of this project was to characterize these $\alpha_2$-deficient mice and observe the consequences – if any – of the complete lack of negative feedback control.  The comparison to our $\alpha_2$-double KO mice allowed us to evaluate the amount of redundancy of the three $\alpha_2$-subtypes.

Having successfully generated a sufficiently large population of $\alpha_{2ABC}$-KO mice, the next goal was to assess the possible actions of $\alpha_2$-agonists possessing an imidazoline structure in these $\alpha_{2ABC}$-KO mice.  Represented by the forerunner clonidine, the class of centrally acting antihypertensive drugs, which includes moxonidine and rilmenidine, is generally believed to act not only by activation of $\alpha_2$-receptors but also via purported $I_1$ imidazoline binding sites in the brain stem.  Our mouse model devoid of all functional $\alpha_2$-receptor subtypes was expected to give us insight into the mechanism of action of clonidine and clonidine-like drugs.  These centrally acting antihypertensive drugs failed to decrease resting blood pressure in the absence of $\alpha_2$-receptors; however, a significant reduction in heart rate both in anesthetized and conscious $\alpha_{2ABC}$-KO mice was determined after clonidine administration.

The final goal of this project was to identify the pharmacological target of this $\alpha_2$-receptor-independent effect of clonidine.  Intriguingly, it became evident that $I_1$ receptors did not mediate the bradycardia observed after clonidine treatment of $\alpha_{2ABC}$-KO mice. My studies identified hyperpolarization activated, cyclic nucleotide-gated cation (HCN) channels as a novel target of an $\alpha_2$ / imidazoline agonist.

# III. Methods

## 1. Generation of $\alpha_2$-deficient mice

### 1.1. Housing facilities

All mice used in the following experiments were housed in individually ventilated cages of up to 5 mice per cage in a specified pathogen free facility. The mice were exposed to 12 hour light and dark cycles and were allowed free access to pelleted food and water. All experiments were approved by the Animal Care Committee of the University of Würzburg and the Government of Unterfranken, and were performed in accordance with the guidelines of the National Institutes of Health.

### 1.2. Generation of $\alpha_{2ABC}$-KO mice

$\alpha_{2ABC}$-knockout mice were generated by crossing the existing $\alpha_{2AC}$-KO and $\alpha_{2B}$-KO lines. Once homozygous $\alpha_{2ABC}$-KOs were obtained, these mice were mated so that all resulting $\alpha_{2ABC}$-KO offspring were of purely homozygous origin. The generation of $\alpha_{2A}$-KO, $\alpha_{2B}$-KO, and $\alpha_{2C}$-KO has been described previously (Altman et al., 1999; Link et al., 1995, 1996).

### 1.3. Genotyping of $\alpha_{2ABC}$-KO mice

#### 1.3.1. Preparation of genomic DNA

Approximately 0.5 cm of tail was biopsied and digested overnight at 55 C, shaking constantly, after addition of 200 $\mu$l lysis buffer and 5 $\mu$l proteinase K (20 mg/ml). The next morning, the samples were briefly vortexed and centrifuged (30 s at 13000 rpm). Next, the samples were heated 8 min at 100 C and then centrifuged again for 3 min at 13000 rpm. 1 $\mu$l of the supernatant was used as described below.

lysis buffer

0.5% sodium lauroylsarcosin
0.1 M NaCl
5% Chelex-100
in $H_2O$

### 1.3.2. Polymerase chain reaction (PCR)

To confirm the absence of all three $\alpha_2$-receptor subtypes, genomic DNA of $\alpha_{2ABC}$-KO mice was subjected to analysis by means of the polymerase chain reaction (PCR). By using oligonucleotides (= "primers") flanking the modified region of the gene in question, it was possible to amplify the targeted sequence and view the resulting gene fragment under UV light after electrophoretic separation on agarose gel. In addition to the samples, tail biopsies of mice of confirmed genotype (control DNA) as well as a negative control (water instead of DNA to insure the absence of impurities of the reactants) were concurrently subjected to the PCR.

| primers: | | $T_m$ | fragment size |
|---|---|---|---|
| $\alpha_{2A}$-WT | 5' – GGT GAC ACT GAC GCT GGT TT<br>5' – AAG GAG ATG ACA GCC GAG AT | 56 C | 410 bp |
| $\alpha_{2A}$-KO | 5' – GGT GAC ACT GAC GCT GGT TT<br>5' – CGA GAT CCA CTA GTT CTA GC | 56 C | 260 bp |
| $\alpha_{2B}$-WT | 5' – CTC TTC TGT ACC TCC TCC AT<br>5' – CAT AGA TTC GCA GGT AGA CG | 55 C | 320 bp |
| $\alpha_{2B}$-KO | 5' – TGG ATG TGG AAT GTG TGC GA<br>5' – CAT AGA TTC GCA GGT AGA CG | 55 C | 212 bp |
| $\alpha_{2C}$-WT | 5' – CAT CTT GTC CTC CTG CAT AG<br>5' – TCT CAT CCG GCT CCA CTT CA | 57 C | 230 bp |
| $\alpha_{2C}$-KO | 5' – GGG AAG ACA ATA GCA GGC AT<br>5' – TCT CAT CCG GCT CCA CTT CA | 57 C | 250 bp |

PCR:

1 $\mu$l genomic DNA from Chelex digestion
1 $\mu$l forward primer, 10 $\mu$M
1 $\mu$l backwards primer, 10 $\mu$M
2 $\mu$l 10x PCR buffer + MgCl$_2$
2 $\mu$l dNTPs, 2 mM
0.2 $\mu$l Taq-polymerase 5 U/$\mu$l
<u>12.8 $\mu$l water for injection</u>
20 $\mu$l total volume for n=1 sample

Over 30 cycles the samples were repeatedly first heated to 94 C (15 s) to denature the double-stranded DNA, then cooled to the appropriate hybridization temperature of the primers (T$_m$) to assure annealing of the primers to the single-stranded DNA (20 s), then finally heated again to 72 C (25 s) to allow for elongation of the complementary DNA strand.

1.3.3. Gel electrophoresis

After the PCR, approximately 2 $\mu$l loading buffer was added to the entire contents of each reaction tube, and the samples were loaded into the pockets of a 2% agarose gel. After electrophoretic separation at about 145 V, the gel was examined under UV light (265 nm) and photographed. The position of the sample fragments was compared to the control DNA.

<u>2% agarose gel:</u>

2% agarose dissolved by heating in 1x TAE buffer

<u>50x TAE buffer:</u>

400 mM Tris-HCl
50 mM Na(CH$_3$COO)
10 mM EDTA
pH = 8

<u>loading buffer:</u>

0.25% (M/V) bromphenol blue

50% (V/V) glycerin
50% (V/V) $H_2O$


## 2.  Basal characterization of $\alpha_{2ABC}$-deficient mice

$\alpha_{2ABC}$-KO mice were generated and maintained on a mixed 129/Sv/C57BL6 genetic background.  Due to the lethality of $\alpha_{2B}$-deficient mice on a pure, congenic C57BL6-background, it was not possible to generate congenic $\alpha_{2ABC}$-deficient mice.  In the initial mating scheme (Results, figure 12), the relative contributions of 129Sv and C57BL6 were 1:16.  C57BL6 wild-type mice housed under identical conditions served as controls.

### 2.1.  Determination of urine catecholamines

The catecholamines norepinephrine, epinephrine, dopamine and L-DOPA were examined extensively in our $\alpha_{2ABC}$-KO mice.  Urine catecholamines were bound and purified using the aluminum oxide method, which makes use of the ability of aluminum oxide to selectively bind catecholamines at pH 8.6 and to release them after washing with acid (pH = 1-2).  Catecholamines were quantified by means of HPLC on a reversed phase RP-18 column.  Peaks were detected electrochemically and quantified using Millennium M32 software (Waters).

Mice (n=2-5) were placed in a metabolic cage for 24 hours and the total urine was collected in a small graduated measuring cylinder containing 1 ml 0.4 M $HClO_4$ and 1 ml mineral oil to prevent loss of urine volume due to evaporation.  Mice had free access to food and water in the metabolic cage.  After 24 hours, the total volume of urine in the measuring cylinder was recorded and the aqueous phase was pipetted into a 15 ml Falcon.  The samples were stored at -20 C until preparation for measurement.  Directly before HPLC analysis, samples were thawed and a 100 $\mu$l sample was added to 500 $\mu$l stabilizing mix (27 mM EDTA, 50 mM $Na_2SO_3$).  Then, 100 $\mu$l 3,4-dihydroxy benzylamine hydrobromide (DHBA) internal standard (100 ng/ml) solution, 300 $\mu$l 2 M Tris pH = 8.2-8.3 and 20 mg aluminum oxide were added.  The mixture was shaken well to allow binding of the catecholamines to the aluminum oxide.  After 5 minutes, the mixture was filtered and the aluminum oxide was washed twice with water.  Finally, the purified catecholamines were eluted twice with

100 $\mu$l 0.1 M HClO$_4$; the eluate was injected directly into the HPLC system by means of an automatic injector (WISP 717, Waters).

## 2.2.   Determination of the degree of cardiac hypertrophy

Following sacrifice of the mouse by cervical dislocation, the heart was removed and all excess tissue and also the atria were excised.  The ventricles were weighed on an analytical balance (Kern, type 370-13).  The tibia was also removed and, after trimming away excess tissue, measured using a vernier caliper.  The quotient of heart weight divided by tibia length is a widely accepted indicator of cardiac hypertrophy.

Another common measure of hypertrophy is the ratio of heart weight to body weight.  Here the mouse was weighed on a balance (Mettler, PM480 DeltaRange) before sacrifice.  However, in this case the atria were not removed from the heart before weighing (these hearts were later used in radioligand binding experiments where the binding characteristics of the whole heart were investigated).

## 2.3.   Histology

### 2.3.1.  Organ removal and fixation

After sacrifice by cervical dislocation, the organ(s) of interest was quickly removed, blotted dry on a paper towel and immersed in 4% paraformaldehyde solution in a 6-well plate.  The plate was sealed tightly and the organs were stored at 4  C until they could be embedded in paraffin (at least 24 hours).

### 2.3.2.  Preparation of paraffin slices

The organs were removed from the paraformaldehyde solution and washed twice with formalin.  Next, water was removed from the tissues by immersing them successively in ethanol / water solutions of increasing concentration (2x 80%, 4x absolute ethanol). Since paraffin is not soluble in ethanol, it was necessary to wash twice with xylol before adding the liquid paraffin.  The tissue was warmed to approximately 60  C and saturated with paraffin of the same temperature.  The previous steps were carried out by an automated tissue processor.  Next the paraffin-coated tissue was positioned in a cassette and embedded in molten paraffin.  After a thin film had formed on the cooling

form, cold water was poured onto the form and the form removed from the cassette. The tissue blocks were cut with a microtome (Leica RM2165) into 3-4 $\mu$M sections. The sections were placed in a water bath (37 C) and mounted onto Superfrost slides (Menzel). The slides were dried at 42 C and then stored at 4 C.

### 2.3.3. Staining with hematoxylin and eosin (HE)

Before staining it was necessary to remove the paraffin coating. This was done by washing the slides with xylol and then rehydrating the tissue with decreasing ethanol / water concentrations (3x absolute ethanol, 1x ethanol 70%) and finally washing with double-distilled water four times. The slides were stained in hemalaun for 10 min, washed with tap water for 10 min, then counterstained with eosin (1% eosin Y ws) for approximately 50 s. The slides were washed twice with Milli-Q® water (30 s each). After staining, it was necessary to dehydrate the tissue again, so slides were immersed in increasing ethanol/water concentrations (reverse of above procedure), then xylol. Finally, slides were embedded in Eukitt®.

hemalaun:

0.1% hematoxylin
5% alaun (AlK(SO$_4$)$_2$ x 12H$_2$O)
0.02% sodium iodate
5% chloral hydrate
0.1% citric acid

### 2.3.4. Staining with Sirius red

After removal of paraffin and rehydration of sections as described in 2.3.3., slides were stained 45 min with Sirius red solution. After staining, slides were washed twice with Milli-Q® water (30 s each) and then dehydrated as described above. Finally, slides were embedded in Eukitt®.

Sirius red:

0.1% Direct Red 80 in saturated picric acid

2.3.5. Photographing and evaluation of slides

Slides showing a transverse section through the whole heart were photographed using a Contax 167MT camera attached to the microscope (Zeiss Axiovert 135). The photographs were stored digitally and could be evaluated later in Photoshop.

To assess the degree of hypertrophy by comparing the sizes of individual cardiac myocytes (HE-stained), a photograph showing approximately 10 myocytes (under 63x magnification) in cross-section was evaluated. Using the lasso tool, the individual myocytes were carefully outlined one after another and filled in with paint. Under the "picture" column and "histogram", the pixel size of the myocyte was calculated by Photoshop. The pixel sizes of the myocytes (approximately 10 per slide x 5 slides) were averaged for each group and the group means were compared.

To assess the degree of fibrosis, Sirius red-stained slides were compared. Under low magnification (5x) the major cavity was centered in the field of view and then photographed. Next, the papillary muscle was focused under 20x magnification and photographed. Finally, the tissue areas directly to the right and left of the papillary muscle (viewed such that the major cavity is directly above the papillary muscle) that do not show the cavity wall were photographed under 20x magnification. In Photoshop the pipette tool was selected. The pipette was clicked on fibrotic areas (red in Sirius red stain) to select the color intensity. A tolerance of 40 was entered under the "selection" column and "select colored region". Then, under the "picture" column and "histogram", the number of pixels shown was recorded.


## 3. Radioligand binding

### 3.1. Preparation of membranes from tissues

After sacrifice of the mouse by cervical dislocation, the organ(s) was quickly removed, freed from excess tissue and frozen immediately in liquid nitrogen. The tissues were stored at -80 C until homogenization. The frozen tissue was homogenized in 2 ml 0.32 M sucrose on ice with a glass Dounce homogenizer. After centrifugation of the homogenate 10 min, 4500 rpm, 4 C in a tabletop centrifuge (Rotina 48 R), the supernatant was poured into an

ultracentrifuge tube, balanced, and centrifuged 40 min at 37000 rpm, 4 C in a Ti70 rotor (Beckman LE-70 ultracentrifuge). The supernatant was discarded and the pellet resuspended in 1 ml Milli-Q® water with a disposable 1 ml syringe. After another 30 minutes of centrifugation at 37000 rpm and 4 C, the pellet was resuspended in 1 ml 50 mM Tris, pH = 7.4 and centrifuged a final 30 min at 37000 rpm, 4 C. The pellet was resuspended in approximately 400 $\mu$l 50 mM Tris, pH = 7.4 per homogenized organ. The protein content of the resulting membrane suspension was determined by the Bradford method (see 3.2.).

3.2.   Quantification of proteins:  Bradford assay

The Bradford dye assay to determine the protein concentration in a solution makes use of the pH-induced changes in equilibrium of Coomassie Blue G dye. Upon binding to a protein, the red doubly-protonated form of Coomassie Blue G goes via an intermediate single-protonated green form into the blue protein-bound unprotonated form (Bradford, 1976). This protein / dye complex is stable and can be quantified photometrically by measuring the absorbance of the sample at 595 nm.

In a disposable plastic cuvette, approximately 1-5 $\mu$l of the membrane solution obtained under 3.1. was added to a 1:5 dilution of the Bradford reagent 5x concentrate (Roti®-Nanoquant, Roth) to yield a total volume of 1 ml. After 20 minutes, the absorbance of the sample at 595 nm was measured against the protein-free Bradford dilution using a spectrophotometer (Shimadzu UV-1601). Each membrane suspension was measured in triplicate.

The protein concentration of the measured membrane suspension was calculated using a calibration curve generated with bovine serum albumine as a standard.

The membrane suspension was diluted with Tris 50 mM, pH = 7.4 to a final concentration of 2 $\mu$g/$\mu$l, aliquoted, and frozen in liquid nitrogen. The aliquots were stored at -80 C until binding was performed.

3.3.   Saturation binding in $\alpha_{2ABC}$-KO membranes

Saturation binding experiments were performed to determine the total number of specific binding sites for [$^3$H]clonidine in $\alpha_{2ABC}$-KO brain and heart

membrane preparations. The nonspecific binding of the radioligand to other sites (determined in the presence of an excess of non-radioactive clonidine) was subtracted from the total binding in $\alpha_{2ABC}$-KO membranes to yield the specific binding of [³H]clonidine.

The specific binding curve obtained by subtraction of the nonspecific binding curve from the total binding curve is characterized by the number of binding sites $B_{max}$ and by the dissociation constant $K_d$, the concentration of ligand at which 50% of the binding sites are occupied. $B_{max}$ and $K_d$ can be determined using the following equation:

$$Y = \frac{B_{max} * X}{K_d + X}$$

$X$      radioligand concentration [nM]

$Y$      specific binding in cpm or fmol/mg at $X$

The above equation assumes one site binding.

To first assess whether or not $\alpha_{2ABC}$-KO mouse membranes exhibited specific binding possibly attributable to $I_1$-imidazoline receptors (originally proposed by Bousquet et al., 1984), membrane preparations of $\alpha_{2ABC}$-KO brain and heart (see 3.1.) were subjected to saturation binding experiments with the "classic" mixed $\alpha_2$ / $I_1$ agonist [³H]clonidine. Total binding and nonspecific binding of the radioligand were determined as follows:

| total binding: | nonspecific binding: |
|---|---|
| 100 µl 50 mM Tris buffer, pH = 7.4 | 50 µl 50 mM Tris buffer, pH = 7.4 |
| 50 µl 2 µg/µl membrane suspension | 50 µl 2 µg/µl membrane suspension |
| 50 µl [³H]clonidine (2-64 nM) | 50 µl 40 µM clonidine |
| | 50 µl [³H]clonidine (2-64 nM) |

[³H]clonidine:

| working conc. | end conc. |
|---|---|
| 2 nM | 0.5 nM |
| 4 nM | 1 nM |
| 8 nM | 2 nM |
| 16 nM | 4 nM |

| | |
|---|---|
| 24 nM | 6 nM |
| 32 nM | 8 nM |
| 64 nM | 16 nM |

The [$^3$H]clonidine stock solution (18 $\mu$M) was first diluted 1:100 with 50 mM Tris buffer, pH = 7.4, then the radioligand dilution was diluted again with Tris buffer to yield the necessary amount of each working concentration.  Each concentration was determined in triplicate (3x total binding, 3x nonspecific binding).  Filter counts (150 $\mu$l 50 mM Tris buffer and 50 $\mu$l radioligand) were determined in duplicate, and total counts were measured once per concentration.  The reagents were pipetted on ice, vortexed briefly, spun down, then incubated at room temperature for 1 hour.  After this time, samples were placed on ice, and the reaction was stopped by rapid vacuum filtration over GF/F glass fiber filters which were incubated at least 20 minutes prior to filtration in 0.33% polyethylenimine (PEI) in 50 mM Tris buffer on ice.  Each filter was washed 3x with ice-cold 50 mM Tris buffer, then placed in a 5 ml scintillation vial.  After all samples were filtered, the vials were filled with 4 ml Lumasafe scintillation solution, closed, and shaken.  After at least 2 hours, the samples were counted in a Beckman LS 1801 $\beta$-counter.  The results were analyzed using Prism GraphPad software to determine $B_{max}$ and $K_d$ values.

## 3.4.    Competition binding in $\alpha_{2ABC}$-KO membranes

Competition binding studies allow the determination of the affinities of a wide range of compounds at a given receptor in the presence of a single concentration of radioligand with a known $K_d$ at that receptor.  Samples are incubated with increasing concentrations of the non-radioactive ligand, and then the amount of radioligand still bound at that concentration is counted.  By plotting the logarithmic concentration of the inhibitor against the bound radioligand (cpm), a sigmoidal dose-response curve is obtained, yielding the $IC_{50}$ value of the ligand of unknown affinity.  This inflection point is where 50% of the specific binding of the radioligand is displaced by the non-radioactive ligand.  With the $IC_{50}$ value, it is possible to calculate the $K_d$ value of the inhibitor [$K_i$] by means of the Cheng-Prusoff equation:

$$K_i = \frac{IC_{50}}{1 + [L]/K_d}$$

[L] = total concentration of radioligand in sample [nM]

[$K_d$] = known $K_d$ of radioligand at the receptor [nM]

To better define the non-$\alpha_2$ binding site for [$^3$H]clonidine in $\alpha_{2ABC}$-KO membranes, other known mixed $\alpha_2$ / $I_1$ agonists with previously defined $I_1$ affinities were examined under the current experimental conditions. Samples were incubated with increasing concentrations of non-radioactive ligand (1 nM, 10 nM, 100 nM, 0.5 $\mu$M, 1 $\mu$M, 10 $\mu$M) and 8 nM [$^3$H]clonidine for one hour at room temperature as follows:

competition binding:

50 $\mu$l 50 mM Tris buffer, pH = 7.4
50 $\mu$l 2 $\mu$g/$\mu$l membrane suspension
50 $\mu$l 4x ligand solution
50 $\mu$l [$^3$H]clonidine (32 nM)

In addition, three blank values (= total binding of radioligand) were included. All samples were analyzed in triplicate. After one hour, samples were placed on ice, and the reaction was stopped by rapid vacuum filtration over GF/F glass fiber filters which were incubated at least 20 minutes prior to filtration in 0.33% PEI in 50 mM Tris buffer on ice. Each filter was washed 3x with ice-cold 50 mM Tris, then placed in a 5 ml scintillation vial. After all samples were filtered, the vials were filled with 4 ml Lumasafe scintillation solution, closed, and shaken. After at least 2 hours, the samples were counted in a Beckman LS 1801 $\beta$-counter. The results were analyzed using Prism GraphPad software to determine $IC_{50}$ values for the tested ligands.

All ligands, with the exception of rilmenidine, were dissolved in Milli-Q$^®$ water to 10 mM stock solutions, then diluted with 50 mM Tris buffer, pH = 7.4 to the working concentration. Due to poor water solubility, rilmenidine was first dissolved in 30% ethanol to yield the 10 mM stock solution, then diluted as above with 50 mM Tris buffer, pH = 7.4.

## 4.    Functional characterization of $\alpha_{2ABC}$-deficient mice after $\alpha_2$-agonist application

### 4.1.   Assessment of analgesic efficacy

A tail-flick test (Ugo Basile model 7360, IR intensity = 40) was used to measure the analgesic efficacy of clonidine, moxonidine and rilmenidine (50

μg per mouse) in wild-type and $\alpha_{2ABC}$-KO mice. The mean duration of 10 measurements taken for the mouse to remove its tail before agonist injection was compared to the mean duration of 10 measurements taken 15 minutes after injection. Only 5 post-injection measurements were performed in wild-type clonidine-injected mice to reduce harm to the animal.

## 4.2.    Measurement of sedative properties

A rotarod model was used to assess the sedative effect of clonidine in wild-type and $\alpha_{2ABC}$-KO mice. The rod rotated at a speed of approximately 15 rpm. After a brief training period, 5 measurements were taken before and 15 minutes after clonidine, moxonidine, rilmenidine or medetomidine (50 μg / mouse) administration in 6 wild-type and 6 $\alpha_{2ABC}$-KO mice.

## 4.3.    Determination of blood glucose

Mice were briefly anesthetized with 4% isoflurane gas in oxygen, administered by a nose mask. Following loss of consciousness, the isoflurane content in the oxygen was reduced to 1.5-2%, depending on the animal's reactivity. 1-2 drops of blood were collected per sample using a 1 cm long glass capillary from the retroorbital venous plexus. The blood sample was immediately applied to the Accu-Chek Sensor Comfort test strip already placed in the Accu-Chek Sensor glucose meter (Roche), and the result was recorded in an Excel sheet.

## 4.4    Measurement of cardiovascular parameters

### 4.4.1.  Blood pressure

In mice anesthetized with 2% isoflurane, blood pressure was determined by catheterization of either the left ventricle or aorta using a 1.4F high-fidelity pressure-volume catheter (Millar Instruments). The measurements were recorded using PowerLab Chart software for Macintosh (AD Instruments, Australia). Agonists and antagonists were administered, unless otherwise stated, intraperitoneally (ip) in a physiological saline solution. Mice remained on a heated table (37 C) throughout the measurements to avoid temperature-dependent changes.

Telemetric measurement of resting blood pressure in awake, unrestrained $\alpha_{2ABC}$-KO and age-matched wild-type mice (n=6 per group) was also performed to eliminate a possible influence of the anesthetic on blood pressure.  10-20 days after implantation of the sensor (PA10; DSI, Transoma Medical, USA), the mean 24-hour blood pressure was recorded in wild-type and $\alpha_{2ABC}$-KO mice (n=6 per group).

### 4.4.2.  Heart rate

In isoflurane-anesthetized mice (2% in $O_2$ via a nose mask), heart rate was monitored after insertion of a 1.4F high-fidelity pressure-volume catheter (Millar Instruments) into the femoral artery.  Blood pressure measurement was not possible in the femoral artery. The measurements were recorded using PowerLab Chart software for Macintosh (AD Instruments, Australia) after the mouse was placed on a heated table (37 C).  Agonists and antagonists were applied, unless otherwise stated, intraperitoneally (ip) in a physiological saline solution.

Baseline heart rate of both wild-type and $\alpha_{2ABC}$-KO mice was determined in conscious, freely-moving mice by means of pressure telemetry (sensor PA10, DSI, Transoma Medical, USA) after implantation of an indwelling catheter in the left carotid artery.  The mean 24-hour heart rate of $\alpha_{2ABC}$-KO and age-matched wild-type mice (n=6 per group) was recorded 10-20 days after surgical implantation of the telemetric sensor. Agonist-induced changes in beating frequency were also evaluated in awake, unrestrained mice using ECG telemetry (sensor TC10, DSI).  Clonidine-induced bradycardia was recorded in $\alpha_{2ABC}$-KO and age-matched wild-type mice (n=6 per group) 10-20 days after surgical implantation.

### 4.4.3.  Contractile function

In order to evaluate left ventricular function in $\alpha_{2ABC}$-KOs, shortening fraction was measured via echocardiography.  After light sedation with tribromoethanol (200 $\mu$l 2.5% solution ip), transthoracic echocardiography Doppler examinations were performed in wild-type and $\alpha_{2ABC}$-KO mice (n=6 per group) with an echocardiographic system (Acuson, Sequoia C512, Siemens AG, Erlangen) utilizing a 15-Mhz linear transducer.  Measurements were performed offline by a blinded observer in accordance with the recommendations of the American Society of Echocardiography.

4.5.    Organ bath

After sacrifice of the mouse by cervical dislocation, the heart was rapidly but carefully removed and placed in a silicon-coated Petri dish filled with a modified Tyrode's solution, pH-adjusted with carbogen gas.  The atria were then completely excised from the ventricles, pinned down with a 27-gauge needle and closely observed to identify the right atrium.  Using a fine thread (Danville's 6/0 Flymaster waxed), a loop was formed and the sides of the atrium were "lassoed" and knotted.  One thread from each knot was removed, and the remaining threads were affixed with tissue adhesive (Histoacryl) to either a thin wire (upper thread) or to the hook (lower thread) of the force transducer.  The four chamber organ bath (FMI GmbH, type IOA-5301) was prefilled with the modified Tyrode's solution, tempered to 37 C by an outer heating coil.  Each atrium was gently stretched by shortening the wire so that a normal contraction rate of 300-500 bpm resumed.  After this, the amplifier was zeroed.  The spontaneous contractions of the right atria were registered by PowerLab Chart software for Macintosh (ADInstruments).

Ligands were added in increasing concentrations from 100x stock solutions (to yield end concentrations of 1 nM – 1 mM in tenfold steps) to the 3 ml bath solution.  Once the effective concentration range of the ligand was determined, only one or two concentrations were administered to the bath.  Both dilution error as well as the accumulation of the ligand was neglected in the evaluation.

modified Tyrode's solution

119.77 mM NaCl
5.36 mM KCl
2.13 mM $MgCl_2$
22.6 mM $NaHCO_3$
0.48 mM $NaH_2PO_4$
1.2 mM $CaCl_2$
10 mM glucose
2 mM sodium pyruvate
0.28 mM ascorbic acid
pH adjusted to 7.4 with carbogen

4.6.    Neurotransmitter release experiments

The release of [$^3$H]norepinephrine from adrenergic neurons was measured in the absence and in the presence of the agonists norepinephrine and medetomidine in isolated cardiac atria from wild-type and $\alpha_{2ABC}$-KO mice. Briefly, the hearts of mice killed by cervical dislocation were quickly removed and placed in Krebs-Henseleit buffer (see below), taking care not to injure the atria.  In a buffer-filled Petri dish the atria were precisely separated from the ventricles and other remaining tissues with the aid of a magnifying glass. Using a small pair of dissection scissors, the atria were opened by cutting from the mitral or tricuspid valve opening along the septum until the atrium resembled a butterfly.  Next, the atria were incubated in ca. 0.1 $\mu$M [$^3$H]norepinephrine for one hour, rinsed, then placed in isolated chambers bounded above and below by electrodes.  Following [$^3$H]norepinephrine uptake, 1 $\mu$M desipramine was added to the buffer for the remainder of the experiment.  After 60 minutes equilibration time in the buffer-perfused chamber, the atria were electrically stimulated according to a fixed protocol (see below) and the perfusate was collected over 8 minutes at 2 minute intervals.  The stimulation protocol below describes only one measurement "set", i.e. for agonist-free (baseline) or for one concentration of agonist.  In a typical experiment, 6 such sets were repeated in succession to establish a dose-response curve.  Medetomidine and norepinephrine were added (separately) to the buffer reservoir in increasing concentrations after an initial baseline measurement.

Krebs-Henseleit buffer (atria)            stimulation protocol

118 mM NaCl                               t = 0-2 min:  basal collection interval
4.8 mM KCl                                t = 2 min:  stimulation interval
2.5 mM CaCl$_2$                                    20 V
1.2 mM MgSO$_4$ x 7H$_2$O                          20 pulses
25 mM NaHCO$_3$                                    2 ms
1.2 mM KH$_2$PO$_4$                                50 Hz
0.03 mM Na$_2$EDTA                        t = 2-4 min:  collection interval
11 mM glucose                             t = 4-6 min:  collection interval
0.57 mM ascorbic acid                     t = 8-20 min:  rinse; no collection
pH adjusted to 7.4 with carbogen

## 5.    Cell culture

### 5.1.    HEK293 cells stably expressing HCN channel subtypes

### 5.1.1.  Culture

Stably transfected HEK293 cells expressing the murine HCN1, the murine HCN2 and the human HCN4 subtypes were generated in the lab of Prof. Dr. Martin Biel at the Ludwig-Maximilians-Universität in Munich.  HCN-HEK293 cells were maintained in DMEM high glucose containing 10% fetal calf serum, 100 U/ml penicillin, 100 $\mu$g/ml streptomycin and G418 (at an end concentration of 0.2 mg/ml) to maintain selection pressure. The cells were incubated at 37 C and 10% $CO_2$.

### 5.1.2.  Electrophysiological measurements in HCN-HEK293 cells

The $I_f$ current in transfected HEK293 cells was measured in Munich using the whole cell patch clamp technique at room temperature.  Measurements were conducted at varying extracellular ion concentrations as well as at different voltages.  Data were recorded at 10 kHz with the aid of an Axopatch 200B amplifier and pClamp 8 (Axon Instruments).  The current amplitude and half-maximum activation voltage $V_{0.5}$ were calculated with the acquired data.  In addition, a dose response curve was created to reflect the dose-dependent inhibition of HCN channels (and therefore the $I_f$ current) by clonidine.

### 5.2.    Sinoatrial node (SAN) cells

Located in the sinus node, these cells are characterized by their unstable resting potential which leads to the generation of each new heart beat.  HCN channels (as well as others which regulate heart rate, see Introduction 1.2.2.) are located at the cell membrane of SAN cells, making these cells an ideal system in which to study the physiological response to HCN blockade.

### 5.2.1.  Isolation

SAN cells were isolated based on the protocol developed by Mangoni and Nargeot (2001) from age-matched adult wild-type and $\alpha_{2ABC}$-KO mice in the lab of Prof. Dr. Martin Biel.  Briefly, the beating heart was removed from the anesthetized mouse and immediately placed in pre-warmed Tyrode's solution,

59

where the sinoatrial region was removed and cut into tissue strips. These strips were then placed in a $Ca^{2+}$- and $Mg^{2+}$-deficient solution. The SAN tissue strips were digested by collagenase type II, elastase, protease, BSA 1 mg/ml and 200 $\mu$M $CaCl_2$, all added to the low $Ca^2$ and $Mg^{2+}$ solution. The tissue strips were intermittently dissociated with a glass Pasteur pipette during 9-13 minutes of digestion at 35 C. Afterwards, SAN strips were washed and placed in a modified high $K^+$ medium. Further agitation of the tissue strips made an isolation of single SAN cells possible, which were returned to a more physiological solution. After readaptation to the physiological extracellular $Ca^{2+}$ concentration, SAN cells were placed in storage medium.

| Tyrode's solution | low $Ca^{2+}$ / low $Mg^{2+}$ | digestion solution |
|---|---|---|
| 140 mM NaCl | 140 mM NaCl | 229 U/ml collagenase |
| 5.4 mM KCl | 5.4 mM KCl | type II |
| 1.8 $CaCl_2$ | 0.2 mM $CaCl_2$ | 1.9 U/ml elastase |
| 1 mM $MgCl_2$ | 0.5 mM $MgCl_2$ | 0.9 U/ml protease |
| 5 mM Hepes-NaOH | 1.2 mM $KH_2PO_4$ | 1 mg/ml BSA |
| 5.5 mM D-glucose | 50 mM taurine | 200 $\mu$M $CaCl_2$ |
| pH = 7.4 | 5.5 mM D-glucose | |
| | 1 mg/ml BSA | |
| | 5 mM Hepes-NaOH | |
| | pH = 6.9 | |

| high $K^+$ solution | storage solution |
|---|---|
| 70 mM L-glutamic acid | 100 mM NaCl |
| 20 mM KCl | 35 mM KCl |
| 80 mM KOH | 1.3 mM $CaCl_2$ |
| 10 mM D-$\beta$-OH-butyric acid | 0.7 mM $MgCl_2$ |
| 10 mM $KH_2PO_4$ | 14 mM L-glutamic acid |
| 10 mM taurine | 2 mM D-$\beta$-OH-butyric acid |
| 1 mg/ml BSA | 2 mM $KH_2PO_4$ |
| 10 mM Hepes-KOH | 2 mM taurine |
| pH = 7.4 | 1 mg/ml BSA |
| | 50 $\mu$g/ml gentamycin |
| | pH = 7.4 |

### 5.2.2. Electrophysiological measurements in SAN cells

$I_f$ currents in SAN cells were measured using the whole cell voltage clamp technique at room temperature. Measurements were conducted at varying extracellular ion concentrations as well as at different voltages. Data were recorded at 10 kHz with the aid of an Axopatch 200B amplifier and pClamp 8 (Axon Instruments). The current amplitude and half-maximum activation voltage $V_{0.5}$ were calculated with the acquired data. In addition, a dose response curve was created to reflect the dose-dependent inhibition of HCN channels (and therefore the $I_f$ current) by clonidine.

# IV.     Materials

## 1.     Oligonucleotides

Oligonucleotide primers were obtained from MWG Biotech GmbH, Ebersberg.

## 2.     Enzymes

collagenase type II                   Worthington
elastase                              Roche
protease                              Sigma

## 3.     Ligands and chemicals

agmatine                              Sigma
AGN 192403                            Tocris
atipamezole                           Antisedan®, Pfizer
carbachol                             Sigma
cimetidine                            Sigma
clonidine                             Sigma
efaroxan                              Tocris
[$^3$H]clonidine                      New England Nuclear
[$^3$H]norepinephrine                 Amersham
[$^3$H]RX 821002                      Amersham
isoflurane (Forene®)                  Abbott
isoproterenol                         Sigma
Lumasafe plus                         Lumac
medetomidine (Domitor®)               Pfizer
moxonidine                            Sigma
pertussis toxin                       Sigma
rilmenidine                           Tocris
ZD 7288                               Tocris

Unless otherwise stated, all chemicals were purchased from Sigma Aldrich, Germany.

## 4.    Solutions

Buffer solutions were prepared with Milli-Q® water according to protocol. Agonists / antagonists were dissolved in water for injections to yield a 10 mM stock solution.  These stock solutions were then diluted with the appropriate buffer (i.e. 50 mM Tris, pH =7.4 for binding and modified Tyrode's solution for organ bath experiments) or with sterile 0.9% NaCl water for injections for in vivo application.  Rilmenidine was an exception; due to its poor water solubility, it was first dissolved in 30 parts ethanol 96%, then filled up with 70 parts Milli-Q® water to yield a 10 mM stock solution.  The rilmenidine stock solution was then diluted as with the other ligands.

## 5.    Cell culture / tissue culture media

| | |
|---|---|
| DMEM high glucose | Invitrogen |
| FCS | Biochrom |
| Penicillin/Streptomycin | Biochrom |
| Trypsin EDTA | Invitrogen |
| G418 (geneticin) | Roche |

## 6.    Other materials

| | |
|---|---|
| Accu-Chek Sensor glucose meter | Roche |
| Accu-Chek Sensor Comfort test strip | Roche |
| Carbogen (95% $O_2$, 5% $CO_2$) | Linde, Unterschließheim |
| Glass slides | SuperFrost Menzel |
| GF/F glass fiber filters | Millipore |

Plastic tubing, syringes, needles, forceps, scissors, glass capillaries and other miscellaneous equipment were obtained from the company Hartenstein in Würzburg.

# V.  Results

## 1.        Characterization of $\alpha_{2ABC}$-KO mice

### 1.1.     Genotyping of $\alpha_{2ABC}$-KO mice

Mice carrying a targeted deletion in one, two, or all three $\alpha_2$-receptor subtypes were generated as described previously (Philipp et al., 2002c).  Figure 12 shows a simplified scheme for the generation of $\alpha_{2ABC}$-KO mice by crossing the two preexisting knock-out lines $\alpha_{2AC}$-KO and $\alpha_{2B}$-KO.  This project began with approximately 10 adult $\alpha_{2ABC}$-KO mice, despite the low survival rate of $\alpha_{2ABC}$-KO embryos.  Interbreeding of mice deficient in $\alpha_{2A}$- and $\alpha_{2C}$-subtypes but heterozygous for $\alpha_{2B}$ ($\alpha_{2A\text{-/-}B\text{+/-}C\text{-/-}}$) suggested that less than one of every 250 ($\alpha_{2A\text{-/-}B\text{-/-}C\text{-/-}}$) embryos was born and survived until weaning at three weeks of age (Philipp, 2002b).  Nevertheless, these mice were paired, and a few litters were produced.  This younger generation of $\alpha_{2ABC}$-KOs produced more offspring than the original breeding pairs.  With each generation, litter size and frequency appeared to increase, until six months later over 100 $\alpha_{2ABC}$-KO mice were recorded.
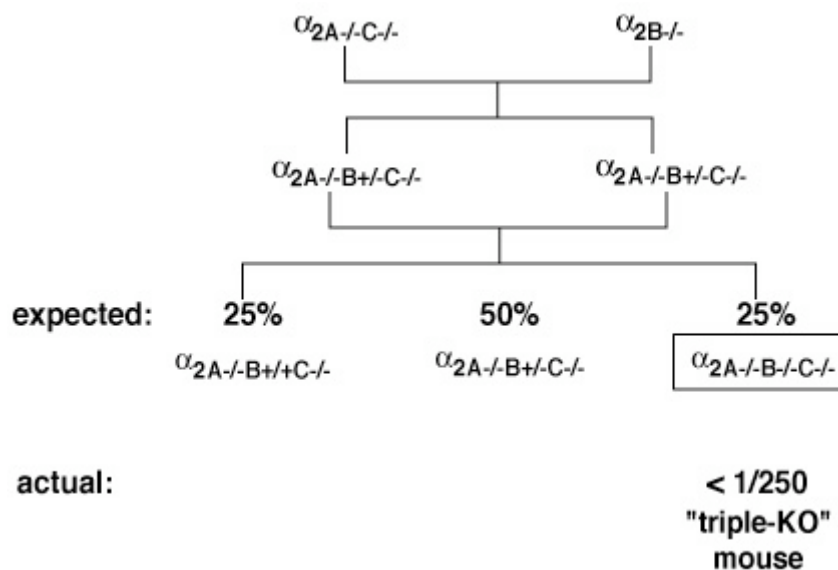


**Fig. 12:**  *Generation scheme for mice deficient in all three $\alpha_2$-receptor subtypes.*  *$\alpha_{2B}$-KOs were mated with $\alpha_{2AC}$-double KOs; their offspring were*

64

*interbred to yield mice lacking $\alpha_{2A}$- and $\alpha_{2C}$-subtypes but heterozygous for $\alpha_{2B}$ ($\alpha_{2A-/-B+/-C-/-}$). These mice were paired. Mendelian genetics predict 25% of their offspring to be $\alpha_{2ABC}$-KOs; however, a much lower percentage of $\alpha_{2ABC}$-KOs were born than expected.*

The $\alpha_{2ABC}$-KO mice studied in the course of this project resulted solely from the homozygous matings of the approximately 10 "original" $\alpha_{2ABC}$-KOs generated by the above scheme. Their genotype had been confirmed by PCR (see Methods, chapter 1.3.) using primers that annealed to the $\alpha_{2}$-DNA contained in the targeted allele on either end of the deleted base pairs as depicted in figure 13a. Four PCR reactions were performed to verify the genotype of $\alpha_{2ABC}$-KOs. While the wild-type and targeted alleles for $\alpha_{2A}$ and $\alpha_{2B}$ could be identified in a single PCR reaction, separate PCR reactions were necessary to distinguish the $\alpha_{2C}$ alleles. Figure 13b depicts a representative PCR analysis for wild-type mice and mice heterozygous and homozygous for the deletion of the given $\alpha_{2}$-subtype.
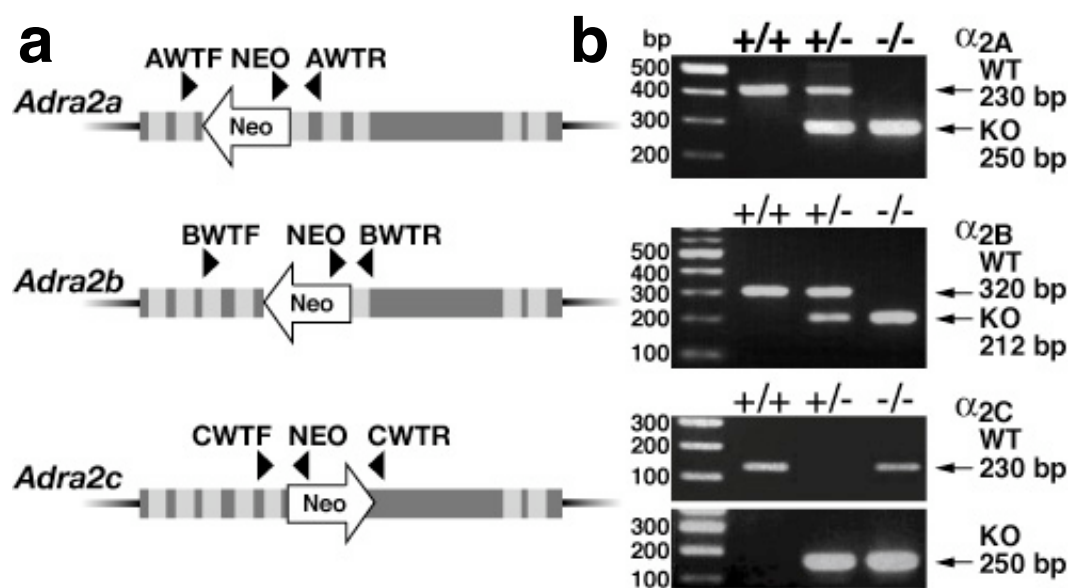


**Fig. 13:** *Generation of mice deficient in $\alpha_{2A}$-, $\alpha_{2B}$- and $\alpha_{2C}$-receptor subtypes. a, A simplified representation of the targeted alleles in $\alpha_{2}$-deficient mice. The DNA coding for each $\alpha_{2}$-subtype was disrupted by the insertion of a neomycin resistance cassette, rendering that $\alpha_{2}$-subtype nonfunctional. b, Representative genotyping analysis showing ethidium bromide-stained gels with PCR products for wild-type or $\alpha_{2}$-KO alleles. Adra2a, Adra2b and Adra2c are the genes encoding the $\alpha_{2}$-adrenergic receptor subtypes $\alpha_{2A}$, $\alpha_{2B}$ and $\alpha_{2C}$,*

65

*respectively. AWTF, BWTF and CWTF: forward primers and AWTR, BWTR and CWTR: reverse primers flanking the modified region of Adra2a, Adra2b and Adra2c, respectively. NEO = neomycin resistance gene.*
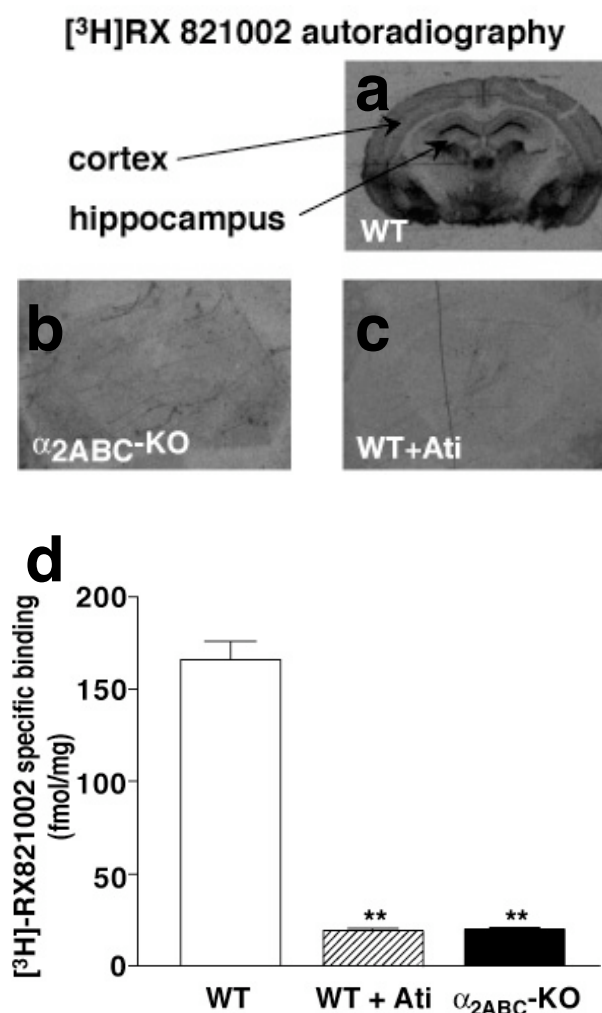
## 1.2. Radioligand binding

To further characterize the $\alpha_{2ABC}$-KO mouse, radioligand binding in $\alpha_{2ABC}$-KO heart and brain membranes was performed. The $\alpha_2$-specific antagonist [$^3$H]RX 821002 confirmed the absence of $\alpha_2$-receptor subtypes in $\alpha_{2ABC}$-KO mice. In addition, [$^3$H]clonidine binding was extensively studied in $\alpha_{2ABC}$-KO membranes. Although $\alpha_2$-receptor binding was absent, [$^3$H]clonidine did display high affinity for an unidentified binding site(s).

### 1.2.1. [$^3$H]RX 821002 autoradiography and membrane binding

Autoradiography of transverse brain sections from wild-type and $\alpha_{2ABC}$-KO mice was performed with 4 nM [$^3$H]RX 821002 (figures 14a-c). No specific binding with the $\alpha_2$-specific antagonist [$^3$H]RX 821002 was detectable in either brain slices or in whole brain membrane preparations of $\alpha_{2ABC}$-KO mice (Fig. 14b, d). The cortex and hippocampus, areas with a high density of $\alpha_2$-receptors, were prominently labeled in wild-type mice (Fig. 14a). No such labeling was seen in $\alpha_{2ABC}$-KO brain slices (Fig. 14b). In the presence of the specific $\alpha_2$-antagonist atipamezole, the binding observed in the wild-type brain slice closely resembled that in the $\alpha_{2ABC}$-KO brain slice (Fig. 14c). Radioligand binding with wild-type and $\alpha_{2ABC}$-KO whole brain membrane preparations was also performed (Fig. 14d). 4 nM [$^3$H]RX 821002 labeled approximately 170 fmol $\alpha_2$-receptors per mg protein in wild-type brain membranes. The very low binding in $\alpha_{2ABC}$-KO membranes was due to non-$\alpha_2$ binding sites, confirmed by the identical level of binding in wild-type membranes in the presence of 1 $\mu$M atipamezole. At this high concentration of specific $\alpha_2$-receptor antagonist, virtually all $\alpha_2$-binding sites in wild-type brain membranes were saturated. Both autoradiography as well as competition binding confirmed the lack of functional $\alpha_2$-subtypes in $\alpha_{2ABC}$-KO mice previously verified by PCR genotyping.

**Fig. 14:** *[³H]RX 821002 binding in wild-type (WT) and $\alpha_{2ABC}$-KO brains. a-c, Autoradiography of brain slices. a, [³H]RX 821002 binding in untreated wild-type brain slices clearly revealed sites containing a high density of $\alpha_2$-receptors. b, In contrast, the complete lack of [³H]RX 821002 binding in $\alpha_{2ABC}$-KO brain slices confirmed the absence of $\alpha_2$-receptors. c, The $\alpha_{2ABC}$-KO autoradiograph was indistinguishable from that of the wild-type brain slice incubated with atipamezole. d, Radioligand binding in whole brain membrane preparations of wild-type and $\alpha_{2ABC}$-KO mice. Bars represent the group means $\pm$ SEM of n=3 experiments. In contrast to wild-type brain membranes, no specific binding could be detected either in atipamezole-treated wild-type or in $\alpha_{2ABC}$-KO brain membranes with [³H]RX 821002 (p < 0.001).*



### 1.2.2. Saturation binding in wild-type and $\alpha_{2ABC}$-KO membranes

In order to test whether imidazoline ligands can detect specific binding sites in $\alpha_{2ABC}$-KO membranes, radioligand binding experiments with [³H]clonidine were performed. [³H]clonidine binding in wild-type brain membranes (figure 15a) demonstrated the high affinity of clonidine for and the density of $\alpha_2$-receptors in this organ. In contrast, most of the [³H]clonidine binding was missing in $\alpha_{2ABC}$-KO brain and heart membranes (Fig. 15b-c). However, $\alpha_{2ABC}$-KO specific binding curves (Fig. 15b) revealed a small but high affinity binding site in $\alpha_{2ABC}$-KO brain membranes for [³H]clonidine. A binding site with similar affinity but lower density was identified in $\alpha_{2ABC}$-KO heart membranes (Fig. 15c).

Clonidine affinity to the $I_1$-imidazoline binding site has been reported to be in a similar range, though values vary greatly depending on the species and tissue examined (Szabo, 2002). This initial observation led us to conduct further binding experiments in $\alpha_{2ABC}$-KO tissue. Since the detection of the presence of a small, high affinity binding site was in and of itself not adequate proof of having identified an imidazoline binding site in the absence of $\alpha_2$-receptors, competition studies were conducted with ligands possessing mixed $\alpha_2$ / imidazoline affinity in order to characterize this binding site.



**Fig. 15:** **_[$^3$H]clonidine saturation binding curves in wild-type and $\alpha_{2ABC}$-KO membranes._ _a_**, _Binding sites for [$^3$H]clonidine in wild-type brain membranes were to a great extent attributable to $\alpha_2$-adrenergic receptors._ _**b**_, $\alpha_{2ABC}$-KO brain membranes displayed approximately one-third of the binding sites of wild-type membranes. _**c**_, The binding sites in $\alpha_{2ABC}$-KO heart membranes, though lower in density, showed a comparable affinity to [$^3$H]clonidine as in $\alpha_{2ABC}$-KO brain membranes. Each data point expresses the triplicate mean ± SEM of a given sample. The saturation curves depicted above are representative of the binding assays performed in wild-type and $\alpha_{2ABC}$-KO brain membranes (n=3) and $\alpha_{2ABC}$-KO heart membranes (n=3), from which the $K_d$ and $B_{max}$ values in the following table (1) were calculated.
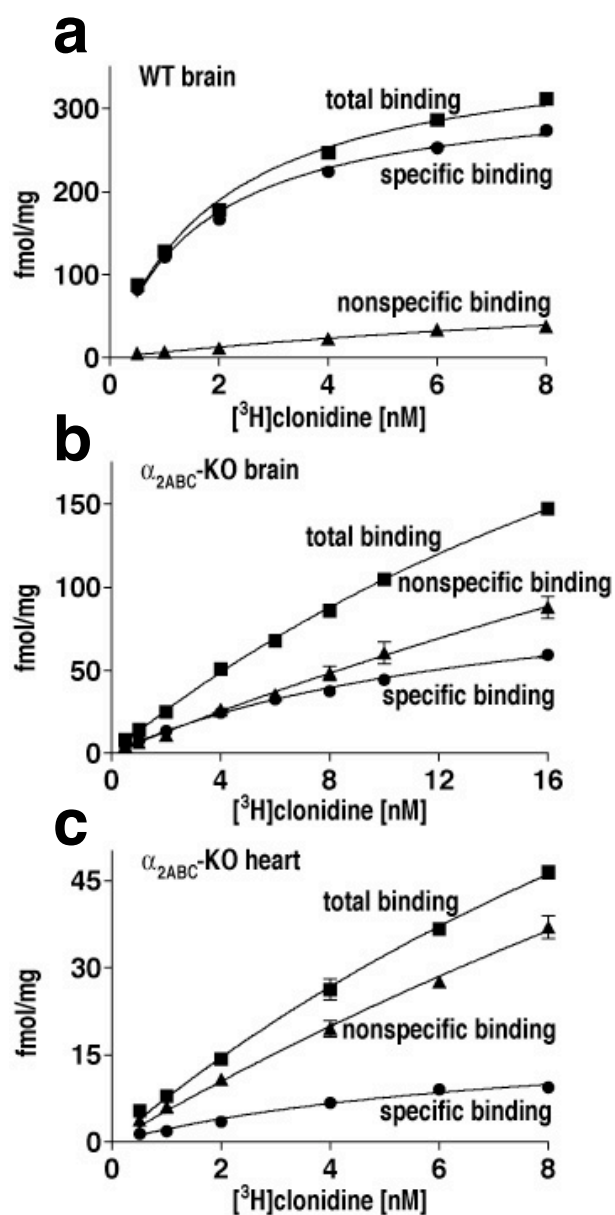
|  | tissue | $K_d$ | $B_{max}$ |
|---|---|---|---|
| **WT** | brain | 1.7 $\pm$ 0.2 nM | 327 $\pm$ 11 fmol/mg |
| $\alpha_{2ABC}$-**KO** | brain | 15.0 $\pm$ 1.6 nM | 113 $\pm$ 7 fmol/mg |
| $\alpha_{2ABC}$-**KO** | heart | 7.8 $\pm$ 2.4 nM | 20 $\pm$ 3 fmol/mg |

**Tab. 1:** *Summary of $K_d$ and $B_{max}$ values for wild-type brain and $\alpha_{2ABC}$-KO brain and heart membranes with [$^3$H]clonidine.* Approximately two-thirds of [$^3$H]clonidine-binding sites in mouse brain could be attributed to $\alpha_2$-receptors, as whole brain membrane preparations from mice deficient in all three $\alpha_2$-receptor subtypes displayed only one-third of the binding site density of those from wild-type mice. Despite the large discrepancy between wild-type and $\alpha_{2ABC}$-KO $B_{max}$ values, [$^3$H]clonidine appeared to possess a similar affinity to one or more common binding sites in both wild-type and $\alpha_{2ABC}$-KO membranes, as $K_d$ values were all in the low nanomolar range.

1.2.3. Competition binding in $\alpha_{2ABC}$-KO membranes

Since the nature of the high affinity binding site for [$^3$H]clonidine in $\alpha_{2ABC}$-KO whole brain and whole heart membranes was not known, competition binding experiments with (non-radioactive) clonidine, moxonidine and rilmenidine were first conducted in order to establish whether or not the binding profile of this site matched that of an imidazoline binding site. While three different imidazoline binding sites have been described (see Introduction 3.5.2.), it was most logical that the $I_1$ binding site, widely distributed and often in close proximity to $\alpha_2$-adrenergic receptors (Dontenwill et al., 1999), would be the best candidate for the "non-$\alpha_2$" binding site found in $\alpha_{2ABC}$-KOs with [$^3$H]clonidine.
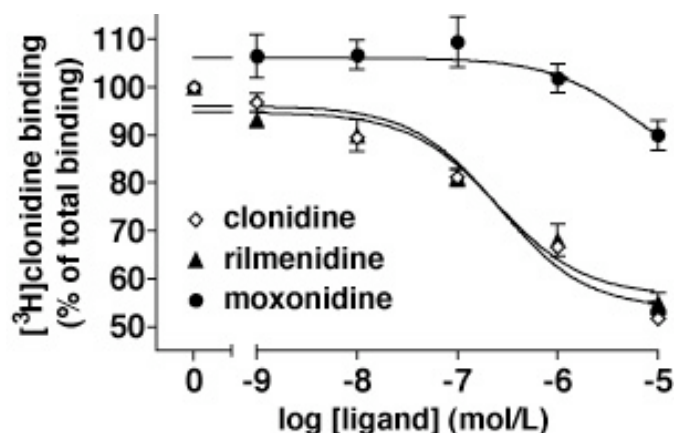
**Fig. 16: [³H]clonidine competition binding in α₂ABC-KO brain membrane preparations.** *Below 1 µM concentration, moxonidine did not displace 8 nM [³H]clonidine from its binding site on α₂ABC-KO brain membranes, while rilmenidine (IC₅₀ = 0.25 µM) and clonidine (IC₅₀ = 0.26 µM) possessed similar affinities to this binding site. Each data point expresses the mean ± SEM of n=3 experiments (moxonidine and rilmenidine) or n=5 experiments (clonidine) performed in triplicate. The IC₅₀ values of clonidine (0.26 µM, 95% confidence interval [CI] 0.17 µM to 0.40 µM) and rilmenidine 0.25 µM, 95% CI 0.11 µM to 0.56 µM) were calculated from these competition curves.*

Moxonidine and rilmenidine are widely accepted to possess higher $I_1$ selectivity as compared to clonidine (Ernsberger et al., 1993), which is believed to account for the occurrence of fewer side effects with these "second-generation" central antihypertensives than with the prototype clonidine. Unexpectedly, these two substances showed very different competition binding profiles than clonidine itself (figure 16). Rilmenidine was, however, able to displace just as much of the radiolabeled clonidine as the non-labeled clonidine, suggesting that rilmenidine competed for this non-$\alpha_2$ binding site in α₂ABC-KO brain membranes as well as clonidine.

A number of imidazoline-containing substances, including the highly selective $I_1$-ligand AGN 192403 and the endogenous clonidine displacing substance agmatine (Meeley et al., 1986), were screened at a single concentration of 1 µM to assess their ability to compete with [³H]clonidine (figure 17). While agmatine, atropine, cimetidine, prazosin, rauwolscine and RX 821002 at 1 µM concentrations did not appear to displace any [³H]clonidine from its binding site, both AGN 192403 and the "selective" $\alpha_2$-antagonist atipamezole were able to do so by approximately 18% and 24% (figure 17), respectively.

70

Moxonidine and efaroxan, a mixed $\alpha_2$ / imidazoline antagonist with apparently similar $I_1$-binding site affinities (Separovic et al., 1996), were comparable in their ability to displace less than 10% of total [$^3$H]clonidine binding; these results were not significant.
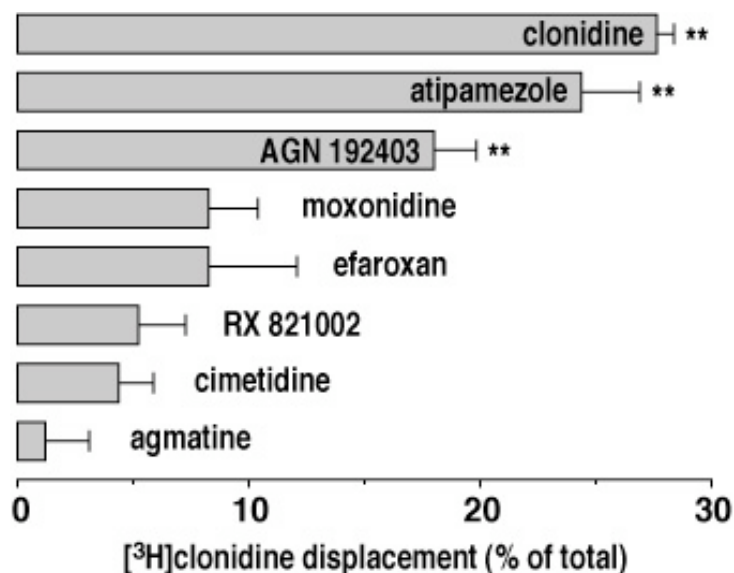


**Fig. 17:** *Displacement of [$^3$H]clonidine by $\alpha_2$ / imidazoline ligands. Assessment of the ability of ligands with reported imidazoline binding site affinity to displace 8 nM [$^3$H]clonidine from $\alpha_{2ABC}$-KO brain membranes. Besides clonidine itself, only the high affinity $I_1$-ligand AGN 192403 and atipamezole were able to significantly compete with the radioligand for this site ($p < 0.001$, one-way ANOVA).*

Although the results from binding experiments indicated that there was a non-$\alpha_2$ high affinity binding site present in $\alpha_{2ABC}$-KO brain and heart tissue, it was not possible to identify this site by means of competition binding. While the appreciable ability of AGN 192403, a ligand found to be highly selective for $I_1$ binding sites (Munk et al., 1996), to compete with [$^3$H]clonidine for this binding site was indicative of an imidazoline $I_1$ site, the complete lack of affinity of the endogenous clonidine displacing substance agmatine for this site was not consistent with an $I_1$ binding profile. The low affinity of moxonidine for this non-$\alpha_2$ site also did not support the plausibility of an imidazoline binding site. All in all, radioligand binding experiments with [$^3$H]clonidine did not confirm the existence of previously proposed $I_1$, $I_2$ or $I_3$ imidazoline binding sites in $\alpha_{2ABC}$-KO membranes.

### 1.3.  Inhibition of [$^3$H]norepinephrine release

Presynaptic $\alpha_2$-autoreceptors control norepinephrine release via a negative feedback mechanism (Starke, 2001).  When this safeguard is absent, as in the case of $\alpha_{2ABC}$-KO mice, catecholamine levels may exceed normal values (see 1.4.).  As a functional control of the absence of $\alpha_2$-receptors, atria from wild-type and $\alpha_{2ABC}$-KO mice were preloaded with [$^3$H]norepinephrine and then electrically stimulated to evoke release of the tritiated neurotransmitter.  The radioactivity released from the atria was measured before and after addition of exogenous norepinephrine in increasing concentrations from 0.1 nM up to 1 $\mu$M.  The agonist norepinephrine stimulated presynaptic $\alpha_2$-receptors in wild-type mice, decreasing the amount of [$^3$H]norepinephrine released in a concentration-dependent manner.  As expected, the amount of radioactivity released following stimulation of $\alpha_{2ABC}$-KO atria remained constant over time (figure 18).
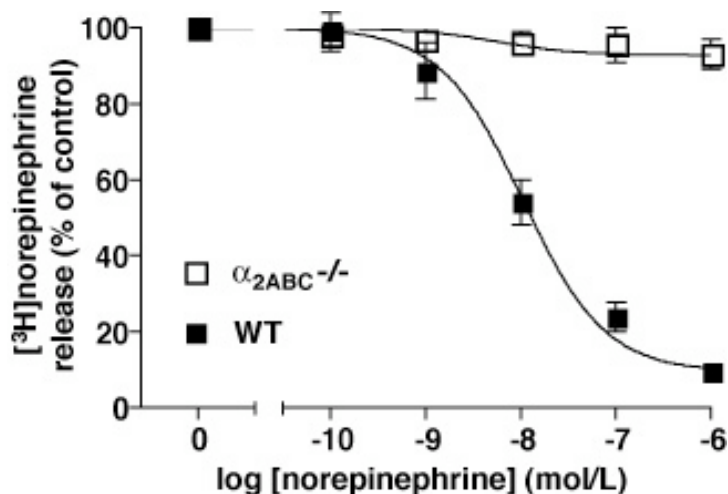


**Fig. 18:  *Inhibition of [$^3$H]norepinephrine release in wild-type and $\alpha_{2ABC}$-KO atria.*** *Electrical stimulation evoked release of the tritiated neurotransmitter in both groups.  Norepinephrine applied to the superfusion medium decreased the electrically induced [$^3$H]norepinephrine release in wild-type atria but not in $\alpha_{2ABC}$-KO atria (n=6 atria per genotype).*

### 1.4.  Urine catecholamine levels

The endogenous catecholamine norepinephrine serves as the postganglionic neurotransmitter in sympathetic fibers. Methylation of norepinephrine primarily in the adrenal medulla by the enzyme phenylethanolamine N-methyl

transferase (PNMT) yields the hormone epinephrine. Levels of these catecholamines and their precursors in urine and blood are often elevated in the early stages of heart failure (where symptoms first become manifest), as well as in the presence of some neuroendocrine tumors (e.g. pheochromocytoma). Determination of catecholamine concentration in urine collected over 24 hours was achieved by HPLC followed by electrochemical detection.
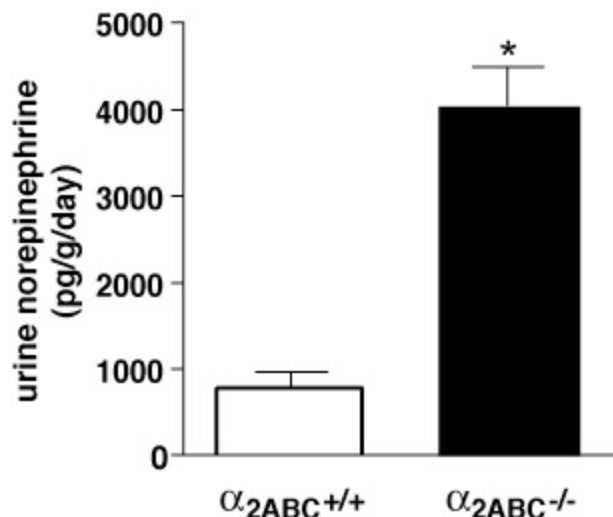


**Fig. 19:** *24-hour urine norepinephrine in wild-type and $\alpha_{2ABC}$-KO mice. HPLC measurement of 24-hour urine collected from wild-type (n=10) and $\alpha_{2ABC}$-KO (n=8) mice revealed significantly elevated norepinephrine levels in mice deficient in all three $\alpha_2$-subtypes (* $p < 0.05$).*

1.5.    Adverse cardiovascular consequences of the deletion of all three $\alpha_2$-receptor subtypes

Because of the critical role played by $\alpha_2$-receptors as autoinhibitors of norepinephrine release in both central and peripheral sympathetic nervous system compartments, it was anticipated that deletion of all three $\alpha_2$-receptor subtypes would have some, if not detrimental, effects on the cardiovascular system. In order to assess any morphological or functional abnormalities in blood vessels and heart, blood pressure, heart rate and left ventricular function were determined and hearts were examined both macroscopically as well as microscopically.

## 1.5.1. Resting blood pressure and heart rate

A microtip catheter inserted into the left ventricle was used to measure resting blood pressure and cardiac function in isoflurane-anesthetized mice. Compared to wild-type mice, $\alpha_{2ABC}$-KO mice showed a significantly higher resting blood pressure (figure 20). Of the three $\alpha_2$-double KO lines, only the $\alpha_{2AC}$-KO mice displayed hypertension in their resting blood pressure. The other two double-KO lines did not differ significantly from wild-type mice (not shown). These findings corroborate previous data demonstrating the relative contribution of each $\alpha_2$-subtype to presynaptic inhibition of norepinephrine release (Hein et al., 1999; Trendelenburg et al., 2003).
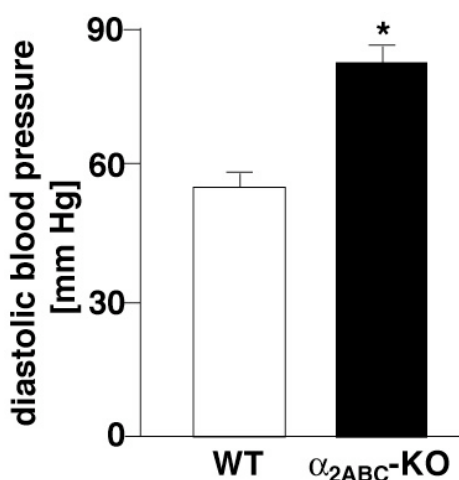


**Fig. 20:** ***Resting diastolic blood pressure in wild-type and $\alpha_{2ABC}$–KO mice.*** *Mice lacking all three $\alpha_2$-receptor subtypes displayed significantly higher resting blood pressure than wild-type mice (p < 0.001, one-way ANOVA, n=6-8).*

In order to confirm that the elevated blood pressure in $\alpha_{2ABC}$-KO mice was not related to the anesthetic, these measurements were later repeated with awake, unrestrained $\alpha_{2ABC}$-KO and age-matched wild-type mice. Resting blood pressure in these mice was determined by pressure telemetry with an indwelling catheter placed in the left carotid artery (figure 21). Although baseline blood pressure was markedly higher in both groups, means of both diastolic and systolic blood pressure recorded over a 24-hour period of $\alpha_{2ABC}$-KO mice were nearly 30 mm Hg higher than the wild-type means. This difference in blood pressure between the groups was similar to that observed in anesthetized mice, suggesting that isoflurane affected both groups equally.
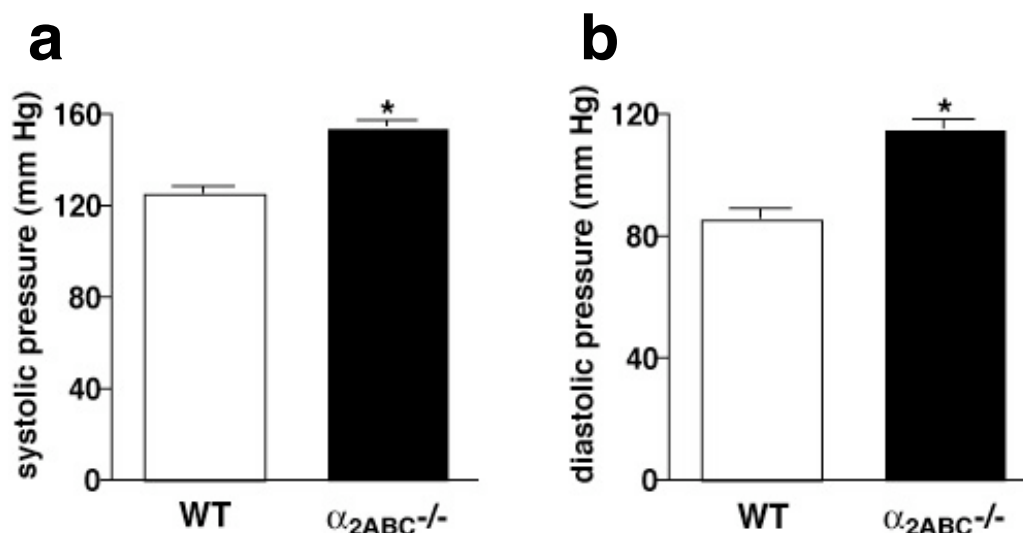
**Fig. 21:** *24-hour mean resting systolic (a) and diastolic (b) blood pressure in awake, freely-moving wild-type and $\alpha_{2ABC}$-KO mice.* With the aid of pressure telemetry, the significantly higher basal blood pressure in $\alpha_{2ABC}$-KOs compared to age-matched wild-type mice could be determined without possible obscuration by anesthesia. Blood pressure measured in the aorta of $\alpha_{2ABC}$-KO mice was higher both during systole and diastole than in wild-type mice (* $p < 0.05$, unpaired t test, n=6 per group).

Resting heart rate was likewise determined by means of pressure telemetry as described above. The lack of feedback inhibition by $\alpha_2$-adrenergic receptors not only significantly increased blood pressure but also basal heart rate in $\alpha_{2ABC}$-KO mice compared to age-matched wild-type controls (figure 22). The mean beating frequency over a 24-hour period measured in $\alpha_{2ABC}$-KO mice was over 50 beats per minute higher than in wild-type controls.



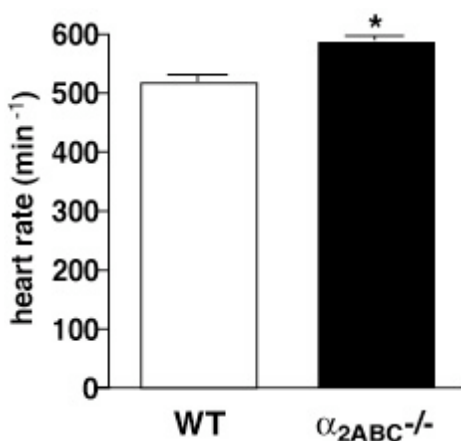**Fig. 22:** *24-hour mean heart rate in awake, unrestrained wild-type and $\alpha_{2ABC}$-KO mice measured with pressure telemetry.* On average, $\alpha_{2ABC}$-KO mice displayed a significantly higher beating frequency (approximately 585 bpm) compared with wild-type controls (520 bpm). Each bar represents the group mean of n=6 mice $\pm$ SEM (* $p < 0.05$, unpaired t test).

75

### 1.5.2. Cardiac hypertrophy

Two common methods to assess the degree of cardiac hypertrophy are the comparison of the heart weight [mg] to tibia length [mm] ratios (figure 23a) as well as the comparison of heart weight [mg] to body weight [g] (figure 23b). The latter ratio in a "normal" healthy mouse without obesity or cardiac hypertrophy or remodeling is approximately 5 or less. Values significantly higher ($\geq 6$) than age-matched healthy controls are indicative of the presence of cardiac hypertrophy.
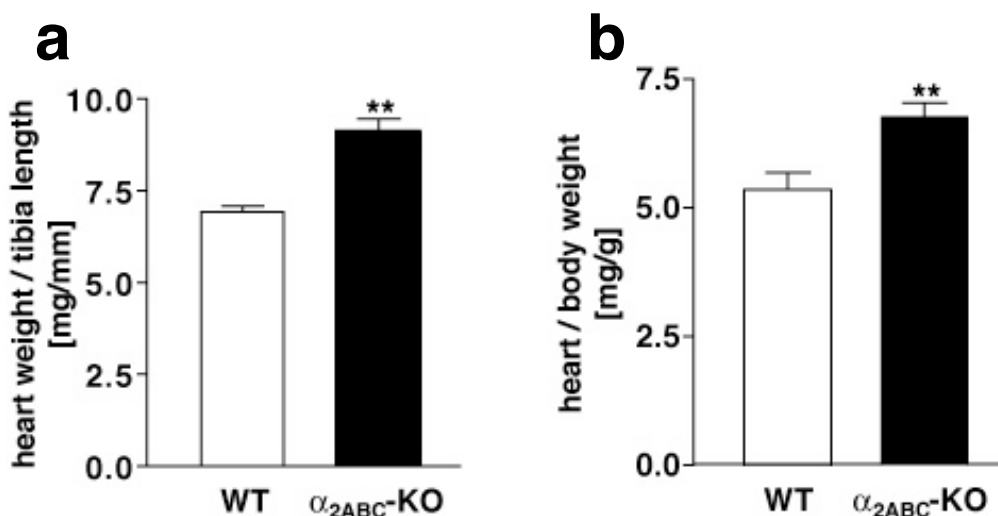


**Fig. 23:** *Cardiac hypertrophy in $\alpha_{2ABC}$-KO mice. a, Ratio of heart weight [mg] to tibia length [mm] in wild-type and $\alpha_{2ABC}$-KO mice. Each bar represents the group mean $\pm$ SEM. Mice deficient in all three $\alpha_2$-receptor subtypes (n=10) showed significantly greater (p = 0.0013, unpaired t test) ratios than age-similar wild-type mice (n=5). b, Comparison of the ratio of heart weight [mg] to body weight [g] of 2-4 month old wild-type and $\alpha_{2ABC}$-KO male mice. Each bar depicts the mean ratio $\pm$ SEM of the respective group. This ratio was again significantly higher (p = 0.0028) in $\alpha_{2ABC}$-KO mice (n=25) compared to age-matched wild-type mice (n=11).*

When examined under a microscope, wild-type and $\alpha_{2ABC}$-KO hearts showed a significant difference in left ventricular myocyte size. Deletion of all three $\alpha_2$-receptor subtypes coincided with increased cross-sectional areas of left ventricular myocytes (figures 24b and 24d). Increased fibrotic tissue was observed in $\alpha_{2ABC}$-KO myocytes as compared to wild-type myocytes after staining with Sirius red (figure 26). The enlarged myocytes, accompanied by

76

fibrotic change, substantiated the role of autoinhibitory $\alpha_2$-receptors when compared with wild-type myocytes.
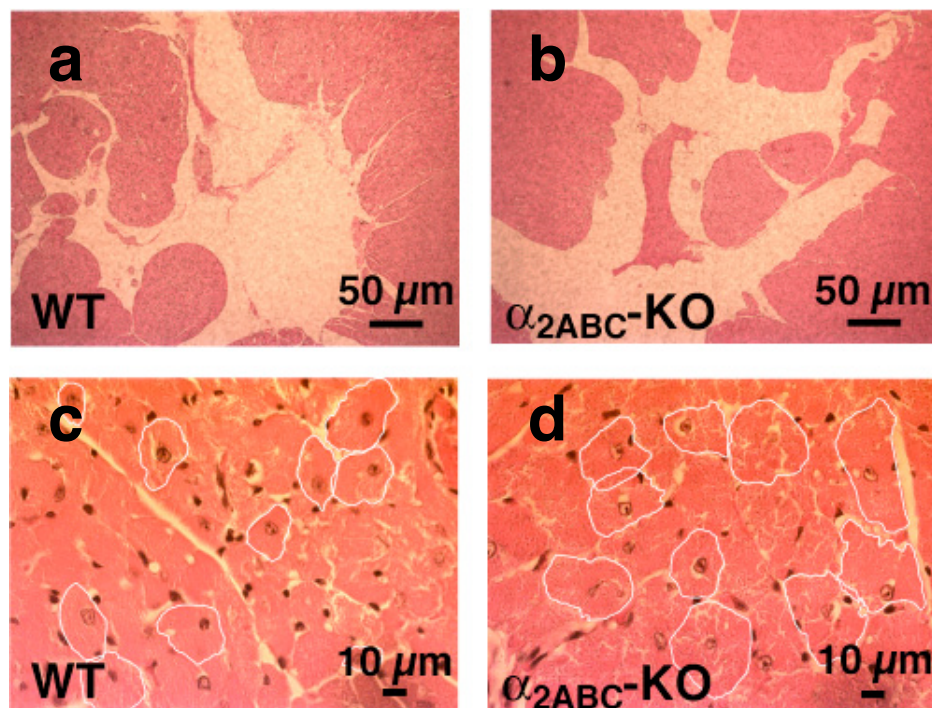


**Fig. 24:** *Cross-sectional view of left ventricle from wild-type and $\alpha_{2ABC}$-KO mice with HE-staining. a-b,* *View of left ventricular cavity at low magnification from a representative wild-type (a) and $\alpha_{2ABC}$-KO (b) mouse.* *c-d, View of left ventricular wall adjacent to the papillary muscle at a higher magnification from a representative wild-type (c) and $\alpha_{2ABC}$-KO (d) mouse. Individual myocytes of WT (n=4) and $\alpha_{2ABC}$-KO (n=4) mice were outlined as shown, and the area of each myocyte was determined morphometrically. A total of 10 regions were selected in 3-4 slides per mouse; between 7 and 10 myocytes were quantified per region (results see figure 25).*



**Fig. 25:** *Mean cross-sectional areas of wild-type and $\alpha_{2ABC}$-KO left ventricular myocytes.* *Left ventricular myocytes from WT (n=4) and $\alpha_{2ABC}$-KO (n=4) mice were obtained as described above (figure 24). Bars depict the group mean $\pm$*

*SEM. In the absence of $\alpha_2$-receptors, myocyte area was significantly increased in comparison to wild-type myocyte area (p=0.0023; two-tailed unpaired t test).*

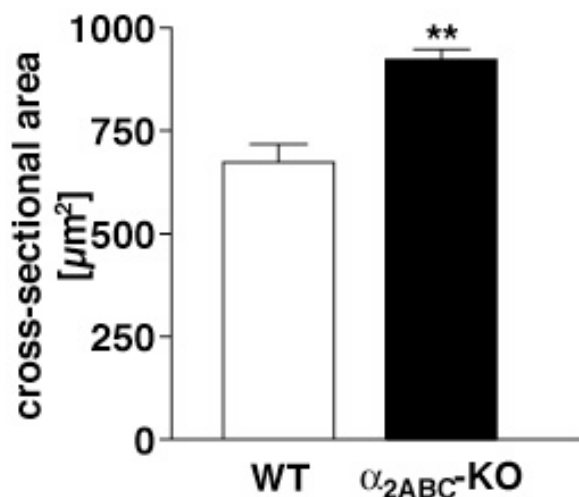### 1.5.3. Fibrosis

Cardiac fibrosis is characterized by an abnormal expansion of the extracellular collagen-rich matrix surrounding cardiac myocytes. Matrix fibers may grow in the presence of an acute stimulus (i.e. myocardial infarct) or after long-term exposure to hypertension or coronary atherosclerosis, resulting in remodeling of cardiac tissue and an impairment of myocyte contractile function. A reduced contractility that results in a sufficiently great impairment of left ventricular function may ultimately precipitate overt heart failure.

Cross-sectional slices of ventricles from male wild-type and $\alpha_{2ABC}$-KO mice (6-9 months) showed widespread interstitial fibrotic changes in the $\alpha_{2ABC}$-KO left ventricle. In contrast, the wild-type ventricle showed virtually no fibrosis (figure 26). This is not surprising given the significantly higher resting blood pressure observed in $\alpha_{2ABC}$-KO mice in comparison to wild-type mice (see figure 20).

**a**
WT
50 µm

**b**
α2ABC-/-
50 µm
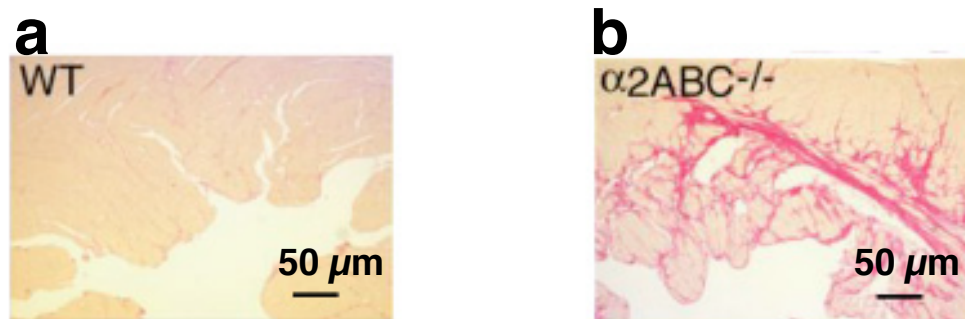
**Fig. 26:** *Cross-sectional view of wild-type (a) and $\alpha_{2ABC}$-KO (b) hearts. Sirius red staining of cross-sectional slices under 5x magnification revealed extensive cardiac fibrosis in the left ventricle of male $\alpha_{2ABC}$-KO mice (b) but not in wild-type mice (a) at 6-9 months of age.*

### 1.5.4. Left ventricular function

One widely used parameter to assess cardiac function is shortening fraction, which measures the percent decrease in left ventricular (LV) diameter during contraction in relation to the left ventricular diameter at the end of diastole.

Both left ventricular systolic and diastolic diameters can be obtained by ultrasonic measurement (echocardiography).

To determine what effect – if any – deletion of all three $\alpha_2$-subtypes had on left ventricular function, echocardiography was performed on wild-type and $\alpha_{2ABC}$-KO mice. The LV end diastolic and end systolic diameters were obtained and the shortening fraction was calculated. In wild-type mice, fractional shortening was 50%, while in $\alpha_{2ABC}$-KO mice this parameter was significantly reduced to 33% (figure 27).
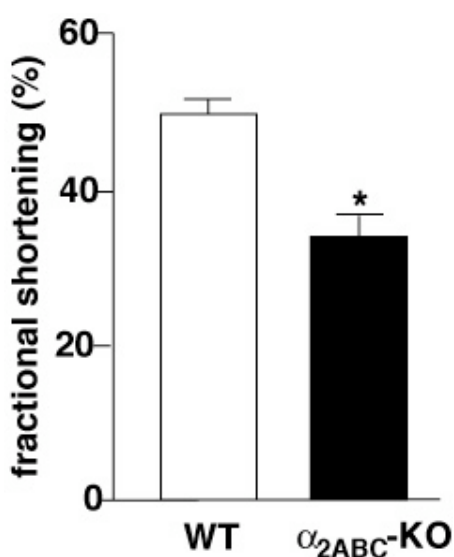


**Fig. 27: *Fractional shortening in wild-type and $\alpha_{2ABC}$-KO mice.*** Bars depict the group mean $\pm$ SEM of the left ventricular function measured in WT (n=6) and $\alpha_{2ABC}$-KO (n=6) mice. Mice lacking all three $\alpha_2$-receptor subtypes showed a significantly lower shortening fraction than wild-type mice (p < 0.05, two-tailed unpaired t test), suggesting that left ventricular function was impaired in the absence of $\alpha_2$-receptors.

## 2. Effects of $\alpha_2$ / imidazoline agonists in $\alpha_{2ABC}$-KO mice

### 2.1. Sedation

One common side effect of clonidine is drowsiness. The sedative qualities of clonidine are believed to be related to its $\alpha_2$-receptor affinity; the observation that moxonidine and rilmenidine may cause less drowsiness than clonidine is generally rationalized by the higher $I_1$-imidazoline selectivity of these drugs compared to clonidine (for review, see Szabo, 2002). Another possible explanation is that these "second-generation" central antihypertensives are simply less potent than clonidine (Macphee et al., 1992).

A rotarod model was used to test the sedative qualities of these $\alpha_2$ / imidazoline agonists in wild-type and $\alpha_{2ABC}$-KO mice (figure 28). Following the baseline (untreated) measurement, clonidine, moxonidine and rilmenidine were each administered as a single ip dose of 50 $\mu$g drug. Due to the high degree of sedation achieved in wild-type mice with the identical dose of medetomidine, both groups received only 25 $\mu$g medetomidine. Fifteen minutes later, the time each mouse could still balance on the rotarod before falling off was determined; this time was expressed in percent of the untreated time. Clonidine greatly impaired the ability of wild-type mice to balance on the rotating rod, while moxonidine showed only a slight sedative effect. Rilmenidine had no significant effect on wild-type coordination. The "selective" $\alpha_2$-agonist medetomidine surpassed clonidine in its sedating effects, affirming its use as a veterinary tranquilizer. Mice deficient in all three $\alpha_2$-receptor subtypes were not hindered in their performance on the rotarod by any of the agonists, clearly demonstrating that the sedative properties of clonidine and moxonidine are indeed $\alpha_2$-mediated.
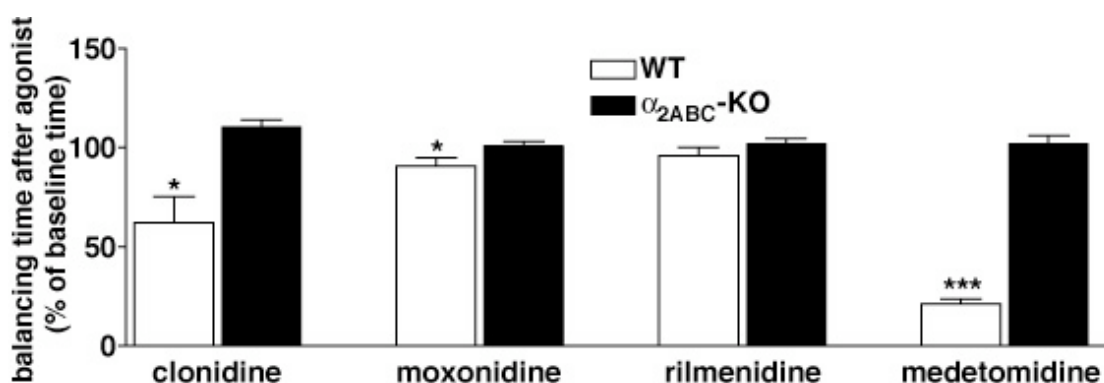


**Fig. 28:** *Rotarod evaluation of the sedative properties of four $\alpha_2$-agonists with imidazoline (or imidazoline-like) structure. Each bar depicts the group mean balancing time on the rotarod following agonist injection, expressed in % of time on the rotarod prior to injection, $\pm$ SEM. In wild-type mice, medetomidine showed the strongest sedative effect (p < 0.0001), followed by clonidine (p = 0.017) and, to a much lesser extent, moxonidine (p = 0.049). $\alpha_{2ABC}$-KO mice displayed no impairment in their performance on the rotarod after agonist treatment. Statistical significance was determined using the two-tailed unpaired t test; n=6 per group.*

## 2.2. Analgesia

The analgesic efficacy of clonidine is well established. If used prior to or during surgery, it may reduce the amount of anesthetic needed (Watanabe et al., 2006). In addition, the analgesic action of clonidine is independent of that of morphine and may complement the efficacy of opioid analgesics (Özdogan et al., 2004). The long use of clonidine in surgery supports its safety and efficacy, and has contributed to its application in pediatric medicine (Bergendahl et al., 2006).

A tail-flick apparatus was used to assess the relative analgesic potencies of clonidine, moxonidine and rilmenidine in wild-type and $\alpha_{2ABC}$-KO mice (figure 29). Each mouse received 50 $\mu$g drug following the baseline (untreated) measurement. The time that passed until each mouse in a given group removed its tail from the thermal stimulus following agonist injection was determined and expressed in percent of the untreated time. Upon comparison of the group means, clonidine significantly increased pain threshold in wild-type mice. Moxonidine and rilmenidine did not appear to produce an analgesic effect in wild-type mice (n=6) under these conditions. None of the three drugs elicited any analgesic response in $\alpha_{2ABC}$-KO mice. These results were not surprising, as previous findings have demonstrated the considerable contribution of the $\alpha_{2A}$-subtype to the analgesic effect of clonidine (Lakhlani et al., 1997).
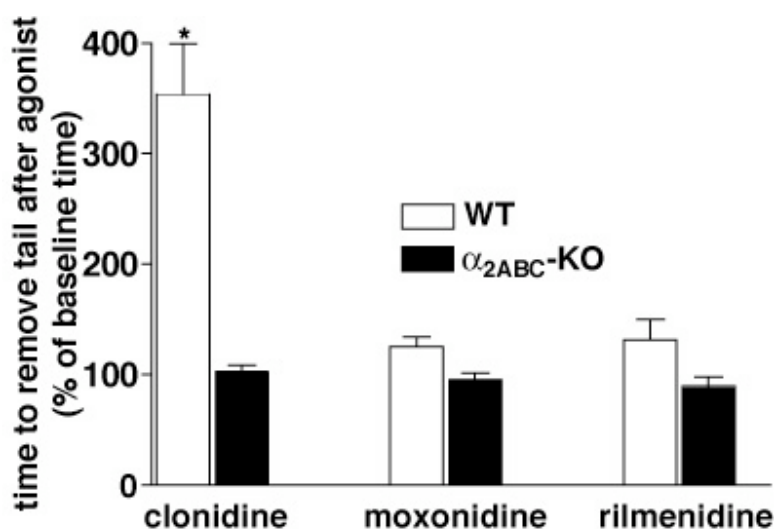


**Fig. 29: Tail-flick assay to assess the analgesic potency of three $\alpha_2$-agonists in wild-type and $\alpha_{2ABC}$-KO mice.** *Each bar depicts the group mean*

*time, expressed as % of mean baseline time, to remove tail from the thermal stimulus, $\pm$ SEM. Of the three $\alpha_2$-agonists, only clonidine was capable of significantly increasing pain threshold in wild-type mice (p = 0.0161, n=3). Although moxonidine has previously been shown to decrease pain sensation in wild-type mice (Fairbanks and Wilcox, 1999), in this experimental design no significant effect of moxonidine or rilmenidine was observed (n=6). $\alpha_{2ABC}$-KO mice (n=7) experienced no analgesic effect from any of these $\alpha_2$-agonists.*

## 2.3.  Glycemic response

Activation of $\alpha_2$-receptors in the pancreas directly inhibits insulin release. Therefore, administration of an $\alpha_2$-agonist to a wild-type mouse should lead to an acute hyperglycemic response within minutes. Plasma glucose concentration was determined for each mouse before and after agonist administration; the mean plasma glucose level of the respective group of mice at 30, 60 and 90 minutes was expressed in percent of the first measurement at t = 0, immediately prior to agonist injection (figure 30).  Wild-type mice displayed significant increases in plasma glucose levels with moxonidine, clonidine and rilmenidine.  In mice lacking all three $\alpha_2$-receptor subtypes, a significant hypoglycemic response only after clonidine administration was observed.
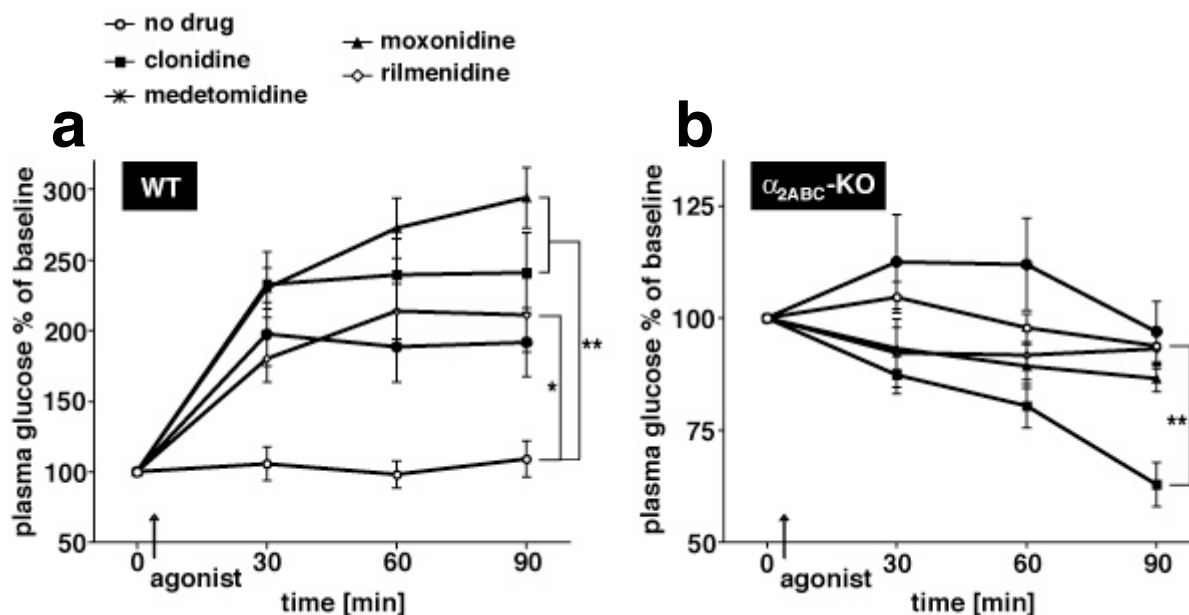


**Fig. 30:  *Acute glycemic response to $\alpha_2$ / imidazoline agonists in wild-type and $\alpha_{2ABC}$-KO mice.  a**, 90 minutes after agonist injection, moxonidine*

*and clonidine elicited a highly significant hyperglycemic response in wild-type mice (p < 0.001); rilmenidine was slightly less effective (p < 0.05).  **b**, In $\alpha_{2ABC}$-KO mice only clonidine showed a significant hypoglycemic effect at t = 90 min (p < 0.001).  The points on the curves represent the group mean ± SEM of n=6-8 wild-type and n=7-13 $\alpha_{2ABC}$-KO mice per group.  Control mice ("no drug") did not receive agonist injection, but blood was sampled at t = 0, 30, 60 and 90 min as with the mice receiving agonist.  Statistical significance was determined by one-way ANOVA.*

## 2.4.  Cardiovascular effects

Blood pressure of anesthetized wild-type and $\alpha_{2ABC}$-KO mice was monitored by catheterization of the femoral artery.  Clonidine was administered via injection into a venous catheter.  In wild-type mice, clonidine dose-dependently reduced diastolic and systolic blood pressure and heart rate (figure 31a).  In contrast, no hypotensive effect could be observed after clonidine injection in $\alpha_{2ABC}$-KO mice (figure 31b).  However, heart rate of $\alpha_{2ABC}$-KO mice was reduced by approximately 60 bpm after injection of 150 $\mu$g/kg clonidine (figure 31b).



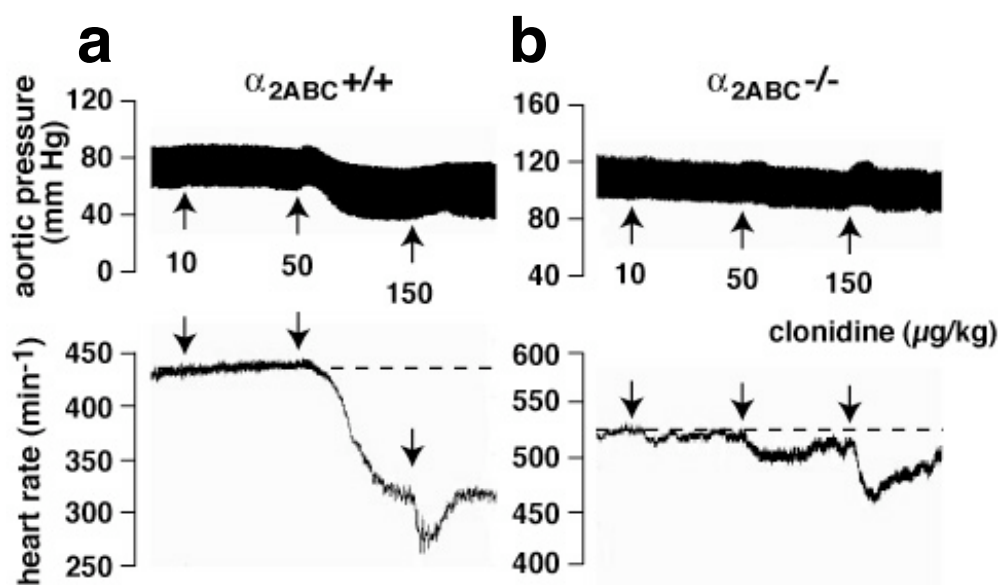**Fig. 31:  *In vivo monitoring of $\alpha_2$ / imidazoline agonist effects in anesthetized $\alpha_{2ABC}$-KO mice.*  *Shown are representative trace recordings of blood pressure and heart rate prior to and following administration of clonidine at doses of 10, 50 and 150 $\mu$g/kg mouse body weight.  No significant decrease in baseline blood pressure was observed in any of the $\alpha_{2ABC}$-KOs tested after*

*clonidine treatment. However, heart rate in both groups did decrease in a dose-dependent manner, $\alpha_{2ABC}$-KO heart rate albeit to a lesser extent.*

To compensate for a possible influence of isoflurane anesthesia on these results, ECG sensors were transplanted into wild-type and $\alpha_{2ABC}$-KO mice, allowing telemetric monitoring of heart rate in conscious, freely moving mice. These experiments were performed by Nadine Beetz and Lutz Hein at the University of Freiburg. Intraperitoneally-administered clonidine decreased resting heart rate in both groups in a dose-dependent manner (figure 32). Although the bradycardic response to clonidine was attenuated in $\alpha_{2ABC}$-KO mice compared to wild-type mice, the $\alpha_2$-independent decrease in $\alpha_{2ABC}$-KO heart rate nevertheless constituted 32%, 27% and 43% of the clonidine-induced bradycardia in wild-type mice at 10, 100 and 300 $\mu g/kg$, respectively.
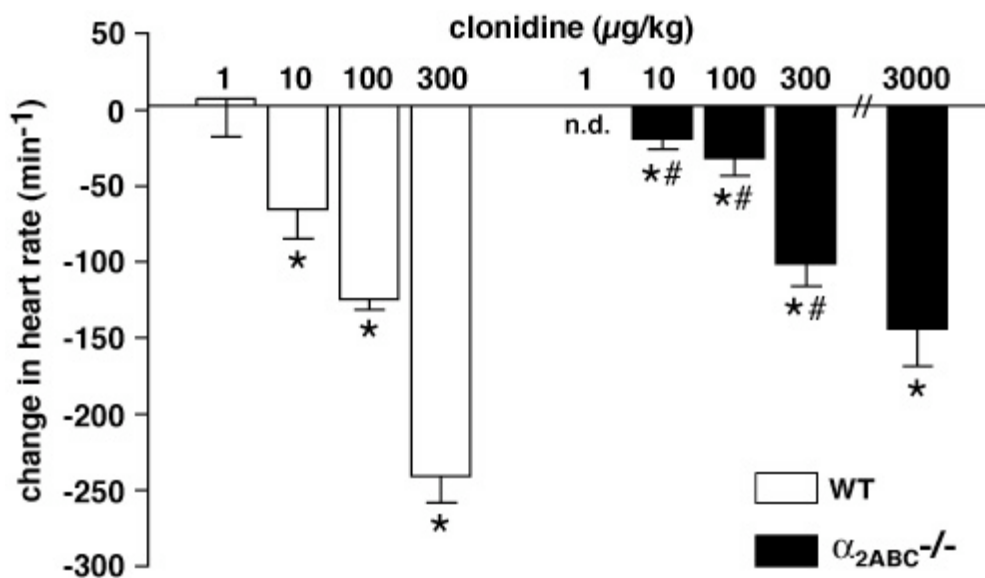


**Fig. 32: *Systemic administration of clonidine in conscious wild-type and $\alpha_{2ABC}$-KO mice.*** *Similar to experiments conducted in anesthetized mice (figure 31), clonidine lowered resting heart rate to a lesser extent in mice lacking $\alpha_2$-receptors than in wild-type mice. In awake mice, the significance of the bradycardic effects of clonidine both within (\* denotes $p < 0.05$) and between (#) the groups became apparent (n=6-9 mice per group). At the highest dose of 300 $\mu g/kg$ tested in both groups, over 40% of the bradycardia observed in $\alpha_{2ABC}$-KO was $\alpha_2$-independent. n.d. = not determined.*

**3. Identification of the target protein(s) responsible for clonidine-induced bradycardia in $\alpha_{2ABC}$-deficient mice**

Clonidine was demonstrated to lower heart rate in both wild-type and $\alpha_{2ABC}$-KO mice. While the bradycardic effect of clonidine was clearly less pronounced in $\alpha_{2ABC}$-deficient mice than in wild-type, a considerable portion of the clonidine-induced decrease in heart rate could not be attributed to $\alpha_2$-receptors. To identify the target or targets of this bradycardic response to clonidine in $\alpha_{2ABC}$-KO mice, it was next necessary to simplify the experimental system. In order to determine whether or not the clonidine effect on heart rate in the absence of $\alpha_2$-receptors was centrally-derived or peripheral in nature, an in vitro system was chosen.

3.1. Isolated spontaneously beating right atria

Organ bath experiments were performed to confirm the location of the bradycardic action of clonidine in $\alpha_{2ABC}$-KO mice. The frequency of isolated, spontaneously beating right atria from $\alpha_{2ABC}$-KO mice was reduced by 100 $\mu$M clonidine by approximately 50% of the beating frequency of wild-type right atria (figure 33), a proportion similar to that observed in conscious wild-type and $\alpha_{2ABC}$-KO mice at 300 $\mu$g/kg clonidine (figure 32). This indicated that the origin of the bradycardic response was in the atrium itself. Organ bath experiments with isolated spontaneously beating right atria yielded clonidine dose-response curves in wild-type and $\alpha_{2ABC}$-KO right atria with similar $IC_{50}$ values in both genotypes (6.2 $\mu$M and 4.8 $\mu$M, respectively).
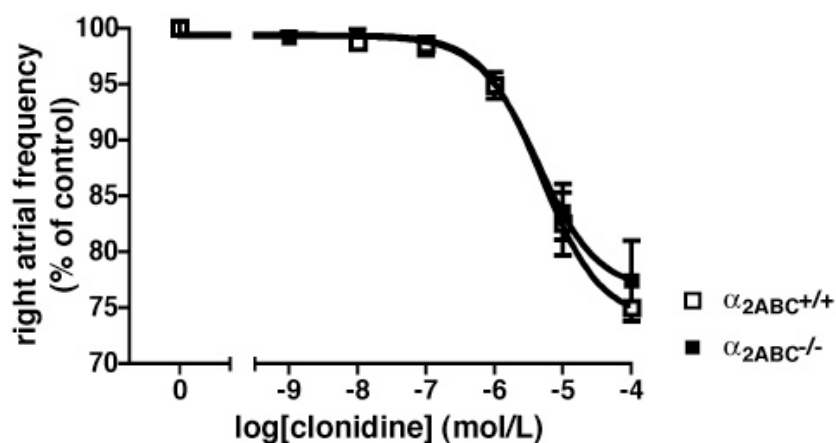


**Fig. 33:** *Decrease in spontaneous beating frequency with clonidine in isolated right atria from wild-type and $\alpha_{2ABC}$-KO mice*. *Clonidine lowered*

85

*spontaneous beating frequency in wild-type (n=6) and $\alpha_{2ABC}$-KO (n=7) right atria with similar affinity (IC$_{50}$ wild-type: 6.2 $\mu$M, IC$_{50}$ $\alpha_{2ABC}$-KO: 4.8 $\mu$M). The points on the curves represent the group mean $\pm$ SEM of the beating frequency, expressed as percent of baseline beating frequency, at the respective clonidine concentration.*

After localization of the $\alpha_2$-independent decrease in spontaneous beating frequency induced by clonidine, various antagonists and inhibitors were tested in an attempt to interfere with this effect in $\alpha_{2ABC}$-KO atria (table 2).

| antagonist / inhibitor | target |
|---|---|
| pertussis toxin | G$_i$ proteins |
| Ba$^{2+}$ (100 $\mu$M) | inward rectifier K$^+$ channels |
| Cs$^+$ (2mM) | most K$^+$ channels |
| ZD 7288 | HCN channels |

**Tab. 2:** ***Antagonists and inhibitors of some atrial regulators of heart rate.*** *These substances were tested for their potential to interact with the bradycardic effect of clonidine in isolated right atria.*

Pertussis toxin (PTX), an unselective inhibitor of G$_i$ proteins, failed to abolish or even reduce the bradycardic effect of clonidine in the right atria of $\alpha_{2ABC}$-KO mice when injected 16 hours prior to sacrifice (figure 34). The administered dose of PTX was sufficient to eliminate the M2-muscarinic receptor-mediated reduction in beating frequency by the agonist carbachol in pretreated $\alpha_{2ABC}$-KO mice (figure 34). The right atrial beating frequency of PTX-untreated $\alpha_{2ABC}$-KO mice was further decreased with carbachol following clonidine administration, suggesting that clonidine did not interact with muscarinic receptors. These results eliminated the involvement of G$_i$-coupled receptors in the bradycardic action of clonidine. As no G$_s$- or G$_q$-coupled receptors could explain the $\alpha_2$-independent decrease in beating frequency, the possible influence of clonidine on ion currents was next examined.
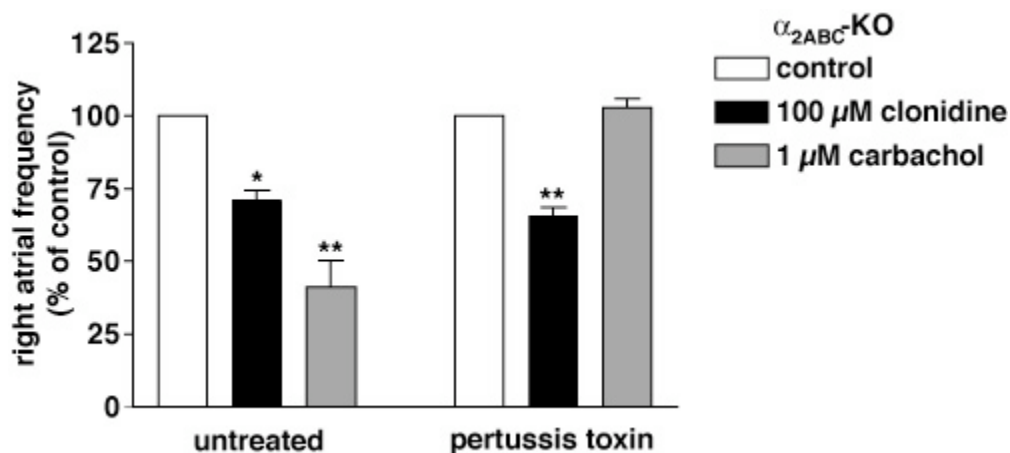
**Fig. 34:** *The bradycardic effect of clonidine in $\alpha_{2ABC}$-KO mice is not dependent on $G_i$ proteins.* *Right atrial frequency, expressed in % of control (baseline), of $\alpha_{2ABC}$-KO mice either untreated or injected 16 h prior to the organ bath experiment with 150 µg/kg pertussis toxin (PTX) ip. Bars depict the mean $\pm$ SEM of untreated (n=4) and PTX-treated (n=4) $\alpha_{2ABC}$-KO mice before (= control) and after addition of clonidine, and – after rinsing – of carbachol to the organ bath. Pretreatment with PTX did not diminish the bradycardic effect of clonidine (\* p < 0.05 untreated vs. control, \*\* p < 0.001 treated vs. control; one-way ANOVA). However, PTX did abolish the ability of carbachol to lower frequency in spontaneously beating right atria.*

In the right atrium, $Ca^{2+}$ and $K^+$ currents are primarily responsible for generation of heart beat (see Introduction, chapter 1.2.2., Heart rate). Figure 35 illustrates the consequences of $K^+$ current inhibition by $Ba^{2+}$ and $Cs^+$ on the reduction of beating frequency by clonidine. The addition of 100 µM $Ba^{2+}$ to the bath fluid did not suppress atrial response to clonidine, excluding the involvement of inward rectifier $K^+$ channels, as these were effectively blocked by $Ba^{2+}$ at this concentration (Stelling and Jacob, 1992). In contrast, $Cs^+$, which blocks most $K^+$ channels but also pacemaker channels as well (Levick, 1998), completely abolished the clonidine-mediated bradycardia. This was the first substantial evidence in support of pacemaker channels, more precisely known as HCN (hyperpolarization activated, cyclic nucleotide-gated cation) channels, as a non-$\alpha_2$ molecular target of clonidine.
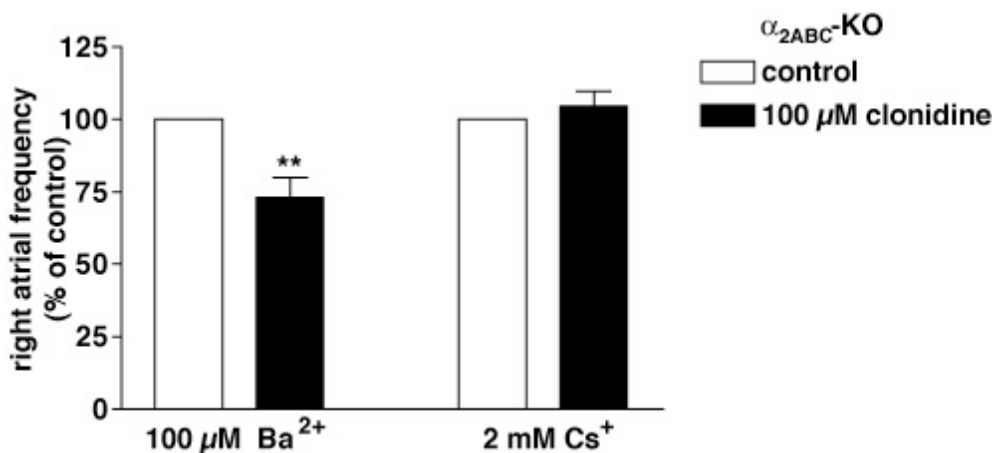
**Fig. 35:** $\alpha_{2ABC}$**-KO right atrial frequency in the presence of Ba$^{2+}$ or Cs$^{+}$.** *Black bars show the mean % change in control frequency ± SEM after addition of clonidine to n=6 right atria in Ba$^{2+}$-containing solution and to n=5 in Cs$^{+}$ containing bath. Ba$^{2+}$ did not affect the ability of clonidine to lower frequency (p = 0.0025, two-tailed unpaired t test), while the presence of Cs$^{+}$ completely abolished the clonidine effect.*

The specific HCN channel blocker ZD 7288 (BoSmith et al., 1993) prevented a further reduction in beating frequency by clonidine. 10 $\mu$M ZD 7288 slowly but significantly lowered beating frequency in $\alpha_{2ABC}$-KO right atria (figure 36). When clonidine was added to the bath, the frequency remained significantly lower than control, but was indistinguishable from that in the presence of ZD 7288 alone. Addition of 1 $\mu$M isoproterenol failed to elevate beating frequency, as HCN channels mediate the effect of increased sympathetic tone on beating frequency (Levick 1998). As proposed by a previous experiment where clonidine inhibited the neuronal $I_h$ current in isolated sciatic nerve, this suggests that clonidine and ZD 7288 may share a common site of action (Kroin et al., 2004).

| | | | | |
|---|---|---|---|---|
| 10 $\mu$M ZD 7288 | - | + | + | + |
| 100 $\mu$M clonidine | - | - | + | + |
| 1 $\mu$M isoproterenol | - | - | - | + |
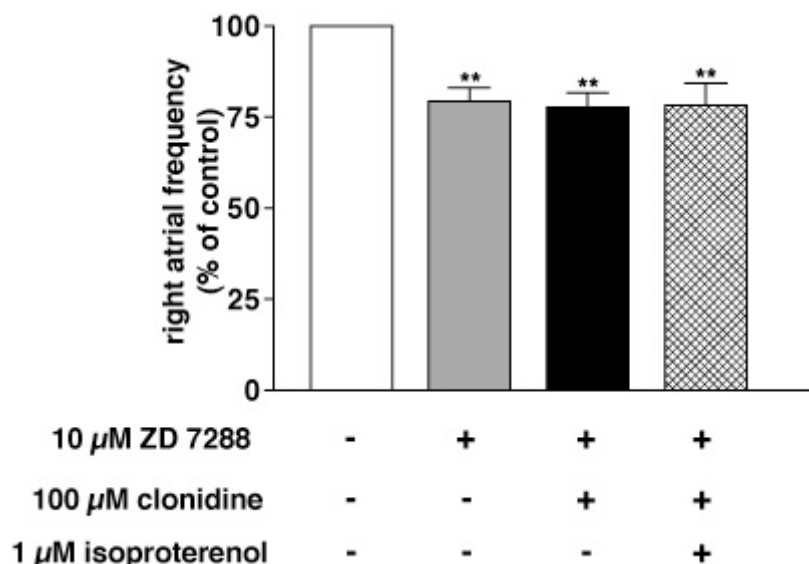
**Fig. 36:** *Inhibition of cardiac HCN channels prevents the bradycardic effect of clonidine in $\alpha_{2ABC}$-KO right atria. Bars represent the mean right atrial frequency in % of control $\pm$ SEM after addition of 10 $\mu$M ZD 7288 and after 100 $\mu$M clonidine to the bath solution of n=6 right atria. Clonidine did not lower the beating frequency of $\alpha_{2ABC}$-KO right atria after pretreatment with the specific HCN channel blocker ZD 7288. Isoproterenol failed to raise frequency in the presence of ZD 7288 and clonidine (n=3 atria). Both ZD 7288 and clonidine lowered frequency significantly from control (p < 0.001; one-way ANOVA); however, none of the three bars differed significantly from each other (two-tailed unpaired t test).*

3.2.    [$^{3}$H]Clonidine binding in $\alpha_{2ABC}$-KO membranes

Competition binding with ZD 7288 was performed in $\alpha_{2ABC}$-KO heart membranes to assess whether or not the specific HCN inhibitor interacted with the [$^{3}$H]clonidine binding site identified in $\alpha_{2ABC}$-KO tissues. Surprisingly, the competition curves of ZD 7288 and clonidine in the presence of 8 nM [$^{3}$H]clonidine nearly overlapped (figure 37).
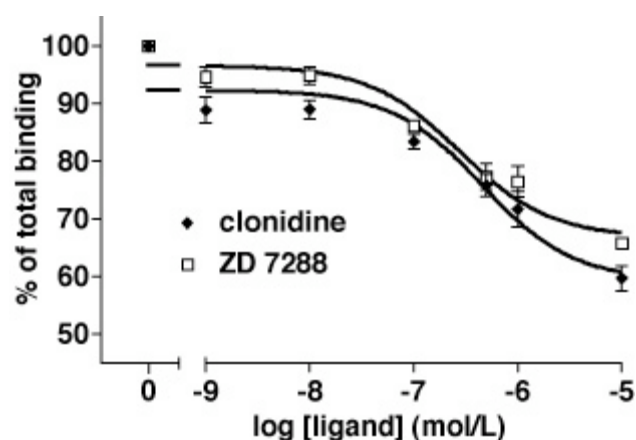
**Fig. 37:** *Displacement of [³H]clonidine (8 nM) binding by the specific HCN blocker ZD 7288 in $\alpha_{2ABC}$-KO heart membranes.* *Binding curves were fit using the one-site competition model. Each symbol depicts the mean of 9 measurements from three experiments performed in triplicate, $\pm$ SEM. Clonidine showed an $IC_{50}$ value of approximately 0.5 µM, while ZD 7288 displayed a very similar $IC_{50}$ value of 0.3 µM.*

3.3.    Effect of clonidine in stably transfected HEK293 cells

In order to test the potential interaction of clonidine with HCN channels, electrophysiological measurements were performed by Dr. Xiangang Zong and Prof. Martin Biel in Munich. HEK293 cells stably expressing the (murine) HCN1, (murine) HCN2 and (human) HCN4 subtypes were chosen to substantiate the interaction of clonidine with pacemaker channels observed in vitro. Electrophysiological measurements indisputably showed a decrease in $I_f$ current upon clonidine administration. Whole-cell patch clamp recordings revealed a dose-dependent reduction of pacemaker current with increasing clonidine concentration from 1 µM to 1 mM (figure 38). The resulting inhibition curve yielded an $IC_{50}$ value in the low micromolar range.
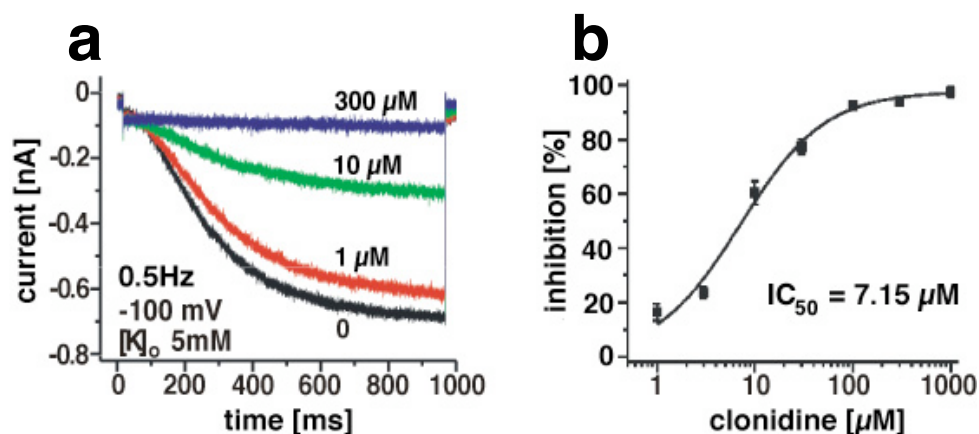
**Fig. 38:** *Clonidine inhibits the HCN2 channel in a concentration-dependent manner.* *Figure 38a depicts a representative recording for clonidine inhibition of HCN2 obtained by whole-cell patch clamp recording of stably transfected HEK cells. At time 0, no clonidine was present and the basal $I_f$ current was apparent. Increasing concentrations of clonidine – 1 µM, 10 µM and 300 µM – continually suppressed the $I_f$ current until it was completely blocked at the highest clonidine concentration. b, In HCN2-stably expressing HEK cells, clonidine inhibited the HCN2 subtype with an $IC_{50}$ value of 7.15 µM. Measurements and diagrams were kindly provided by Dr. Xiangang Zong and Prof. Martin Biel from the Ludwig-Maximilians Universität in Munich, Department of Pharmacy.*

Analogous experiments were conducted in HEK cells stably expressing the HCN1 and HCN4 subtypes. The $IC_{50}$ value of clonidine for the HCN4 subtype, the predominant subtype in sinoatrial node cells (Ishii et al., 1999), was nearly identical to that of the HCN2 subtype (9.7 µM vs. 7.2 µM, respectively). Clonidine affinity to the HCN1 subtype was 4-6 fold lower (42 µM) as compared with HCN2 and HCN4 (table 3).

| HCN channel subtype | $IC_{50}$ clonidine |
|---------------------|---------------------|
| HCN1 | 42 µM |
| HCN2 | 7.2 µM |
| HCN4 | 9.7 µM |

**Tab. 3:** *$IC_{50}$ values of clonidine for the HCN channel subtypes HCN1, HCN2 and HCN4.* *Clonidine blocked HCN2 and HCN4 channel subtypes with nearly equal potency ($IC_{50} < 10$ µM), while the affinity for the HCN1 subtype was slightly lower (42 µM). Data were kindly provided by Dr. Xiangang Zong and Prof. Martin Biel, Munich.*

3.4.    Effect of clonidine in cultured isolated sinoatrial node cells

After the clonidine-mediated inhibition of HCN channel subtypes was well established in stably transfected HEK cells, it was necessary to test whether or not this occurred in the atrium.  The $I_f$ current from the sinoatrial node (SAN) cells isolated from both wild-type and $\alpha_{2ABC}$-KO mice was measured using the whole-cell voltage clamp technique.  Clonidine reduced the $I_f$ current dose-dependently in both wild-type and $\alpha_{2ABC}$-KO SAN cells (individual traces not shown).  This inhibition was nearly identical in both genotypes, as the clonidine dose-response curves generated from these measurements nearly overlapped (figure 39).  The $IC_{50}$ values from the SAN cells (approximately 3 $\mu$M in both genotypes) were in accordance with those from stably transfected HEK cells ($IC_{50}$[HCN4] = 9.7 $\mu$M, table 3).
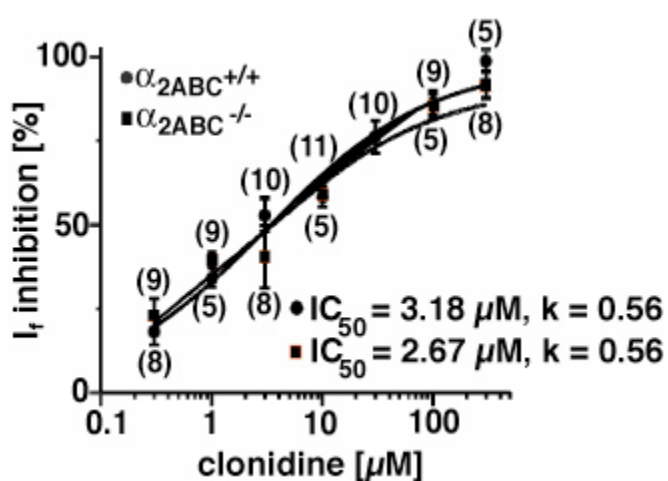


**Fig. 39:  _Clonidine inhibition curves in SAN cells._** _Clonidine inhibited HCN channels in isolated SAN cells from $\alpha_{2ABC}$-KO mice with the same affinity and potency as in wild-type SAN cells.  The resulting inhibition curve from n (the number in parenthesis) recordings is shown.  The points on the two curves express the mean and SEM of n values. Data were kindly provided by Dr. Xiangang Zong and Prof. Martin Biel, Munich._

Once it was established that clonidine indeed inhibited the $I_f$ current in the sinus node, the question arose as to the mechanism by which it interacted with the HCN channels.  To demonstrate the link between clonidine-induced $I_f$ inhibition and bradycardia in $\alpha_{2ABC}$-KO mice, the perforated patch technique with amphotericin B was used to measure spontaneous action potentials of wild-type and $\alpha_{2ABC}$-KO SAN cells (figure 40a, 40b).
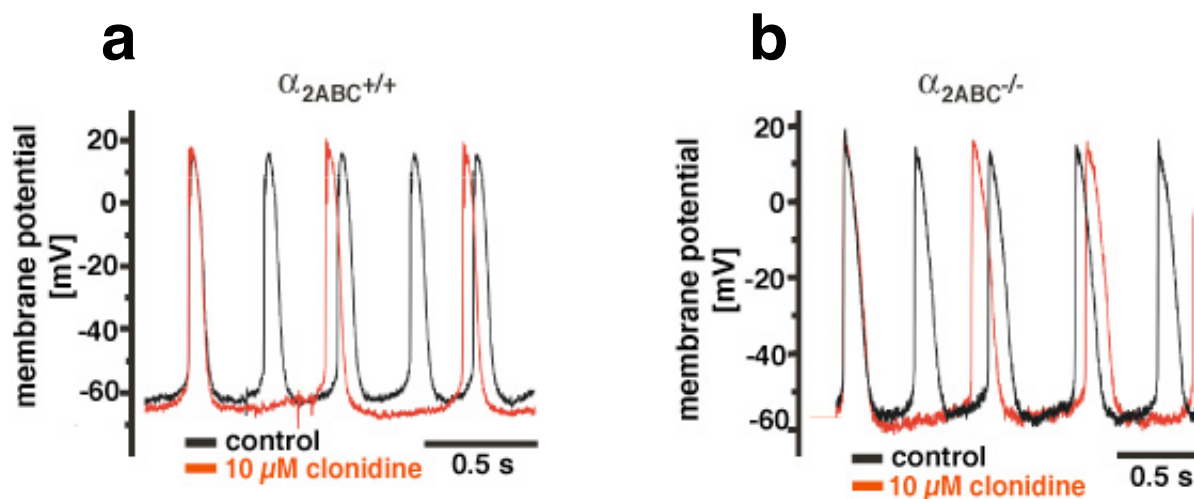
**Fig. 40:** *Action potential recordings in SAN cells from wild-type and* $\alpha_{2ABC}$*-KO mice.* *In both genotypes, clonidine evoked a marked increase in cycle length, or the time between two consecutive action potentials. Inhibition of the I$_f$ current was evidenced by a delay in return to threshold potential following clonidine treatment. The action potential duration during systole remained unchanged after clonidine. Data were kindly provided by Dr. Xiangang Zong and Prof. Martin Biel, Munich.*

Analysis of the individual components of the action potential provided much insight (table 4). As demonstrated by the recorded spontaneous action potentials in the previous figure, the cycle length in SAN cells from both wild-type and $\alpha_{2ABC}$-KO mice was significantly increased with clonidine. This appeared to be mainly, if not exclusively, due to a decrease in the speed of diastolic depolarization, as all other measured parameters remained unchanged. While the proportional decrease of diastolic depolarization by clonidine was equal in wild-type and $\alpha_{2ABC}$-KO SANs (approximately 55%), cycle length was increased by a much higher percentage in wild-type (ca. 240%) than compared to $\alpha_{2ABC}$-KO (ca. 150%).

| parameter | $\alpha_{2ABC}$+/+ control (n) | clonidine | $\alpha_{2ABC}$-/- control (n) | clonidine |
|---|---|---|---|---|
| CL [ms] | 455±48 (6) | 1105±223* | 605±45 (4) | 895±98* |
| **DD [mV/s]** | 79.7±8.1 (6) | 45.6±6.6* | 62.1±9.9 (4) | 34.1±7.9* |
| RP [mV] | -56.7±1.5 (6) | -57.8±2.1 | -58.4±1.2 (4) | -58.9±1.0 |
| OS [mV] | 18.2±3.5 (6) | 18.2±3.6 | 17.5±2.4 (4) | 18.2±3.8 |
| APD50 [ms] | 68.7±14 (6) | 67.7±11.9 | 72.6±20.7 (4) | 70.0±20.6 |
| APD90 [ms] | 116±17.8 (6) | 118±14.8 | 129±21.6 (4) | 130±20.2 |

**Tab. 4:** *Effects of clonidine on various action potential parameters in isolated SAN cells from wild-type and $\alpha_{2ABC}$-KO mice. Clonidine significantly increased the time between two consecutive action potentials (cycle length) by decreasing the speed with which membrane potential returned to threshold potential (diastolic depolarization). Significant changes (p < 0.05) from baseline are denoted with an asterisk *. CL: cycle length; DD: diastolic depolarization; RP: resting potential; OS: overshoot; APD50 and APD90: 50% and 90% of the action potential duration. Data were kindly provided by Dr. Xiangang Zong and Prof. Martin Biel, Munich.*

3.5.    Effect of moxonidine in stably transfected HEK293 cells

The mixed $\alpha_2$ / imidazoline agonist moxonidine was evaluated to determine whether it showed similar effects on HCN channels as clonidine. Application of 50 $\mu$M moxonidine failed to significantly lower $I_f$ current in HEK293 cells expressing either the HCN2 (figure 41a) or the HCN1 (figure 41b) subtype. Clonidine administration (50 $\mu$M) following moxonidine decreased $I_f$ current as observed previously. This finding correlated well with in vivo heart rate measurements in anesthetized $\alpha_{2ABC}$-KO mice, where moxonidine only slightly lowered the frequency of the beating heart.
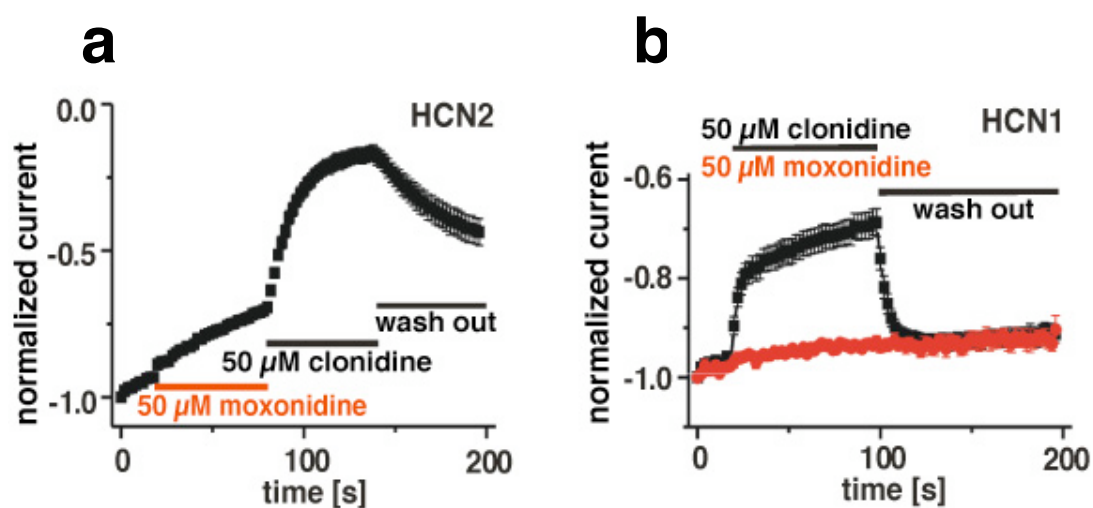
**Fig. 41:** *Moxonidine does not inhibit HCN1 and HCN2 channel subtypes.* *The effects of identical concentrations of moxonidine and clonidine on HEK293 cells stably transfected with murine HCN2 (**a**) and HCN1(**b**) channels were determined by whole-cell voltage clamp measurement. Moxonidine showed no significant inhibition of either HCN1 or HCN2 channel subtype. Data were kindly provided by Dr. Xiangang Zong and Prof. Martin Biel, Munich.*

# VI.        Discussion

Prior to the generation of $\alpha_2$-deficient mice, it was very difficult to assign a particular physiological role to a specific $\alpha_2$-subtype with much certainty.  No $\alpha_2$-ligands with sufficient subtype specificity were available, and, as two or all three $\alpha_2$-subtypes are often expressed together, it was not always possible to infer function unique to one subtype based merely on its (sub)cellular location.  $\alpha_2$-deficient mice presented an opportunity to examine each subtype in the absence of the remaining subtype(s).  Not until this powerful tool was available did it become clear, for example, that each $\alpha_2$-subtype played a distinct role in the modulation of norepinephrine release (Hein et al., 1999; Trendelenburg et al., 2003).

## 1.    Analysis of $\alpha_{2ABC}$-deficient mice

Equally intriguing were the characteristics displayed in $\alpha_{2ABC}$-deficient mice.  Although at first the generation of this line did not appear feasible due to the extremely high embryonic lethality (less than 1 of 250 embryos survived until birth), over time enough $\alpha_{2ABC}$-KO survivors were recovered to establish a breeding colony.  The mixed genetic background of these founding mice apparently compensated for the insufficient placental vascularization due to deletion of the $\alpha_{2B}$-subtype in congenic mice (Philipp et al., 2002c).

The complete absence of $\alpha_2$-receptors was verified both on a molecular as well as on a functional level.  Routine PCR genotyping (figure 13) as well as initial Southern blotting concurrent with the generation of $\alpha_2$-single KOs (Philipp et al., 2002c) confirmed the insertion of the neomycin resistance cassette into the coding region of each $\alpha_2$-subtype, rendering all three $\alpha_2$-receptor genes nonfunctional.  Radioligand binding both in whole brain slices as well as in brain membrane preparations with the selective $\alpha_2$-antagonist [$^3$H]RX 821002 failed to detect any specific binding in $\alpha_{2ABC}$-KO brain, analogous to that observed in wild-type brain in the presence of the $\alpha_2$-antagonist atipamezole at saturating levels (figure 14d).  The lack of presynaptic control by $\alpha_2$-autoreceptors was manifest by the inability of norepinephrine to suppress the release of [$^3$H]norepinephrine following electrical stimulation of $\alpha_{2ABC}$-KO atrial tissue (figure 18).  Dysregulated

sympathetic activity in $\alpha_{2ABC}$-KO mice was also evident by elevated norepinephrine levels in $\alpha_{2ABC}$-KO urine (figure 19). The deleterious consequences of absent negative feedback control and resulting elevated catecholamine levels later became visible at both a microscopic level (fibrosis and hypertrophy of left ventricular myocytes, figures 24-26) and at a functional level as well (impaired shortening fraction, figure 27).

## 2. Mechanisms of action of clonidine and clonidine-like drugs

There is still much controversy as to the exact mechanism by which clonidine and similar $\alpha_2$-agonists possessing an imidazoline structure lower blood pressure. The older $\alpha_2$-hypothesis, which attributes the antihypertensive effect of clonidine to $\alpha_2$-receptors alone (van Zwieten et al., 1984; Guyenet, 1997), has lost ground to the newer imidazoline hypothesis. This hypothesis was originally proposed by Bousquet and colleagues after the observation that many $\alpha_1$ / $\alpha_2$-imidazoline-containing ligands were able to lower blood pressure when microinjected into the rostral ventrolateral medulla (Bousquet et al., 1984). The specificity for $\alpha_1$- or $\alpha_2$-adrenergic receptors appeared to play less of a role in the ligand's ability to centrally inhibit sympathetic tone; crucial, however, seemed the presence of an imidazoline moiety, as this effect was not observed when catecholamine $\alpha$-adrenergic ligands were injected into the same brainstem region (Ernsberger and Haxhiu, 1997). While the existence of this central imidazoline "receptor" is generally recognized today, there is still an ongoing debate as to whether it alone is responsible for the sympathoinhibitory (and therefore therapeutic) effects of clonidine and clonidine-like antihypertensives, or if the imidazoline $I_1$-binding site is merely that, with no physiological importance. In addition to its antihypertensive effect, clonidine lowers heart rate as well. Clonidine-elicited bradycardia is ascribed to its stimulation of presynaptic $\alpha_2$-autoreceptors, thereby reducing sympathetic activity (van Zwieten et al., 1984).

Outside of the cardiovascular system, clonidine is known for its strong sedative properties. This unwanted "side" effect of daily antihypertensive treatment likely spurred the search for $\alpha_2$ / $I_1$ imidazoline agonists with less pronounced sedative effects. While moxonidine and rilmenidine have been shown to be less sedating, there is disagreement as to how much less pronounced this side effect is compared to with clonidine. These differences in amount of sedation have been attributed to the higher affinities of moxonidine and rilmenidine to $I_1$ binding sites (Szabo, 2002). When clonidine is used as a pre- or post-operative sedative, the additional analgesic properties of this drug are desirable.

Mice lacking all three $\alpha_2$-receptor subtypes were an ideal model with which to test the validity of the imidazoline hypothesis. If indeed imidazoline $I_1$-binding sites are physiologically functional and independent of $\alpha_2$-adrenergic receptors, a similar, although perhaps diminished, effect of clonidine and other centrally acting antihypertensives would be expected in $\alpha_{2ABC}$-KO mice compared to in wild-type mice. The absence of sympathetic inhibition in these mice after drug administration could be interpreted in two ways: either $I_1$-binding sites are unable to evoke a physiological response (Munk et al., 1996), or they are only functional in the presence of $\alpha_2$-receptors, acting - in a manner not yet understood - in cooperation with them (Bruban et al., 2002).

### 3. Cardiovascular effects of clonidine in $\alpha_{2ABC}$-deficient mice

The effects of clonidine on blood pressure and heart rate in $\alpha_{2ABC}$-KO mice were observed. In anesthetized $\alpha_{2ABC}$-KO mice, the femoral artery was chosen for catheter insertion for blood pressure measurement, as insertion and vessel constriction at this location were much less likely to disturb the baroflex than in the carotid artery. Not only clonidine (figure 31), but moxonidine and rilmenidine as well (not shown) failed to significantly decrease mean arterial pressure in $\alpha_{2ABC}$-KO mice. Since clonidine was observed to significantly lower heart rate in $\alpha_{2ABC}$-KOs as well as in wild-type mice, this drug was studied more closely, and the effects at different doses were assessed in both groups of mice. Even at doses as high as 150 $\mu$g/kg, clonidine failed to show any hypotensive effect in the absence of $\alpha_2$-receptors. These results are in good agreement with those from previous studies examining the hypotensive effect of $\alpha_2$-agonists in mice deficient in functional $\alpha_{2A}$-receptors, due either to point mutation – D79N $\alpha_{2A}$-mutant (MacMillan et al., 1996; Zhu et al., 1999) – or to deletion – $\alpha_{2A}$-KO (Altman et al., 1999). Taken together, these findings substantiate that the presence of functional $\alpha_2$-receptors is indeed required for these $\alpha_2$ / imidazoline agonists to lower blood pressure (Szabo, 2002).

Despite its failure to lower blood pressure, clonidine did markedly decrease heart rate in anesthetized $\alpha_{2ABC}$-KOs. This bradycardic effect was much less pronounced with moxonidine; rilmenidine did not appear to influence heart rate at all (not shown). In conscious, unrestrained wild-type and $\alpha_{2ABC}$-KO mice monitored via telemetry, clonidine again produced a dose-dependent decrease in baseline heart rate in the absence of $\alpha_2$-receptors. At the highest clonidine dose in both groups (300 $\mu$g/kg in conscious mice), clonidine lowered baseline heart rate by 50% in wild-type and by approximately 25% in $\alpha_{2ABC}$-KO mice (figure 32). While $\alpha_2$-receptors clearly played the predominant

role in the clonidine-induced bradycardia, the substantial contribution of a non-$\alpha_2$-adrenergic target of clonidine was unmistakable.

### 4. Other effects of clonidine in $\alpha_{2ABC}$-deficient mice

Activation of $\alpha_2$-receptors in the pancreas indirectly regulates the release of insulin into the blood stream via $G_{i/o}$-mediated inhibition of adenylyl cyclase and reduction of intracellular $Ca^{2+}$ levels, thereby inhibiting $Ca^{2+}$ sensitive $K^+(ATP)$ channels which control the exocytotic release of insulin (Ullrich and Wollheim, 1985; Hsu et al., 1991). As expected, clonidine evoked an immediate increase in plasma glucose in wild-type mice (figure 30). In contrast, $\alpha_{2ABC}$-KO mice responded to clonidine application with a mild but significant decrease in plasma glucose levels. Moxonidine and rilmenidine did not appear to elicit a hypoglycemic response in $\alpha_{2ABC}$-KO mice; medetomidine displayed absolutely no effect in $\alpha_{2ABC}$-KOs (Lee et al., 1995). Some imidazoline-containing compounds, such as efaroxan, are known to stimulate insulin secretion due – at least in part – to interaction with the Kir6.2 pore component of the $K^+(ATP)$ channel via an $I_3$ imidazoline binding site (Morgan and Chan, 2001). While this may provide an explanation for the hypoglycemic action of clonidine in $\alpha_{2ABC}$-KO mice, its confirmation is beyond the scope of this project.

Sedation and analgesia are two well known properties of clonidine that have long been recognized to be mediated by $\alpha_2$-adrenergic receptors (van Zwieten et al., 1984; Correa-Sales et al., 1992). Studies with $\alpha_{2A}$-deficient mice have demonstrated that this subtype plays the predominant role in clonidine-induced elevation of pain threshold (Özdogan et al., 2004, Röser, 2005). As expected, clonidine failed to produce either a sedative or an analgesic effect in $\alpha_{2ABC}$-KO mice (figures 28-29). Although both drugs elicited significant effects in wild-type mice, clonidine was a far more potent sedative and analgesic than moxonidine. While differences in $\alpha_2$ and $I_1$ affinities could explain the lack of "side effects" with moxonidine, perhaps another explanation contributes to this observation as well. In spontaneously hypertensive rats, clonidine was found to be 10-fold more potent than moxonidine in lowering blood pressure (Ernsberger et al., 1997). As both drugs produced an equal antihypertensive response at identical doses when microinjected into the RVLM, the authors attributed the lower potency of peripherally applied moxonidine to a lesser degree of penetration of the blood-brain barrier than clonidine. A lower lipophilicity of moxonidine could well account for both the lack of analgesic response, as well as the greatly reduced sedation, with moxonidine compared to with clonidine in wild-type mice in this study. Many of the experiments confirming the analgesic potency of moxonidine are performed via intrathecal

injection of moxonidine, thereby circumventing the blood-brain barrier and offering a possible explanation for this discrepancy.

### 5.    Bradycardic effect of clonidine in $\alpha_{2ABC}$-deficient mice is mediated by inhibition of pacemaker (HCN) channels

After establishing the bradycardic effect of clonidine in $\alpha_{2ABC}$-KO mice, we turned to in vitro experiments to pinpoint the target(s) of this action. Organ bath experiments with spontaneously beating wild-type and $\alpha_{2ABC}$-KO right atria confirmed in vivo findings and narrowed the location of the molecular target(s) of clonidine to the right atrium. Clonidine dose-dependently decreased spontaneous beating frequency in wild-type and $\alpha_{2ABC}$-KO right atria with nearly equal affinity. Assuming that the entire clonidine dose is retained in the plasma, a rough estimate of the clonidine concentration after administration of 300 $\mu$g/kg clonidine to a 30 g mouse with 2.4 ml blood volume (Mitruka and Rawnsley, 1981; Harkness and Wagner, 1989) is approximately 14 $\mu$M. This value is well within range of the higher clonidine concentrations used in organ bath experiments and further confirms that this indeed is the molecular target mediating the bradycardia induced by clonidine in $\alpha_{2ABC}$-KO mice.

Next, antagonists and inhibitors of likely candidates for this non-$\alpha_2$ target of clonidine were tested (table 2). Pretreatment of $\alpha_{2ABC}$-KO mice with pertussis toxin to inactivate $G_{i/o}$ proteins did not diminish the decrease in spontaneous beating frequency by clonidine in isolated $\alpha_{2ABC}$-KO atria, therefore excluding all $G_i$ protein coupled receptors as possible targets (figure 34). Although many ion channels (particularly $K^+$ channels) contribute to pacemaker activity in the right atria, three major regulators of action potential predominate. L-type $Ca^{2+}$ channels generate the $I_{CaL}$ current, regarded as the most important pacemaker current, as the $I_{CaL}$ channel threshold potential is nearly the same as that of the pacemaker potential of SAN cells (Satoh, 2003). T-type $Ca^{2+}$ channels play only an insignificant role in maintaining the pacemaker current. Diltiazem and mibefradil, inhibitors of L-type and T-type $Ca^{2+}$ currents, respectively, did not interfere with clonidine-induced reduction of beating frequency when added to the bath (not shown). $Ba^{2+}$ is a known inhibitor of delayed rectifier $K^+$ channels which are responsible for repolarization and return to resting potential (Satoh, 2003). $Ba^{2+}$, too, failed to influence the effect of clonidine (figure 35). The pacemaker, or $I_f$, current is characteristic of SAN cells. The pacemaker HCN channel is both $K^+$ and $Na^+$ permeable, depolarizing slowly until threshold potential is reached (DiFrancesco, 1981). Other $K^+$ channels play lesser roles in the regulation of pacemaker activity. Many $K^+$ channels, including HCN channels, are inhibited by $Cs^+$ (Levick, 1998). In the presence of 2 mM $Cs^+$,

clonidine was no longer able to lower the beating frequency of $\alpha_{2ABC}$-KO atria (figure 35). In addition, after incubation with the specific HCN channel inhibitor ZD 7288 (BoSmith et al., 1993), clonidine did not (further) reduce the frequency of spontaneously beating $\alpha_{2ABC}$-KO right atria (figure 36). Two previous studies have indicated that clonidine inhibited the $I_h$ current (the $I_f$ current equivalent in neurons) in both rat sciatic nerve (Kroin et al., 2004) and in desheathed rabbit vagus nerve (Dalle et al., 2001); this inhibition was presumed to be at least partly responsible for the analgesic prolongation of local anesthetics, such as lidocaine, when clonidine was added (Dalle et al., 2001). The interaction between ZD 7288 and clonidine described above is similar to that of Kroin and colleagues (2004), who demonstrated that clonidine was not able to further lower $I_h$ in sciatic nerve pretreated with ZD 7288, suggesting a common site of action.

To confirm that HCN channels were indeed directly targeted by clonidine, we then began a collaboration with Dr. Xiangang Zong and Prof. Dr. Martin Biel at the Ludwig-Maximilians-Universität in Munich, in whose group the HCN channels were originally cloned and molecularly characterized (Ludwig et al., 1998; see also Santoro et al., 1998). In HEK293 cells stably transfected with HCN subtypes HCN1, HCN2 and HCN4, as well as in sinoatrial node (SAN) cells isolated from wild-type and $\alpha_{2ABC}$-KO mice, clonidine directly inhibited HCN currents (figures 38-39). Clonidine displayed equal affinity and potency for HCN channels in SAN cells from both groups of mice. In contrast, moxonidine failed to inhibit recombinant HCN channels expressed in HEK293 cells (figure 41). Of all the parameters contributing to cycle length in isolated SAN cells, only diastolic depolarization was significantly decreased (table 4). These results are consistent with a previous study of the effects of clonidine and moxonidine in rabbit SAN cells. In tissue strips excised from the sinoatrial node region of rabbit right atrium, both drugs (0.1 mM – 30 mM) decreased rate of pacemaker firing and increased cycle length; however, preincubation with yohimbine completely blocked the effects of moxonidine but only partially blocked those of clonidine (Zhao and Ren, 2003). The authors concluded that while moxonidine decreased pacemaker activity via $\alpha_2$-receptors alone, clonidine lowered rate of pacemaker firing via an unidentified $\alpha_2$-independent target as well.

## 6.    No evidence for involvement of $I_1$ binding sites in the bradycardic action of clonidine

Although saturation binding experiments revealed a non-$\alpha_2$ high affinity binding site for [$^3$H]clonidine in $\alpha_{2ABC}$-KO mouse membranes with a similar affinity to that of clonidine for the purported $I_1$ binding site (Szabo, 2002),

characterization of this non-$\alpha_2$ binding site during competition binding with other high affinity $I_1$ ligands did not support the equivalence of these two binding sites. The imidazoline hypothesis evolved around the binding properties of clonidine and its derivatives [$^3$H]p-aminoclonidine and [$^3$H]p-iodoclonidine (Dontenwill et al., 1999). Clonidine was reported to possess affinity to both $\alpha_2$-receptors and $I_1$ binding sites in the low nanomolar range (Bousquet et al., 2003). The newer, centrally acting antihypertensives moxonidine and rilmenidine are characterized by their higher affinity to $I_1$ binding sites than to $\alpha_2$-receptors (Bousquet and Feldman, 1999). The precise affinities of these drugs vary, sometimes greatly, depending on the tissue type and species from which the tissue was taken (Szabo, 2002). Moxonidine was found to be 70-fold more selective for $I_1$ sites than $\alpha_2$ in bovine ventrolateral medulla membranes (Ernsberger et al., 1993), the tissue in which the $I_1$ site was originally studied. Yet other studies reported a nearly equal $I_1$ / $\alpha_2$ affinity for moxonidine (Szabo, 2002); one study failed to find any $I_1$ affinity for moxonidine (Bricca et al., 1994). One binding study in cattle brain stem reported a 30fold higher affinity of rilmenidine for $I_1$ receptors compared to $\alpha_2$-receptors (Ernsberger et al., 1993); however, other studies could not substantiate the low nanomolar affinity determined previously (Szabo, 2002). In summary, numerous binding studies have been performed in support of $I_1$ binding sites, yet the evidence confirming the existence and nature of these sites has been weakened by conflicting results (Szabo, 2002). Since no uniform binding characteristics of the $I_1$ site are clearly defined, it is not possible to compare the non-$\alpha_2$ binding site found in $\alpha_{2ABC}$-KO mouse membranes with the purported $I_1$ site with any certainty. Considering the nonconformity of several of the tested "selective" imidazoline $I_1$ ligands (moxonidine, efaroxan, cimetidine and agmatine) to [$^3$H]clonidine binding in $\alpha_{2ABC}$-KO mouse membranes, it seems highly unlikely this non-$\alpha_2$ binding site is identical or even related to the purported $I_1$ site.

Not only were the binding characteristics of these two sites incongruous; the pharmacological effects of the $\alpha_2$ / $I_1$ agonist clonidine in $\alpha_{2ABC}$-KO mice were not in accordance with the purported actions of clonidine at the $I_1$ receptor (Bousquet, 2001). Clonidine failed to lower blood pressure in $\alpha_{2ABC}$-deficient mice in several experimental settings (Results, 2.4.). While this could have been attributed to an insufficient concentration of clonidine in the rostral ventrolateral medulla (RVLM) after systemic application, other central effects such as sedation and analgesia were clearly visible in wild-type mice after identical doses of clonidine. At the highest clonidine doses administered, no change in blood pressure was observed (figure 31); most likely these clonidine doses were sufficient to achieve a nanomolar concentration in the RVLM necessary for activation of $I_1$ receptors. Taken together, our findings do not support the involvement of $I_1$ binding sites in the hypotensive effect of

clonidine and clonidine-like agonists. If indeed these sites do play a physiological role in the pharmacological action of these drugs, then it appears they do so only in concert with $\alpha_2$-receptors, as suggested by Dontenwill and colleagues (1999). Or perhaps these $I_1$ binding sites are devoid of any physiological effect, as was proposed by the group of Munk et al., the creators of a high-affinity $I_1$-ligand which showed neither agonistic nor antagonistic properties in animals tested (1996).

Clonidine-induced bradycardia has been shown to result from both a reduction in sympathetic tone as well as an increase in vagal activity and consequent baroreceptor activation (Tangri et al., 1974). $\alpha_2$-adrenergic receptors in the nucleus tractus solitarius were later demonstrated to be required for activation of the baroflex (Sved et al., 1992). $I_1$ receptors do not appear to contribute to the heart rate lowering effects of clonidine, moxonidine and rilmenidine. No presynaptic $I_1$ binding sites have been identified on sympathetic nerve endings (Göthert et al., 1999). In addition, clonidine and moxonidine did not inhibit [$^3$H]norepinephrine release in the presence of the irreversible $\alpha_2$-antagonist phenoxybenzamine (Schlicker et al., 1997). $\alpha_2$-receptors have repeatedly been shown to moderate sympathetic tone, offering the most plausible explanation for the bradycardic action of these centrally acting antihypertensives (Szabo et al., 2001).

## 7. Therapeutic consequences of HCN blockade in human patients

Clonidine reduced the action potential frequency in mice by decreasing the speed of diastolic depolarization. However, it is not certain to what extent – if at all – clonidine lowers heart rate in humans via inhibition of HCN channels. The affinity of clonidine for the human HCN4 subtype expressed in HEK cells ($IC_{50}$ = ca. 10 $\mu$M) was in the same range as the $IC_{50}$ value of clonidine determined in isolated mouse SAN cells ($IC_{50}$ = ca. 3 $\mu$M), where the HCN4 subtype predominates in both humans and mice (Ishii et al., 1999).

Assuming that the affinities of clonidine for recombinant HCN subtypes in HEK293 cells as well as for native HCN channels in murine SAN cells are similar to those for human HCN channels, the plasma concentration attained following a typical antihypertensive dose of clonidine (150 – 900 $\mu$g/day) in humans (Onesti et al., 1971) would not be likely to inhibit HCN channels. Chronic administration of 75 $\mu$g clonidine twice daily was shown to correspond to a maximum plasma concentration of 0.66 $\pm$ 0.06 ng/ml clonidine (Anavekar et al., 1989); another study with 300 $\mu$g oral clonidine determined a peak plasma concentration of 1.34 $\pm$ 0.28 ng/ml in hypertensive patients (Wing et al., 1977). Although the hypotensive effect of clonidine has been shown to

diminish at plasma levels greater than 1.5 ng/ml (Wing et al., 1977; Frisk-Holmberg et al., 1984), higher clonidine plasma concentrations are not uncommon when used as an analgesic (Bernard et al., 1995). Patients self-administering iv clonidine attained a peak plasma concentration of 2.5 $\pm$ 0.6 ng/ml (Bernard et al., 1995). However, even in the highest therapeutic range clonidine concentration in human plasma remains below 10 nM, approximately a thousand fold less than the $IC_{50}$ value of clonidine determined in isolated murine SAN cells. Therefore, the bradycardic effect of clonidine in human patients appears to be solely $\alpha_2$-mediated. This does not, however, exclude the possibility that bolus iv injection of clonidine during hypertensive emergency or rapid opioid detoxification may result in transiently elevated plasma concentrations sufficient to inhibit cardiac HCN channels in humans (Kienbaum et al., 2002).

The comparison of $I_f$ inhibition by clonidine and that of a new class of selective $I_f$ current inhibitors, the bradines, does however support the possibility of the contribution of this action to the bradycardic effect of clonidine in humans. To date, only ivabradine has been approved for the symptomatic treatment of patients with stable angina and who have a contraindication for $\beta$-blockers (Servier, 2006). Ivabradine provides an attractive alternative for the symptomatic treatment of ischemic heart disease without the decrease in blood pressure and cardiac contractility associated with $\beta$-blockers and $Ca^{2+}$ channel blockers (Vilaine, 2006). Not only does the reduction in heart rate reduce the frequency of ischemic episodes (Borer et al., 2003), but it reduces the mortality associated with an increased heart rate as well (DiFrancesco and Camm, 2004). Therapeutic doses in humans range from 7.5 mg – 10 mg ivabradine, divided into two doses daily (Tardif et al., 2005). In mice, however, the $EC_{50}$ value of ivabradine is nearly 5 mg/kg (Stieber et al., 2006). In contrast, clonidine reduced baseline heart rate in $\alpha_{2ABC}$-KO mice by almost 50% at doses between 100 $\mu$g/kg – 300 $\mu$g/kg (figure 32). If the same discrepancy in the effective concentration between humans and mice exists for clonidine as is the case with ivabradine, then human HCN channels may indeed be (at least partially) inhibited at therapeutic plasma concentrations during antihypertensive treatment with clonidine.

## 8. Conclusion

In conclusion, clonidine was shown to directly inhibit cardiac HCN pacemaker channels in mice. It is not certain whether this may contribute to its strong bradycardic effect in humans. While the $\alpha_2$-mediated reduction of sympathetic tone is inarguably the predominant bradycardic mechanism of clonidine, a possible direct inhibition of $I_f$ current by clonidine, however slight, could

enhance the overall benefits from a reduction in heart rate and prove advantageous to the patient suffering the effects from sympathetic overstimulation. It is also conceivable that HCN channels ubiquitously expressed in the nervous system may be similarly inhibited by clonidine, and this might partially mediate some of the neuronal effects of clonidine previously attributed to $\alpha_2$-receptors (Kroin et al., 2004). While its poor selectivity for HCN channels will exclude its use solely for this purpose, clonidine may provide a lead structure for the development of novel HCN inhibitors, not only in the treatment of tachycardia, but perhaps also to target neuronal disorders in which HCN channels are involved.
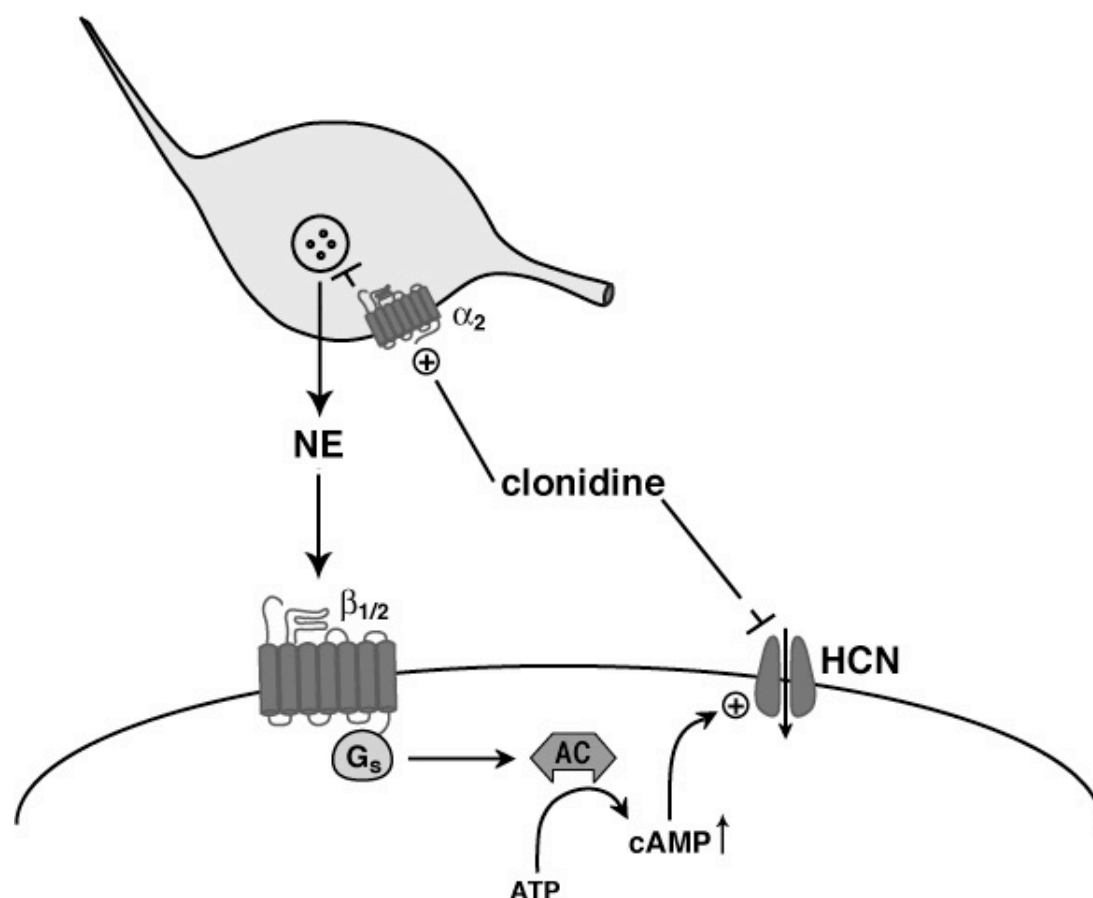


**Fig. 42:** *Clonidine lowers heart rate in wild-type mice via two distinct mechanisms. At doses sufficient to significantly lower blood pressure in wild-type mice (10 µg/kg), clonidine significantly decreased heart rate in both wild-type and $\alpha_{2ABC}$-KO mice (figure 32). This finding demonstrates that clonidine elicits its bradycardic effect in mice not only via activation of $\alpha_2$-adrenergic receptors, but also via an $\alpha_2$-independent mechanism. Experiments with the spontaneously beating isolated right atria from $\alpha_{2ABC}$-KO mice localized this*

*effect, and, with recombinant HCN channel subtypes as well as with SAN cells isolated from $\alpha_{2ABC}$-KO mice, clonidine was shown to inhibit the $I_f$ pacemaker current.*

# VII. References

Altman JD, Trendelenburg AU, MacMillan L, Bernstein D, Limbird L, Starke K, Kobilka BK and Hein L (1999) Abnormal regulation of the sympathetic nervous system in alpha2A-adrenergic receptor knockout mice. *Mol Pharmacol* **56**:154-61.

Anavekar SN, Howes LG, Jarrott B, Syrjanen M, Conway EL and Louis WJ (1989) Pharmacokinetics and antihypertensive effects of low dose clonidine during chronic therapy. *J Clin Pharmacol* **29**:321-6.

Armah BI (1988) Unique presynaptic alpha 2-receptor selectivity and specificity of the antihypertensive agent moxonidine. *Arzneimittelforschung* **38**:1435-42.

Arnsten AF, Steere JC and Hunt RD (1996) The contribution of alpha 2-noradrenergic mechanisms of prefrontal cortical cognitive function. Potential significance for attention-deficit hyperactivity disorder. *Arch Gen Psychiatry* **53**:448-55.

Avbelj F and Hadzi D (1985) Potential energy functions and the role of the conformational entropy of clonidine-like imidazolidines in determining their affinity for alpha-adrenergic receptors. *Mol Pharmacol* **27**:466-70.

Baruscotti M and Difrancesco D (2004) Pacemaker channels. *Ann N Y Acad Sci* **1015**:111-21.

Bennett MR (2000) The concept of transmitter receptors: 100 years on. *Neuropharmacology* **39**:523-46.

Bergendahl H, Lonnqvist PA and Eksborg S (2006) Clonidine in paediatric anaesthesia: review of the literature and comparison with benzodiazepines for premedication. *Acta Anaesthesiol Scand* **50**:135-43.

Bernard C (1883) Lecons sur les Effets des Substances Toxiques et Medicamenteuses, Bailliere, Paris.

Bernard JM, Kick O and Bonnet F (1995) Comparison of intravenous and epidural clonidine for postoperative patient-controlled analgesia. *Anesth Analg* **81**:706-12.

Bjorklund M, Sirvio J, Sallinen J, Scheinin M, Kobilka BK and Riekkinen P, Jr. (1999) Alpha2C-adrenoceptor overexpression disrupts execution of spatial and non-spatial search patterns. *Neuroscience* **88**:1187-98.

Black JW (1976) Ahlquist and the development of beta-adrenoceptor antagonists. *Postgrad Med J* **52 Suppl 4**:11-13.

Black JW and Stephenson JS (1962) Pharmacology of a new adrenergic beta-receptor-blocking compound (Nethalide). *Lancet* **2**:311-4.

Bonner TI, Buckley NJ, Young AC and Brann MR (1987) Identification of a family of muscarinic acetylcholine receptor genes. *Science* **237**:527-32.

Borer JS, Fox K, Jaillon P and Lerebours G (2003) Antianginal and antiischemic effects of ivabradine, an I(f) inhibitor, in stable angina: a randomized, double-blind, multicentered, placebo-controlled trial. *Circulation* **107**:817-23.

BoSmith RE, Briggs I and Sturgess NC (1993) Inhibitory actions of ZENECA ZD7288 on whole-cell hyperpolarization activated inward current (If) in guinea-pig dissociated sinoatrial node cells. *Br J Pharmacol* **110**:343-9.

Bousquet P (2001) I1 receptors, cardiovascular function, and metabolism. *Am J Hypertens* **14**:317S-321S.

Bousquet P and Feldman J (1999) Drugs acting on imidazoline receptors: a review of their pharmacology, their use in blood pressure control and their potential interest in cardioprotection. *Drugs* **58**:799-812.

Bousquet P, Feldman J and Schwartz J (1984) Central cardiovascular effects of alpha adrenergic drugs: differences between catecholamines and imidazolines. *J Pharmacol Exp Ther* **230**:232-6.

Bousquet P, Greney H, Bruban V, Schann S, Ehrhardt JD, Monassier L and Feldman J (2003) I(1) imidazoline receptors involved in cardiovascular regulation: where are we and where are we going? *Ann N Y Acad Sci* **1009**:228-33.

Bradford MM (1976) A rapid and sensitive method for the quantitation of microgram quantities of protein utilizing the principle of protein-dye binding. *Anal Biochem* **72**:248-54.

Brede M, Nagy G, Philipp M, Sorensen JB, Lohse MJ and Hein L (2003) Differential control of adrenal and sympathetic catecholamine release by alpha 2-adrenoceptor subtypes. *Mol Endocrinol* **17**:1640-6.

Bricca G, Greney H, Zhang J, Dontenwill M, Stutzmann J, Belcourt A and Bousquet P (1994) Human brain imidazoline receptors: further characterization with [3H]clonidine. *Eur J Pharmacol* **266**:25-33.

Bruban V, Estato V, Schann S, Ehrhardt JD, Monassier L, Renard P, Scalbert E, Feldman J and Bousquet P (2002) Evidence for synergy between alpha(2)-adrenergic and nonadrenergic mechanisms in central blood pressure regulation. *Circulation* **105**:1116-21.

Bünemann M, Bücheler MM, Philipp M, Lohse MJ and Hein L (2001) Activation and deactivation kinetics of alpha 2A- and alpha 2C-adrenergic receptor-activated G protein-activated inwardly rectifying K+ channel currents. *J Biol Chem* **276**:47512-7.

Bylund DB, Eikenberg DC, Hieble JP, Langer SZ, Lefkowitz RJ, Minneman KP, Molinoff PB, Ruffolo RR, Jr. and Trendelenburg U (1994) International Union of Pharmacology nomenclature of adrenoceptors. *Pharmacol Rev* **46**:121-36.

Bylund DB and Martinez JR (1980) alpha 2-Adrenergic receptors appear in rat salivary glands after reserpine treatment. *Nature* **285**:229-30.

Bylund DB and Martinez JR (1981) Postsynaptic localization of alpha 2-adrenergic receptors in rat submandibular gland. *J Neurosci* **1**:1003-7.

Cano E and Mahadevan LC (1995) Parallel signal processing among mammalian MAPKs. *Trends Biochem Sci* **20**:117-22.

Chang EB, Field M and Miller RJ (1982) alpha 2-Adrenergic receptor regulation of ion transport in rabbit ileum. *Am J Physiol* **242**:G237-42.

Chappell PB, Riddle MA, Scahill L, Lynch KA, Schultz R, Arnsten A, Leckman JF and Cohen DJ (1995) Guanfacine treatment of comorbid attention-deficit hyperactivity disorder and Tourette's syndrome: preliminary clinical experience. *J Am Acad Child Adolesc Psychiatry* **34**:1140-6.

Chotani MA, Flavahan S, Mitra S, Daunt D and Flavahan NA (2000) Silent alpha(2C)-adrenergic receptors enable cold-induced vasoconstriction in cutaneous arteries. *Am J Physiol Heart Circ Physiol* **278**:H1075-83.

Chruscinski AJ, Rohrer, DK, Schauble, E, Desai, KH, Bernstein, D and Kobilka, BK (1999) Targeted disruption of the beta2 adrenergic receptor gene. *J Biol Chem* **274**:16694-700.

Correa-Sales C, Rabin BC and Maze M (1992) A hypnotic response to dexmedetomidine, an alpha 2 agonist, is mediated in the locus coeruleus in rats. *Anesthesiology* **76**:948-52.

Cussac D, Schaak S, Denis C and Paris H (2002) alpha 2B-adrenergic receptor activates MAPK via a pathway involving arachidonic acid metabolism, matrix metalloproteinases, and epidermal growth factor receptor transactivation. *J Biol Chem* **277**:19882-8.

Dale D (1914) Hydrogen ion concentrations limiting automaticity in different regions of the frog's heart. *J Physiol* **47**:493-508.

Dalle C, Schneider M, Clergue F, Bretton C and Jirounek P (2001) Inhibition of the I(h) current in isolated peripheral nerve: a novel mode of peripheral antinociception? *Muscle Nerve* **24**:254-61.

Dam J, Ryde L, Svejso J, Lauge N, Lauritsen B and Bech P (1998) Morning fluoxetine plus evening mianserin versus morning fluoxetine plus evening placebo in the acute treatment of major depression. *Pharmacopsychiatry* **31**:48-54.

Daub H, Weiss FU, Wallasch C and Ullrich A (1996) Role of transactivation of the EGF receptor in signalling by G-protein-coupled receptors. *Nature* **379**:557-60.

Daunt DA, Hurt C, Hein L, Kallio J, Feng F and Kobilka BK (1997) Subtype-specific intracellular trafficking of alpha2-adrenergic receptors. *Mol Pharmacol* **51**:711-20.

Delfs JM, Zhu Y, Druhan JP and Aston-Jones G (2000) Noradrenaline in the ventral forebrain is critical for opiate withdrawal-induced aversion. *Nature* **403**:430-4.

Delgado PL and Moreno FA (2000) Role of norepinephrine in depression. *J Clin Psychiatry* **61 Suppl 1**:5-12.

Della Rocca GJ, van Biesen T, Daaka Y, Luttrell DK, Luttrell LM and Lefkowitz RJ (1997) Ras-dependent mitogen-activated protein kinase activation by G protein-coupled receptors. Convergence of Gi- and Gq-mediated pathways on calcium/calmodulin, Pyk2, and Src kinase. *J Biol Chem* **272**:19125-32.

Delmas P, Abogadie FC, Milligan G, Buckley NJ and Brown DA (1999) betagamma dimers derived from Go and Gi proteins contribute different components of adrenergic inhibition of Ca2+ channels in rat sympathetic neurones. *J Physiol* **518 ( Pt 1)**:23-36.

Devoto P, Flore G, Pira L, Diana M and Gessa GL (2002) Co-release of noradrenaline and dopamine in the prefrontal cortex after acute morphine and during morphine withdrawal. *Psychopharmacology (Berl)* **160**:220-4.

DiFrancesco D (1981) A study of the ionic nature of the pace-maker current in calf Purkinje fibres. *J Physiol* **314**:377-93.

DiFrancesco D and Camm JA (2004) Heart rate lowering by specific and selective I(f) current inhibition with ivabradine: a new therapeutic perspective in cardiovascular disease. *Drugs* **64**:1757-65.

Dixon WE (1906) Vagus inhibition. *British Medical Journal*:1807.

Dohlman HG, Thorner J, Caron MG and Lefkowitz RJ (1991) Model systems for the study of seven-transmembrane-segment receptors. *Annu Rev Biochem* **60**:653-88.

Dontenwill M, Vonthron C, Greney H, Magnier C, Heemskerk F and Bousquet P (1999) Identification of human I1 receptors and their relationship to alpha 2-adrenoceptors. *Ann N Y Acad Sci* **881**:123-34.

Duman RS and Nestler, EJ (1995) Signal Transduction Pathways for Catecholamine Receptors, in *Psychopharmacology: The Fourth Generation of Progress* (Bloom, FE and Kupfer DJ eds), Raven Press, New York.

Eason MG and Liggett SB (1992) Subtype-selective desensitization of alpha 2-adrenergic receptors. Different mechanisms control short and long term agonist-promoted desensitization of alpha 2C10, alpha 2C4, and alpha 2C2. *J Biol Chem* **267**:25473-9.

Ehrlich P (1900) Croonian lecture.  On immunity with special reference to cell life, in *Proceedings of the Royal Society* pp 424-448, London.

Ehrlich P (1914) Chemotherapy, in *The Collected Papers of Paul Ehrlich, (1960)* (Himmelweit F ed) pp 505-518, Pergamon Press, London.

Ernsberger P, Damon TH, Graff LM, Schafer SG and Christen MO (1993) Moxonidine, a centrally acting antihypertensive agent, is a selective ligand for I1-imidazoline sites. *J Pharmacol Exp Ther* **264**:172-82.

Ernsberger P, Friedman JE and Koletsky RJ (1997) The I1-imidazoline receptor: from binding site to therapeutic target in cardiovascular disease. *J Hypertens Suppl* **15**:S9-23.

Ernsberger P and Haxhiu MA (1997) The I1-imidazoline-binding site is a functional receptor mediating vasodepression via the ventral medulla. *Am J Physiol* **273**:R1572-9.

Fairbanks CA and Wilcox GL (1999) Moxonidine, a selective alpha2-adrenergic and imidazoline receptor agonist, produces spinal antinociception in mice. *J Pharmacol Exp Ther* **290**:403-12.

Ferro A, Coash M, Yamamoto T, Rob J, Ji Y and Queen L (2004) Nitric oxide-dependent beta2-adrenergic dilatation of rat aorta is mediated through activation of both protein kinase A and Akt. *Br J Pharmacol* **143**:397-403.

Foote SL and Aston-Jones, GS (1995) Pharmacology and physiology of central noradrenergic systems, in *Psychopharmacology: The Fourth Generation of Progress* (Bloom, FE and Kupfer DJ eds) pp 335-346, Raven Press, New York.

Franowicz JS, Kessler LE, Borja CM, Kobilka BK, Limbird LE and Arnsten AF (2002) Mutation of the alpha2A-adrenoceptor impairs working memory performance and annuls cognitive enhancement by guanfacine. *J Neurosci* **22**:8771-7.

Frisk-Holmberg M, Paalzow L and Wibell L (1984) Relationship between the cardiovascular effects and steady-state kinetics of clonidine in hypertension. Demonstration of a therapeutic window in man. *Eur J Clin Pharmacol* **26**:309-13.

Gembal M, Gilon P and Henquin JC (1992) Evidence that glucose can control insulin release independently from its action on ATP-sensitive K+ channels in mouse B cells. *J Clin Invest* **89**:1288-95.

Gibson SK and Gilman AG (2006) Gialpha and Gbeta subunits both define selectivity of G protein activation by alpha2-adrenergic receptors. *Proc Natl Acad Sci U S A* **103**:212-7.

Gilman AG (1987) G proteins: transducers of receptor-generated signals. *Annu Rev Biochem* **56**:615-49.

Gold MS, Redmond DE, Jr. and Kleber HD (1978) Clonidine blocks acute opiate-withdrawal symptoms. *Lancet* **2**:599-602.

Göthert M, Bruss M, Bonisch H and Molderings GJ (1999) Presynaptic imidazoline receptors. New developments in characterization and classification. *Ann N Y Acad Sci* **881**:171-84.

Guelfi JD, Ansseau M, Timmerman L and Korsgaard S (2001) Mirtazapine versus venlafaxine in hospitalized severely depressed patients with melancholic features. *J Clin Psychopharmacol* **21**:425-31.

Guimaraes S and Moura D (2001) Vascular adrenoceptors: an update. *Pharmacol Rev* **53**:319-56.

Guo TZ, Jiang JY, Buttermann AE and Maze M (1996) Dexmedetomidine injection into the locus ceruleus produces antinociception. *Anesthesiology* **84**:873-81.

Guyenet PG (1997) Is the hypotensive effect of clonidine and related drugs due to imidazoline binding sites? *Am J Physiol* **273**:R1580-4.

Harkness JE and Wagner JE (1989) Biology and husbandry, in *The biology and medicine of rabbits and rodents* (Harkness JEaW, J.E. ed) p 372, Lea & Febiger, Philadelphia.

Hein L, Altman JD and Kobilka BK (1999) Two functionally distinct alpha2-adrenergic receptors regulate sympathetic neurotransmission. *Nature* **402**:181-4.

Hoefke W and Kobinger W (1966) [Pharmacological effects of 2-(2,6-dichlorophenylamino)-2-imidazoline hydrochloride, a new, antihypertensive substance]. *Arzneimittelforschung* **16**:1038-50.

Hoffman BB (2001) Catecholamines, Sympathomimetic Drugs, and Adrenergic Receptor Antagonists, in *Goodman and Gilman's The Pharmacological Basis of Therapeutics* (Hardman JG, Limbird, L.E. and Goodman Gilman, A. ed) pp 215-268, McGraw-Hill.

Hoffman BB and Taylor P (2001) Neurotransmission; The Autonomic and Somatic Motor Nervous Systems, in *Goodman and Gilman's The Pharmacological Basis of Therapeutics* (Hardman JG, Limbird, L.E. and Goodman Gilman, A. ed) pp 115-153, McGraw-Hill.

Hornykiewicz O (1982) Brain catecholamines in schizophrenia -- a good case for noradrenaline. *Nature* **299**:484-6.

Hsu WH, Xiang HD, Rajan AS and Boyd AE, 3rd (1991) Activation of alpha 2-adrenergic receptors decreases Ca2+ influx to inhibit insulin secretion in a hamster beta-cell line: an action mediated by a guanosine triphosphate-binding protein. *Endocrinology* **128**:958-64.

Hunt R and Taveau RM (1906) On the physiological action of certain cholin derivatives and new methods for detecting cholin. *British Medical Journal* **II**:1788-1791.

Hunt RD, Arnsten AF and Asbell MD (1995) An open trial of guanfacine in the treatment of attention-deficit hyperactivity disorder. *J Am Acad Child Adolesc Psychiatry* **34**:50-4.

Hurt CM, Feng FY and Kobilka B (2000) Cell-type specific targeting of the alpha 2c-adrenoceptor. Evidence for the organization of receptor microdomains during neuronal differentiation of PC12 cells. *J Biol Chem* **275**:35424-31.

Ishii TM, Takano M, Xie LH, Noma A and Ohmori H (1999) Molecular characterization of the hyperpolarization-activated cation channel in rabbit heart sinoatrial node. *J Biol Chem* **274**:12835-9.

Jacob S, Klimm HJ, Rett K, Helsberg K, Haring HU and Godicke J (2004) Effects of moxonidine vs. metoprolol on blood pressure and metabolic control in hypertensive subjects with type 2 diabetes. *Exp Clin Endocrinol Diabetes* **112**:315-22.

Jewell-Motz EA and Liggett SB (1996) G protein-coupled receptor kinase specificity for phosphorylation and desensitization of alpha2-adrenergic receptor subtypes. *J Biol Chem* **271**:18082-7.

Jeyaraj SC, Chotani MA, Mitra S, Gregg HE, Flavahan NA and Morrison KJ (2001) Cooling evokes redistribution of alpha2C-adrenoceptors from Golgi to plasma membrane in transfected human embryonic kidney 293 cells. *Mol Pharmacol* **60**:1195-200.

Jimenez-Jimenez FJ and Garcia-Ruiz PJ (2001) Pharmacological options for the treatment of Tourette's disorder. *Drugs* **61**:2207-20.

Keefer JR, Kennedy ME and Limbird LE (1994) Unique structural features important for stabilization versus polarization of the alpha 2A-adrenergic receptor on the basolateral membrane of Madin-Darby canine kidney cells. *J Biol Chem* **269**:16425-32.

Kienbaum P, Heuter T, Michel MC, Scherbaum N, Gastpar M and Peters J (2002) Sympathetic neural activation evoked by *μ*-receptor blockade in patients addicted to opioids is abolished by intravenous clonidine. *Anesthesiology* **96**:346-51.

Kiowski W, Hulthen UL, Ritz R and Buhler FR (1983) Alpha 2 adrenoceptor-mediated vasoconstriction of arteries. *Clin Pharmacol Ther* **34**:565-9.

Knaus A, Zong X, Beetz N, Jahns R, Lohse MJ, Biel M and Hein L (2007) Direct inhibition of cardiac hyperpolarization-activated cyclic nucleotide-gated pacemaker channels by clonidine. *Circulation* **115**:872-80.

Kobilka BK, Matsui H, Kobilka TS, Yang-Feng TL, Francke U, Caron MG, Lefkowitz RJ and Regan JW (1987) Cloning, sequencing, and expression of the gene coding for the human platelet alpha 2-adrenergic receptor. *Science* **238**:650-6.

Krauss G (1997) *Biochemie der Regulation und Signaltransduktion*. VCH Verlagsgesellschaft mbH, Weinheim.

Kribben A, Herget-Rosenthal S, Lange B, Erdbrugger W, Philipp T and Michel MC (1997) Alpha2-adrenoceptors in opossum kidney cells couple to stimulation of mitogen-activated protein kinase independently of adenylyl cyclase inhibition. *Naunyn Schmiedebergs Arch Pharmacol* **356**:225-32.

Kroin JS, Buvanendran A, Beck DR, Topic JE, Watts DE and Tuman KJ (2004) Clonidine prolongation of lidocaine analgesia after sciatic nerve block in rats Is mediated via the hyperpolarization-activated cation current, not by alpha-adrenoreceptors. *Anesthesiology* **101**:488-94.

Lakhlani PP, MacMillan LB, Guo TZ, McCool BA, Lovinger DM, Maze M and Limbird LE (1997) Substitution of a mutant alpha2a-adrenergic receptor via "hit and run" gene targeting reveals the role of this subtype in sedative, analgesic, and anesthetic-sparing responses in vivo. *Proc Natl Acad Sci U S A* **94**:9950-5.

Langley JN (1905) On the reaction of cells and of nerve endings to certain poisons, chiefly as regards the reaction of striated muscle to nicotine and to curari. *Journal of Physiology* **XXXIII**:374-413.

Lanier SM, Ivkovic B, Singh I, Neumeyer JL and Bakthavachalam V (1993) Visualization of multiple imidazoline/guanidinium-receptive sites. *J Biol Chem* **268**:16047-51.

Laubie M, Poignant JC, Scuvee-Moreau J, Dabire H, Dresse A and Schmitt H (1985) Pharmacological properties of (N-dicyclopropylmethyl) amino-2-oxazoline (S 3341), an alpha-2 adrenoceptor agonist. *J Pharmacol* **16**:259-78.

Lee K, Groh WJ, Blair TA, Maylie JG and Adelman JP (1995) Imidazoline compounds inhibit KATP channels in guinea pig ventricular myocytes. *Eur J Pharmacol* **285**:309-12.

Leinonen E, Skarstein J, Behnke K, Agren H and Helsdingen JT (1999) Efficacy and tolerability of mirtazapine versus citalopram: a double-blind, randomized study in patients with major depressive disorder. Nordic Antidepressant Study Group. *Int Clin Psychopharmacol* **14**:329-37.

Levick JR (1998) *Physiologie des Herz-Kreislauf-Systems*. Johann Ambrosius Barth Verlag, Heidelberg, Leipzig.

Lindström LH (2000) Schizophrenia, the dopamine hypothesis and alpha2-adrenoceptor antagonists. *Trends Pharmacol Sci* **21**:198-9.

Link RE, Desai K, Hein L, Stevens ME, Chruscinski A, Bernstein D, Barsh GS and Kobilka BK (1996) Cardiovascular regulation in mice lacking alpha2-adrenergic receptor subtypes b and c. *Science* **273**:803-5.

Link RE, Stevens MS, Kulatunga M, Scheinin M, Barsh GS and Kobilka BK (1995) Targeted inactivation of the gene encoding the mouse alpha 2c-adrenoceptor homolog. *Mol Pharmacol* **48**:48-55.

Lomasney JW, Lorenz W, Allen LF, King K, Regan JW, Yang-Feng TL, Caron MG and Lefkowitz RJ (1990) Expansion of the alpha 2-adrenergic receptor family: cloning and characterization of a human alpha 2-adrenergic receptor subtype, the gene for which is located on chromosome 2. *Proc Natl Acad Sci U S A* **87**:5094-8.

Lopez-Ilasaca M (1998) Signaling from G-protein-coupled receptors to mitogen-activated protein (MAP)-kinase cascades. *Biochem Pharmacol* **56**:269-77.

Lotti LV, Lanfrancone L, Migliaccio E, Zompetta C, Pelicci G, Salcini AE, Falini B, Pelicci PG and Torrisi MR (1996) Sch proteins are localized on endoplasmic reticulum membranes and are redistributed after tyrosine kinase receptor activation. *Mol Cell Biol* **16**:1946-54.

Ludwig A, Zong X, Jeglitsch M, Hofmann F and Biel M (1998) A family of hyperpolarization-activated mammalian cation channels. *Nature* **393**:587-91.

MacMillan LB, Hein L, Smith MS, Piascik MT and Limbird LE (1996) Central hypotensive effects of the alpha2a-adrenergic receptor subtype. *Science* **273**:801-3.

Macphee GJ, Howie CA, Elliott HL and Reid JL (1992) A comparison of the haemodynamic and behavioural effects of moxonidine and clonidine in normotensive subjects. *Br J Clin Pharmacol* **33**:261-7.

Mangoni ME and Nargeot J (2001) Properties of the hyperpolarization-activated current (I(f)) in isolated mouse sino-atrial cells. *Cardiovasc Res* **52**:51-64.

Mannion S, Hayes I, Loughnane F, Murphy DB and Shorten GD (2005) Intravenous but not perineural clonidine prolongs postoperative analgesia after psoas compartment block with 0.5% levobupivacaine for hip fracture surgery. *Anesth Analg* **100**:873-8, table of contents.

Meeley MP, Ernsberger PR, Granata AR and Reis DJ (1986) An endogenous clonidine-displacing substance from bovine brain: receptor binding and hypotensive actions in the ventrolateral medulla. *Life Sci* **38**:1119-26.

Milanés MV, Martinez MD, Gonzalez-Cuello A and Laorden ML (2001) Evidence for a peripheral mechanism in cardiac opioid withdrawal. *Naunyn Schmiedebergs Arch Pharmacol* **364**:193-8.

Miller JW, Hu ZW, Okazaki M, Fujinaga M and Hoffman BB (1996) Expression of alpha 1 adrenergic receptor subtype mRNAs in the rat cardiovascular system with aging. *Mech Ageing Dev* **87**:75-89.

Mitruka BM and Rawnsley HM (1981) *Clinical, biochemical and hematological reference values in normal experimental animals and normal humans*. Masson Publishing, New York.

Morgan NG and Chan SL (2001) Imidazoline binding sites in the endocrine pancreas: can they fulfil their potential as targets for the development of new insulin secretagogues? *Curr Pharm Des* **7**:1413-31.

Morris P, Hopwood M, Maguire K, Norman T and Schweitzer I (2004) Blunted growth hormone response to clonidine in post-traumatic stress disorder. *Psychoneuroendocrinology* **29**:269-78.

Munk SA, Lai RK, Burke JE, Arasasingham PN, Kharlamb AB, Manlapaz CA, Padillo EU, Wijono MK, Hasson DW, Wheeler LA and Garst ME (1996) Synthesis and pharmacologic evaluation of 2-endo-amino-3-exo-isopropylbicyclo[2.2.1]heptane: a potent imidazoline1 receptor specific agent. *J Med Chem* **39**:1193-5.

Mutschler E (1997) *Arzneimittelwirkungen: Lehrbuch der Pharmakologie und Toxikologie*. Wissenschaftliche Verlagsgesellschaft mbH, Stuttgart.

Nakaki T, Nakadate T, Ishii K and Kato R (1981) Postsynaptic alpha-2 adrenergic receptors in isolated rat islets of Langerhans: inhibition of insulin release and cyclic 3':5'-adenosine monophosphate accumulation. *J Pharmacol Exp Ther* **216**:607-12.

Neer EJ (1995) Heterotrimeric G proteins: organizers of transmembrane signals. *Cell* **80**:249-57.

Neer EJ and Clapham DE (1988) Roles of G protein subunits in transmembrane signalling. *Nature* **333**:129-34.

Nicholas AP, Pieribone V and Hokfelt T (1993) Distributions of mRNAs for alpha-2 adrenergic receptor subtypes in rat brain: an in situ hybridization study. *J Comp Neurol* **328**:575-94.

Oda S, Ohneda A, Tsuda T and Sasaki Y (1990) Glucagon and insulin responses to alpha-adrenergic subtype receptor blockade in sheep. *Comp Biochem Physiol C* **96**:405-9.

Onesti G, Schwartz AB, Kim KE, Paz-Martinez V and Swartz C (1971) Antihypertensive effect of clonidine. *Circ Res* **28**:Suppl 2:53-69.

Özdogan UK, Lahdesmaki J, Hakala K and Scheinin M (2004) The involvement of alpha 2A-adrenoceptors in morphine analgesia, tolerance and withdrawal in mice. *Eur J Pharmacol* **497**:161-71.

Perry BD, Giller EL, Jr. and Southwick SM (1987) Altered platelet alpha 2-adrenergic binding sites in posttraumatic stress disorder. *Am J Psychiatry* **144**:1511-2.

Pertovaara A, Kauppila T, Jyvasjarvi E and Kalso E (1991) Involvement of supraspinal and spinal segmental alpha-2-adrenergic mechanisms in the medetomidine-induced antinociception. *Neuroscience* **44**:705-14.

Peterhoff M, Sieg A, Brede M, Chao CM, Hein L and Ullrich S (2003) Inhibition of insulin secretion via distinct signaling pathways in alpha2-adrenoceptor knockout mice. *Eur J Endocrinol* **149**:343-50.

Philipp M (2002b) Die Rolle von alpha2-adrenergen Rezeptoren während der Embryonalentwicklung der Maus, in *Institut für Pharmakologie* pp 116, Julius-Maximilians-Universität Würzburg, Würzburg.

Philipp M, Brede M and Hein L (2002a) Physiological significance of alpha(2)-adrenergic receptor subtype diversity: one receptor is not enough. *Am J Physiol Regul Integr Comp Physiol* **283**:R287-95.

Philipp M, Brede ME, Hadamek K, Gessler M, Lohse MJ and Hein L (2002c) Placental alpha(2)-adrenoceptors control vascular development at the interface between mother and embryo. *Nat Genet* **31**:311-5.

Pierce KL, Maudsley S, Daaka Y, Luttrell LM and Lefkowitz RJ (2000) Role of endocytosis in the activation of the extracellular signal-regulated kinase cascade by sequestering and nonsequestering G protein-coupled receptors. *Proc Natl Acad Sci U S A* **97**:1489-94.

Pierce KL, Tohgo A, Ahn S, Field ME, Luttrell LM and Lefkowitz RJ (2001) Epidermal growth factor (EGF) receptor-dependent ERK activation by G protein-coupled receptors: a co-culture system for identifying intermediates upstream and downstream of heparin-binding EGF shedding. *J Biol Chem* **276**:23155-60.

Piletz JE, Andorn AC, Unnerstall JR and Halaris A (1991) Binding of [3H]-p-aminoclonidine to alpha 2-adrenoceptor states plus a non-adrenergic site on human platelet plasma membranes. *Biochem Pharmacol* **42**:569-84.

Piletz JE, Ivanov TR, Sharp JD, Ernsberger P, Chang CH, Pickard RT, Gold G, Roth B, Zhu H, Jones JC, Baldwin J and Reis DJ (2000) Imidazoline receptor antisera-selected (IRAS) cDNA: cloning and characterization. *DNA Cell Biol* **19**:319-29.

Pliszka SR (2003) Non-stimulant treatment of attention-deficit/hyperactivity disorder. *CNS Spectr* **8**:253-8.

Prenzel N, Zwick E, Daub H, Leserer M, Abraham R, Wallasch C and Ullrich A (1999) EGF receptor transactivation by G-protein-coupled receptors requires metalloproteinase cleavage of proHB-EGF. *Nature* **402**:884-8.

Regan JW, Kobilka TS, Yang-Feng TL, Caron MG, Lefkowitz RJ and Kobilka BK (1988) Cloning and expression of a human kidney cDNA for an alpha 2-adrenergic receptor subtype. *Proc Natl Acad Sci U S A* **85**:6301-5.

Remko M, Swart M and Bickelhaupt FM (2006) Theoretical study of structure, pKa, lipophilicity, solubility, absorption, and polar surface area of some centrally acting antihypertensives. *Bioorg Med Chem* **14**:1715-28.

Roberts RE (2004) The role of Rho kinase and extracellular regulated kinase-mitogen-activated protein kinase in alpha2-adrenoceptor-mediated vasoconstriction in the porcine palmar lateral vein. *J Pharmacol Exp Ther* **311**:742-7.

Röser C (2005) Rezeptor-Signaltransduktion in transgenen Mausmodellen: Prä- versus postsynaptische Funktion (alpha)2-adrenerger Rezeptoren, in *Fakultät für Biologie* pp 71, Bayerische Julius-Maximilians-Universität Würzburg, Würzburg.

Rosin DL, Talley EM, Lee A, Stornetta RL, Gaylinn BD, Guyenet PG and Lynch KR (1996) Distribution of alpha 2C-adrenergic receptor-like immunoreactivity in the rat central nervous system. *J Comp Neurol* **372**:135-65.

Ross EM and Gilman AG (1977) Resolution of some components of adenylate cyclase necessary for catalytic activity. *J Biol Chem* **252**:6966-9.

Roth HJ and Fenner H (2000) *Arzneistoffe*. Deutscher Apotheker Verlag Stuttgart, Stuttgart.

Ruffolo RR, Jr. and Waddell JE (1982) Stereochemical requirements of alpha 2-adrenergic receptors for alpha-methyl substituted phenethylamines. *Life Sci* **31**:2999-3007.

Sallinen J, Haapalinna A, Viitamaa T, Kobilka BK and Scheinin M (1998) Adrenergic alpha2C-receptors modulate the acoustic startle reflex, prepulse inhibition, and aggression in mice. *J Neurosci* **18**:3035-42.

Salminen T, Varis M, Nyronen T, Pihlavisto M, Hoffren AM, Lonnberg T, Marjamaki A, Frang H, Savola JM, Scheinin M and Johnson MS (1999) Three-dimensional models of alpha(2A)-adrenergic receptor complexes provide a structural explanation for ligand binding. *J Biol Chem* **274**:23405-13.

Santoro B, Liu DT, Yao H, Bartsch D, Kandel ER, Siegelbaum SA and Tibbs GR (1998) Identification of a gene encoding a hyperpolarization-activated pacemaker channel of brain. *Cell* **93**:717-29.

Satoh H (2003) Sino-atrial nodal cells of mammalian hearts: ionic currents and gene expression of pacemaker ionic channels. *J Smooth Muscle Res* **39**:175-93.

Saunders C and Limbird LE (1999) Localization and trafficking of alpha2-adrenergic receptor subtypes in cells and tissues. *Pharmacol Ther* **84**:193-205.

Scheinin M, Lomasney JW, Hayden-Hixson DM, Schambra UB, Caron MG, Lefkowitz RJ and Fremeau RT, Jr. (1994) Distribution of alpha 2-adrenergic receptor subtype gene expression in rat brain. *Brain Res Mol Brain Res* **21**:133-49.

Schlicker E, Fink K, Kathmann M, Molderings GJ and Gothert M (1997) Effects of imidazolines on noradrenaline release in brain: an investigation into their relationship to imidazoline, alpha 2 and H3 receptors. *Neurochem Int* **30**:73-83.

Scholz H (2002) Some historical aspects of the development of cardiovascular drugs. *Z Kardiol* **91 Suppl 4**:34-42.

Segal IS, Jarvis DJ, Duncan SR, White PF and Maze M (1991) Clinical efficacy of oral-transdermal clonidine combinations during the perioperative period. *Anesthesiology* **74**:220-5.

Seger R, Benard O, Bonfil D, Fitoussi N, Friedman Y, Hanoch T, Michael D, Raviv Z, Rubinfeld H, Wolf I, Yung Y and Yao Z (2000) The mitogen-activated protein kinase (MAPK) signaling cascades, in *Life Science Book* pp 166-167, The Weizmann Institute of Science, Israel.

Separovic D, Kester M and Ernsberger P (1996) Coupling of I1-imidazoline receptors to diacylglyceride accumulation in PC12 rat pheochromocytoma cells. *Mol Pharmacol* **49**:668-75.

Servier (2006) Procorolan, Product Description.

Siess W (1989) Molecular mechanisms of platelet activation. *Physiol Rev* **69**:58-178.

Silver LM (1995) *Mouse Genetics*. Oxford University Press.

Starke K (2001) Presynaptic autoreceptors in the third decade: focus on alpha2-adrenoceptors. *J Neurochem* **78**:685-93.

Stelling JW and Jacob TJ (1992) The inward rectifier K+ current underlies oscillatory membrane potential behaviour in bovine pigmented ciliary epithelial cells. *J Physiol* **458**:439-56.

Stephens GJ and Mochida S (2005) G protein {beta}{gamma} subunits mediate presynaptic inhibition of transmitter release from rat superior cervical ganglion neurones in culture. *J Physiol* **563**:765-76.

Stieber J, Hofmann F and Ludwig A (2004) Pacemaker channels and sinus node arrhythmia. *Trends Cardiovasc Med* **14**:23-8.

Stieber J, Wieland K, Stockl G, Ludwig A and Hofmann F (2006) Bradycardic and proarrhythmic properties of sinus node inhibitors. *Mol Pharmacol* **69**:1328-37.

Stryer L (1995) *Biochemistry*. W.H. Freeman and Company, New York.

Sved AF, Tsukamoto K and Schreihofer AM (1992) Stimulation of alpha 2-adrenergic receptors in nucleus tractus solitarius is required for the baroreceptor reflex. *Brain Res* **576**:297-303.

Szabo B (2002) Imidazoline antihypertensive drugs: a critical review on their mechanism of action. *Pharmacol Ther* **93**:1-35.

Szabo B, Fritz T and Wedzony K (2001) Effects of imidazoline antihypertensive drugs on sympathetic tone and noradrenaline release in the prefrontal cortex. *Br J Pharmacol* **134**:295-304.

Takeda M, Phillips JK, Dubey R, Polson JW and Lipski J (2001) Modulation of ACh-induced currents in rat adrenal chromaffin cells by ligands of alpha2 adrenergic and imidazoline receptors. *Auton Neurosci* **88**:151-9.

Talley EM, Rosin DL, Lee A, Guyenet PG and Lynch KR (1996) Distribution of alpha 2A-adrenergic receptor-like immunoreactivity in the rat central nervous system. *J Comp Neurol* **372**:111-34.

Tangri KK, Bhargava AK and Bhargava KP (1974) Interrelation between monoaminergic and cholinergic mechanisms in the hypothalamic thermoregulatory centre of rabbits. *Neuropharmacology* **13**:333-46.

Taraviras S, Olli-Lahdesmaki T, Lymperopoulos A, Charitonidou D, Mavroidis M, Kallio J, Scheinin M and Flordellis C (2002) Subtype-specific neuronal differentiation of PC12 cells transfected with alpha2-adrenergic receptors. *Eur J Cell Biol* **81**:363-74.

Tardif JC, Ford I, Tendera M, Bourassa MG and Fox K (2005) Efficacy of ivabradine, a new selective I(f) inhibitor, compared with atenolol in patients with chronic stable angina. *Eur Heart J* **26**:2529-36.

Tesson F, Limon-Boulez I, Urban P, Puype M, Vandekerckhove J, Coupry I, Pompon D and Parini A (1995) Localization of I2-imidazoline binding sites on monoamine oxidases. *J Biol Chem* **270**:9856-61.

Trendelenburg AU, Philipp M, Meyer A, Klebroff W, Hein L and Starke K (2003) All three alpha2-adrenoceptor types serve as autoreceptors in postganglionic sympathetic neurons. *Naunyn Schmiedebergs Arch Pharmacol* **368**:504-12.

Tripi PA, Palmer JS, Thomas S and Elder JS (2005) Clonidine increases duration of bupivacaine caudal analgesia for ureteroneocystostomy: a double-blind prospective trial. *J Urol* **174**:1081-3.

Ullrich S and Wollheim CB (1985) Expression of both alpha 1- and alpha 2-adrenoceptors in an insulin-secreting cell line. Parallel studies of cytosolic free Ca2+ and insulin release. *Mol Pharmacol* **28**:100-6.

Valentino RJ and Aston-Jones, GS (1995) Physiological and anatomical determinants of locus coeruleus discharge: behavior and clinical implications, in *Psychopharmacology: The Fourth Generation of Progress* (Bloom, FE and Kupfer DJ eds) pp 373-386, Raven Press, New York.

van Zwieten PA, Thoolen MJ and Timmermans PB (1984) The hypotensive activity and side effects of methyldopa, clonidine, and guanfacine. *Hypertension* **6**:II28-33.

Vanhoutte PM (2001) Endothelial adrenoceptors. *J Cardiovasc Pharmacol* **38**:796-808.

Vilaine JP (2006) The discovery of the selective I(f) current inhibitor ivabradine. A new therapeutic approach to ischemic heart disease. *Pharmacol Res* **53**:424-34.

Vulpian EF (1866) Lecons sur la Physiologie Generale et Comparee du Systeme Nerveux.

Wallace DP, Reif G, Hedge AM, Thrasher JB and Pietrow P (2004) Adrenergic regulation of salt and fluid secretion in human medullary collecting duct cells. *Am J Physiol Renal Physiol* **287**:F639-48.

Watanabe T, Inagaki Y and Ishibe Y (2006) Clonidine premedication effects on inhaled induction with sevoflurane in adults: a prospective, double-blind, randomized study. *Acta Anaesthesiol Scand* **50**:180-7.

Weinshank RL, Zgombick JM, Macchi M, Adham N, Lichtblau H, Branchek TA and Hartig PR (1990) Cloning, expression, and pharmacological characterization of a human alpha 2B-adrenergic receptor. *Mol Pharmacol* **38**:681-8.

Wing LM, Reid JL, Davies DS, Neill EA, Tippett P and Dollery CT (1977) Pharmacokinetic and concentration-effect relationships of clonidine in essential hypertension. *Eur J Clin Pharmacol* **12**:463-9.

Wozniak M, Schramm, N.L. and Limbird, L.E. (1995) The Noradrenergic Receptor Subtypes, in *Psychopharmacology: The Fourth Generation of Progress* (Bloom, FE and Kupfer DJ eds), Raven Press, New York.

Zalunardo MP, Zollinger A, Spahn DR, Seifert B, Radjaipour M, Gautschi K and Pasch T (1997) Effects of intravenous and oral clonidine on hemodynamic and plasma-catecholamine response due to endotracheal intubation. *J Clin Anesth* **9**:143-7.

Zhao D and Ren LM (2003) Electrophysiological responses to imidazoline/alpha2-receptor agonists in rabbit sinoatrial node pacemaker cells. *Acta Pharmacol Sin* **24**:1217-23.

Zhu QM, Lesnick JD, Jasper JR, MacLennan SJ, Dillon MP, Eglen RM and Blue DR, Jr. (1999) Cardiovascular effects of rilmenidine, moxonidine and clonidine in conscious wild-type and D79N alpha2A-adrenoceptor transgenic mice. *Br J Pharmacol* **126**:1522-30.

# VIII. Attachments

## 8.1. List of abbreviations

| | |
|---|---|
| $\alpha_{2A}$D79N-mutant | transgenic mouse line expressing an $\alpha_{2A}$-adrenergic receptor with a D→N point mutation at position 79 |
| AA | arachidonic acid |
| AC | adenylyl cyclase |
| ADHD | attention deficit hyperactivity disorder |
| ADP | adenosine diphosphate |
| ANOVA | analysis of variance |
| APD50 | 50% of action potential duration |
| APD90 | 90% of action potential duration |
| ATP | adenosine triphosphate |
| AV | atrioventricular |
| | |
| BaCl | barium chloride |
| $\beta$ARK | $\beta$-adrenergic receptor kinase |
| $B_{max}$ | total number of binding sites |
| bp | base pairs |
| BSA | bovine serum albumin |
| | |
| C | degrees centigrade |
| $CaCl_2$ | calcium chloride |
| cAMP | cyclic adenosine monophosphate |
| cDNA | complementary DNA (deoxyribonucleic acid) |
| CHO | cell line derived from Chinese hamster ovary tissue |
| CL | cycle length |
| CNS | central nervous system |
| $CO_2$ | carbon dioxide |
| COMT | catechol-O-methyltransferase |
| COX | cyclooxygenase |
| cpm | counts per minute |
| | |
| DD | diastolic depolarization |
| DHBA | 3,4-dihydroxy benzylamine hydrobromide |
| DMEM | Dulbecco's modified Eagle's medium |
| DNA | deoxyribonucleic acid |

| | |
|---|---|
| dNTP | deoxyribonucleoside triphosphate |
| | |
| ECG | electrocardiogram |
| EDTA | ethylenediamine tetraacetic acid |
| EGF | epidermal growth factor |
| ERK | extracellular signal regulated kinase |
| ES cells | embryonic stem cell line |
| | |
| FRET | fluorescence resonance energy transfer |
| | |
| G418 | geneticin; a selection agent in transfection |
| GAP | GTPase activating protein |
| GDP | guanosine diphosphate |
| GEF | guanine nucleotide exchange factor |
| GIRK channel | G protein-activated inward rectifier $K^+$ channel |
| GPCR | G protein coupled receptor |
| GTP | guanosine triphosphate |
| | |
| HB-EGF | heparin-binding EGF-like growth factor |
| $HClO_4$ | perchloric acid |
| HCN | hyperpolarization activated, cyclic nucleotide-gated cation |
| HE | hematoxylin and eosin (HE) |
| HEK293 | human embryonic kidney cell line |
| HeLa | Henrietta Lacks, donor of cervix carcinom cells |
| HEPES | N-(2-hydroxyethyl)piperazine-N'-2-ethanesulfonic acid |
| HPLC | high performance liquid chromatography |
| | |
| $IC_{50}$ | inhibitory concentration 50 |
| $I_f$ | pacemaker current ("funny" current) |
| ip | intraperitoneal |
| IRAS-1 | imidazoline receptor antisera-selected type 1 cDNA |
| iv | intravenous |
| | |
| JNK | c-jun N-terminus kinase (synonymous with SAPK) |
| | |
| $K^+_{ATP}$ channel | ATP-sensitive $K^+$ channel |
| KCl | potassium chloride |
| $K_d$ | dissociation equilibrium constant |
| $KH_2PO_4$ | potassium dihydrogen phosphate |
| KO | knockout |
| KOH | potassium hydroxide |

| | |
|---|---|
| L2 | second lumbar vertebra |
| L-DOPA | 3,4-dihydroxy-L-phenylalanine |
| LOX | lipoxygenase |
| LV | left ventricular |
| | |
| M effect | mesomeric effect |
| MAO | monoamine oxidase |
| MAPK | mitogen-activated protein kinase |
| MDCKII | Madin-Darby canine kidney II cell line |
| MEK | mitogen-activated protein kinase kinase (MAP2K; MKK) |
| $MgCl_2$ | magnesium chloride |
| $MgSO_4$ x $7H_2O$ | magnesium sulfate (heptahydrate) |
| MKKK | mitogen-activated protein kinase kinase kinase (MAP3K) |
| MMP | membrane metalloproteinase |
| mRNA | messenger RNA (ribonucleic acid) |
| | |
| $Na(CH_3COO)$ | sodium acetate |
| NaCl | sodium chloride |
| $NaHCO_3$ | sodium bicarbonate |
| $NaH_2PO_4$ | sodium dihydrogen phosphate |
| NaOH | sodium hydroxide |
| $Na_2SO_3$ | sodium sulfite |
| $NH_4Cl$ | ammonium chloride |
| NO | nitric oxide |
| NRL | nucleus reticularis lateralis |
| NTS | nucleus tractus solitarius |
| | |
| OS | overshoot |
| | |
| PBS | phosphate buffered saline |
| PC-12 | rat pheochromocytoma cell line |
| PCR | polymerase chain reaction |
| PEI | polyethylenimine |
| PKC | protein kinase C |
| PLC | phospholipase C |
| PLA2 | phospholipase A2 |
| PNMT | phenylethanolamine N-methyl transferase |
| PNS | peripheral nervous system |
| | |
| RGS | regulator of G protein signaling |

| | |
|---|---|
| RP | resting potential |
| RP-18 | reversed phase chromatographic column (non-polar) |
| rpm | rotations per minute |
| RVLM | rostral ventrolateral medulla |
| | |
| $S1P_1$ | sphingosine-1-phosphate receptor |
| SAN | sino-atrial node |
| SAPK | stress-activated protein kinase (synonymous with JNK) |
| SH domain | Src homology domain; binds phosphotyrosine residues |
| | |
| T1 | first thoracic vertebra |
| TAE | Tris-acetate-EDTA |
| $T_m$ | hybridization temperature of primer |
| TXA2 | thromboxane |
| | |
| $V_{0.5}$ | half-maximum activation voltage |
| | |
| WT | wild-type |

## 8.2. Acknowledgements

I would like to thank my advisor, Prof. Dr. Lutz Hein, for his outstanding comments, critique and suggestions throughout the preparation and completion of my dissertation. I am grateful for having had the opportunity to work in a group of such high scientific standards.

Dr. Xiangang Zong and Prof. Dr. Martin Biel at the Ludwig-Maximilians-Universität in Munich contributed their long-standing expertise in HCN channels and provided us the means to demonstrate that clonidine indeed inhibits HCN channels, and also the mechanism by which it does so.

Both Marianne Babl and Reinhard Wölfel from the Institut für Pharmakologie und Toxikologie in Würzburg played instrumental roles in the preparation of and measuring of catecholamine samples, respectively.

Roland Jahns kindly performed the echocardiographic measurements of the mice.

Above all, I would like to thank my family for their encouragement, patience and understanding during preparation of my dissertation. Without their support this work would very likely not have come to fruition.

## 8.3.  Past publications and lectures

**publications**

Knaus A, Zong XG, Beetz N, Jahns R, Lohse MJ, Biel M and Hein L (2007) Direct inhibition of cardiac hyperpolarization-activated cyclic nucleotide-gated pacemaker channels by clonidine. *Circulation* **115**:872-80.

Brede M, Philipp M, Knaus A, Muthig V and Hein L (2004) alpha2-adrenergic receptor subtypes – novel functions uncovered in gene-targeted mouse models. *Biol Cell* **96**:343-8.

**lectures**

47th Spring Meeting of the Deutsche Gesellschaft für experimentelle und klinische Pharmakologie und Toxikologie, April 4-6, 2006 Mainz, Germany: Knaus A, Zong X, Biel M and Hein L (2006) Clonidine induces bradycardia in mice lacking all three alpha(2)-adrenergic receptor subtypes via inhibition of HCN channels. *Naunyn-Schmiedebergs Arch Pharmacol* **372**:39-39 107 Suppl. 1 Mar 2006.

Hein L, Muthig V, Knaus A, Brede M, Beetz N and Gilsbach, R (2006) Subtype-specific functions of alpha2-adrenergic receptors – insights from transgenic mouse models. *Acta Pharmacol Sin* **27**:17-17 Suppl. 1 Jul 2006.

46th Spring Meeting of the Deutsche Gesellschaft für experimentelle und klinische Pharmakologie und Toxikologie, April 15-17, 2005 Mainz, Germany:  Knaus A and Hein L (2005) Clonidine exhibits bradycardic and hypoglycemic effects in mice lacking all three alpha(2)-adrenergic receptor subtypes. *Naunyn-Schmiedebergs Arch Pharmacol* **371**:R26-R26 106 Suppl. 1 Feb 2005.

45th Spring Meeting of the Deutsche Gesellschaft für experimentelle und klinische Pharmakologie und Toxikologie, March 9-11, 2004 Mainz, Germany:  Knaus A and Hein L (2004) alpha(2)-adrenergic receptor subtypes: All three control the sympathetic system. *Naunyn-Schmiedebergs Arch Pharmacol* **369**:R24-R24 93 Suppl. 1 Mar 2004.

## 8.4. Curriculum vitae

Anne Elizabeth Knaus
Fichtenstr. 23
97199 Ochsenfurt
09331-20871
thorald@aol.com

| | |
|---|---|
| Education: | One year internship, 2000-2001, completed with 3$^{rd}$ State Exams |
| | Universität Würzburg, 1996-2000 School of Pharmacy completed with 2$^{nd}$ State Exams, (grade point average 1.5) |
| | Western Michigan University, 1991-1996 Bachelor of Arts, summa cum laude |
| Certification: | Licensed pharmacist (Germany) since 2002 |
| | Radiopharmacy, postgraduate diploma, according to the guidelines of the European Association of Nuclear Medicine, completed 2004 |
| | Training as Radiation protection officer, completed 2003 |
| Experience: | Pharmacist, Stadt Apotheke Ochsenfurt Nov. 2006-current |
| | Research assistant / doctoral student, Department of Pharmacology, Universität Würzburg, March 2003-Nov. 2006 |
| | Pharmacist, Engel Apotheke Ochsenfurt Jan. 2002-March 2003 |

Pharmacist, Schloß-Apotheke Würzburg-
Rottenbauer
Jan. 2002-March 2003

Internship spring 2001-fall 2001
Kneipp Werke, Hohestadt,
Analytical Department
Objective: development of a new
quantitative assay of *Plantago lanceolata*
preparations for pharmacopeia

Internship fall 2000-spring 2001
Stadt Apotheke Ochsenfurt